

Analysis of Historical and Future Heavy Precipitation

City of Virginia Beach, Virginia
CIP 7-030, PWCN-15-0014, Work Order 9A

Final Report
Date: March 26, 2018
Submitted to: City of Virginia Beach
Department of Public Works



CONTRIBUTORS

Technical Lead:

Dmitry Smirnov, Ph.D.

Technical Contributions:

Jason Giovannettone, Ph.D., P.E., Seth Lawler, Mathini Sreetharan, Ph.D., P.E., Joel Plummer, Brad Workman

Project Manager, Technical Editor:

Brian Batten, Ph.D.

Copy Editors:

Samuel Rosenberg, Dana McGlone

REVISION HISTORY

July 24, 2017 - Draft Report

October 23, 2017 - Draft Final Report, addressing review comments

November 14, 2017 - Final Report, adding consideration of medium resolution Representative Concentration Pathway scenarios 4.5 and 8.5 for future rainfall projections.

March 26, 2018 – Revised Final Report, added revision history, re-formatted Table 1, completed minor typographical edits.

EXECUTIVE SUMMARY

This report summarizes changes in heavy rainfall frequency and intensity using historical observations and bias-corrected future projections. In addition, a comprehensive evaluation of three heavy rainfall events that were responsible for flooding in the City of Virginia Beach during 2016, and comparison to regional Probable Maximum Precipitation estimates is provided. Finally, we provide a review of rainfall design guidance in the context of non-stationarity and future conditions. Based on the analyses and findings within the report, subsequent discussions with City engineers, as well as our own subject matter expertise, we recommend that the City increase design rainfall intensities by 20% to account for already occurring and/or future increases in heavy rainfall. Below we present the findings that support this recommendation.

Historical trends show increases in 24-hour Annual Maximum Series. Chapter 1 of the report calculates trends in Annual Maximum Series (AMS) in the Virginia Beach region. AMS is the key variable used to develop design rainfall guidance such as NOAA Atlas 14, hence it carries significant weight for design purposes. Over the 70-year period of the Norfolk Airport rain gage, there has been a 0.2 inch per decade trend, or about 7% per decade, showing increases in the Annual Maximum Series of 24-hour rainfall. Extending the rainfall record further back to the early 1900s suggests a smaller increase of about 3% per decade, though this is statistically significant. Given that land development planning considers time scales of several decades or more, it is very likely that the already observed changes have resulted in an increase in runoff to current levels that exceed the original design specifications. An analogous argument applies for current planning for future land development.

Moreover, Chapter 1 showed the increases are not just limited to Virginia Beach but are observed along the entire coastline of the northeast United States, strongly suggesting the changes are not simply localized statistical artifacts.

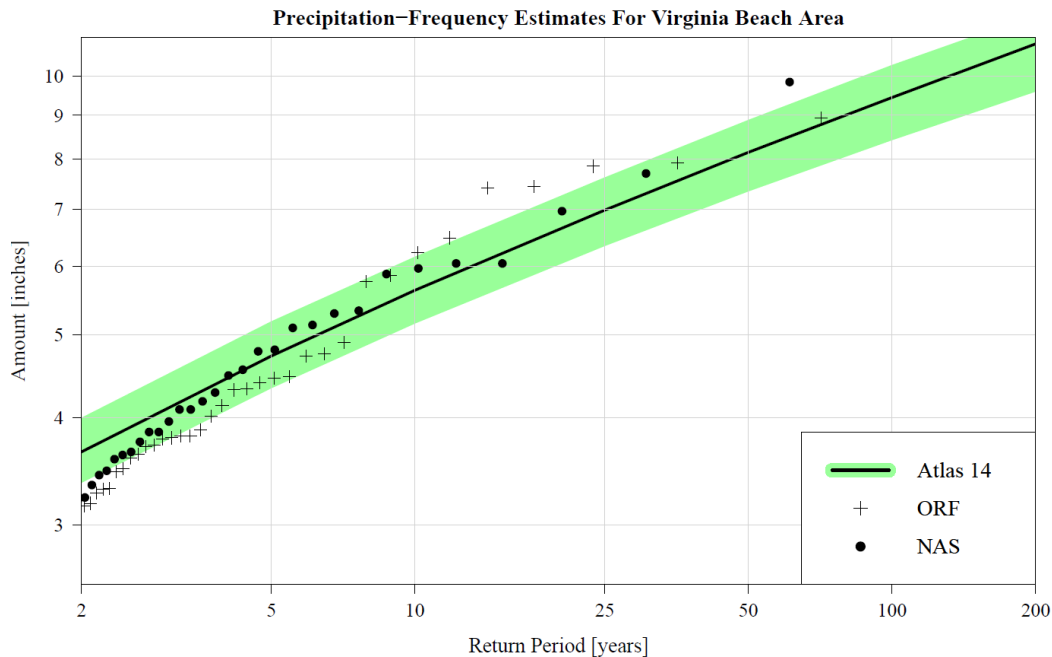
Future Projections Generally Show Increases In Heavy Precipitation. Chapter 2 of the report used bias-corrected future projections of heavy rainfall derived from downscaled global climate models to estimate changes in the Precipitation-Frequency Curve. Two future scenarios were considered: the intermediate emission Representative Concentration Pathway (RCP) 4.5, and the high emission RCP8.5. Furthermore, for RCP8.5, two different sets of simulations were analyzed: one using high resolution models and one using medium resolution models. The high resolution model simulations were unavailable for the RCP4.5 scenario at the time of the analysis.

Across the entire PF curve, the RCP4.5 scenario showed an increase of 4% by 2045 and 6% by 2075. However, the increases were most drastic for the more frequent events; for example, the 1 in 2 year event was projected to increase by 16%. **Assuming an estimated planning time frame of 40 years into the future (~2060), averaging the 2045 and 2075 projections for the RCP4.5 scenario suggests a ~5% increase in the PF curve.**

Meanwhile, the analogous RCP8.5 scenario projected an overall increase of 16% by 2045 and 32% by 2075. The higher resolution models projected similar or even greater overall increases of 22% by 2045 and 31% by 2075. Once again, **assuming an estimated planning time frame of 40 years into the future (~2060), the RCP8.5 scenarios suggest increases in the PF curve of about 24% to 27%, depending on model resolution.**

Historical gage-based Precipitation-Frequency curve estimates are on the higher end of NOAA Atlas 14. NOAA Atlas 14 Precipitation-Frequency (PF) guidance for Virginia Beach was developed by fitting several statistical distributions to local gage estimates, followed by selecting the one with the best fit. However, it is essential to note that the distribution is statistical, and not physical based. In turn, there are frequently situations where parts of the Atlas 14 PF curve may differ from the empirical PF curve of gages contributing to Atlas 14. To illustrate, the plot below shows the Atlas 14 PF estimates for 24-hour rainfall at Virginia Beach, compared to two long-record gages for the area: Norfolk Airport (ORF) and the Oceana Naval Air Station (NAS). Note that overall, the Atlas 14 fit does a reasonable job of capturing the gage estimates. On the other hand, a closer inspection shows potentially noteworthy differences. **For example, the Atlas 14 estimate for the 10 year event is 5.6 inches, with a range of 5.2 to 6.2 inches when incorporating uncertainty. However, the analogous empirical estimates from ORF and NAS are 6.2 and 6.0 inches, which is 7-10% higher than Atlas 14 guidance. The 10-year rainfall for is of particular importance because it is currently used for runoff modeling especially in the context of land development. It is possible that without any changes in future conditions, the Atlas 14 guidance is currently underestimating the local 10-year rainfall amount.**

The differences between empirical gage estimates and Atlas 14 are not readily apparent but may be due to the fact that different processes are responsible for relatively more frequent events (e.g. 2-8 year) versus less frequent events (e.g. 10-100 year). For example, Nor'easters can be responsible for a given year's Annual Maximum 24-hour rainfall, but generally do not produce precipitation exceeding the 1 in 10 year value. Meanwhile, tropical events, while less frequent, produce the majority of the more extreme rainfall events.



Atlas 14 Precipitation-Frequency estimates compared to Norfolk Airport and Oceana Naval Air Station (most likely value is the black line; the green band is the 90% confidence level). Both gages show precipitation values above the Atlas 14 guidance above the approximate 7-yr recurrence interval.

In summary,

- Historically, precipitation Annual Maximum Series have trended upward between 3-7% per decade. Using an average of 5% would suggest a 20% increase given a 40-year horizon.
- Future projections support increases of 5% for the intermediate scenario to 24-27% in the high scenario by 2060. A blend of the two to account for uncertainty in the actual outcome warrants a 15-16% increase.
- Current Atlas 14 guidance for the 10 year rainfall event may be 7-10% below the actual localized value based on analysis of two long-record rain gages in the area. If such is the case, then even using the intermediate RCP4.5 projections of 5% would already warrant a 12-15% increase in the Precipitation Frequency curve.

Given these observations, an increase of the City’s design guideline for rainfall intensity is justified. We recommend an increase of 20% over existing guidance for projects that have a typical lifecycle of 40 years.

TABLE OF CONTENTS

CONTRIBUTORS.....	i
REVISION HISTORY	i
EXECUTIVE SUMMARY.....	ii
TABLE OF CONTENTS	v
LIST OF FIGURES.....	vii
LIST OF TABLES	xi
ACRONYMS	xiii
INTRODUCTION.....	1
CHAPTER 1: HISTORICAL ANALYSIS	3
Climatology	3
Gage-Level Stationarity Assessment	5
Local-Level Stationarity Assessment.....	12
Regional-Level Stationarity Assessment	16
CHAPTER 2: FUTURE PROJECTION.....	22
Overview.....	22
RCP8.5 Analysis (11 km model resolution)	23
Peaks-Over-Threshold (POTs)	25
Precipitation-Frequency Curve.....	28
RCP4.5 and RCP8.5 Analysis (44km model resolution).....	32
Comparing RCP scenarios	38
Limitation of Using Annual Maximum Series.....	38
CHAPTER 3: CHECK STORM ANALYSIS AND COMPARISON WITH PROBABLE MAXIMUM PRECIPITATION	42
Background	42
Design Storm.....	44
Precipitation data.....	45
Event Summaries	47
July 31, 2016 Heavy Rainfall	47
Tropical Storm Julia.....	50

Hurricane Matthew	53
Comparison to Probable Maximum Precipitation	57
Hyetograph Deliverables	59
CHAPTER 4: REVIEW OF RAINFALL DESIGN GUIDANCE	60
Introduction	60
Federal Guidance	61
State Guidance	64
Interviews.....	64
CONCLUSIONS	66
Historical Analysis	66
Future Projections	67
Check Storm Analysis	67
July 31, 2016	67
September 19 – September 22, 2016 (Tropical Storm Julia)	68
October 8 – October 9, 2016 (Hurricane Matthew)	68
Rainfall Design Guidance	68
REFERENCES	71
APPENDIX A: Historical Climate Modeling	74
APPENDIX B: NOAA Atlas 14 Point Rainfall for Virginia Beach	75
APPENDIX C: Hurricane Matthew	76
APPENDIX D: PROJECTED ANNUAL MAXIMUM SERIES	77
APPENDIX E: INTERVIEW SUMMARY	80

LIST OF FIGURES

Figure 1: Observed change in very heavy precipitation events (i.e. downpours, the heaviest 1% of annual rainfall events). Source is 3rd National Climate Assessment, <http://nca2014.globalchange.gov/report/our-changing-climate/heavy-downpours-increasing>..... 1

Figure 2: NOAA Atlas 14 precipitation-frequency curves for 24-hour rainfall for a location near VB. The black curve is the “most likely” estimate, while the green and red curves denote the high and low bounds using the 90% confidence level.3

Figure 3: Seasonality analysis for 24-hour precipitation for a location near VB. The percent chance of observing an event exceeding the indicated threshold is shown for the 2-, 5-, 10-, 25- 50- and 100-year recurrence interval. Note that the late summer and fall months show the highest probabilities of occurrence.4

Figure 4: Annual Maximum Series of daily rainfall at the Norfolk Airport rain gage..... 8

Figure 5. Same as Figure 4 except for annual daily rainfall events exceeding 1.25 inches. 9

Figure 6: Scatter plot and R-squared value correlating AMS at the Diamond Springs (y-axis) and Norfolk Airport (x-axis) gages using the 24-hour (left) and 48-hour (right) durations..10

Figure 7: Trend in the 48-hour AMS at the blended Norfolk gage (combining Norfolk Airport and Diamond Springs rain gage data). 11

Figure 8: Same as Figure 7 except for annual 48-hour Peaks-Over-Threshold, with a threshold of two inches. 12

Figure 9: Method used for conducting a “local-level” rainfall analysis. This shows the qualifying gages during 2015, along with their “coverage” area..... 13

Figure 10: Results of local-level rainfall analysis. 15

Figure 11: Estimates of 100-year 24-hour precipitation across the eastern United States. 16

Figure 12: A total of 175 qualifying, long-record GHCN gages were used for the historical analysis. 17

Figure 13: Trends in Annual Maximum Series (a and b) and Peaks Over Threshold (c and d). Panels (a) and (c) restrict data to 2004, while panels (b) and (d) use values through 2016. Peaks-Over-Threshold time series are calculated using number of annual days exceeding 1.25 inches at each gage. The legend shows the number of statistically significant trends at the 95% confidence level. 19

Figure 14: Regional analysis of changes in the (a) 99th and (b) 70th percentile of rainy day (i.e. dry days are excluded) rainfall. At Norfolk, the 99th percentile is about 2.7 inches per day and is representative of heavy rainfall events, while the 70th percentile is about 0.3 inches per day and is representative of light rainfall events. The legend provides a summary of the number of gages that fall in each category..... 21

Figure 15: Historical and projected total anthropogenic RF (W m-2) relative to preindustrial (about 1765) between 1950 and 2100. Source: Reproduced from Cubasch et al. (2013), their Figure 1.15..... 23

Figure 16: Quantile-quantile maps comparing observed daily precipitation of historical 11-km model simulations. 24

Figure 17: Accumulation of POT exceeding the 24-hour two-year rainfall (3.7 inches). 26

Figure 18: Same as Figure 17 except for 24-hour, five-year rainfall.27

Figure 19: Historical modeled GEV (black line), with a 90% uncertainty band, compared to empirical estimates using 24-hour AMS from the Norfolk Airport. 29

Figure 20: Precipitation-Frequency curve centered on 2045 (orange) compared to the historical curve (black and gray)..... 30

Figure 21: Same as Figure 20 except for the long-term period centered on 2075. 30

Figure 22: Seasonality of AMS occurrence, by month, for the Norfolk gage (left column) and the four RCMs contributing to the future projections (right four columns)..... 32

Figure 23: Quantile-quantile maps comparing observed daily precipitation of historical 44-km model simulations. 34

Figure 24: Precipitation-Frequency curve centered on 2045 (red) compared to the historical curve (black and gray) using the 44-km model simulations for the RCP4.5 scenario.....35

Figure 25: Same as Figure 24 except centered on 2075.....35

Figure 26: Precipitation-Frequency curve centered on 2045 (red) compared to the historical curve (black and gray) using the 44-km model simulations for the RCP8.5 scenario..... 36

Figure 27: Same as Figure 26 except centered on 2075..... 36

Figure 28: Comparisons of the AMS and PDS estimates at the Norfolk Airport rainfall gage. . 39

Figure 29: Precipitation-Frequency curve centered on 2045 (orange) compared to the historical curve (black and gray) using the PDS method. This should be compared to Figure 20, which was based on the AMS method. 40

Figure 30: Estimated rainfall totals (color fill) from the NOAA Stage IV gridded precipitation product for (a) July 31, 2016, (b) Tropical Storm Julia and (c) Hurricane Matthew. Individual rain gage totals are overlaid in (b) and (c). Note that gage totals may not exactly match the gridded data due to averaging effects in the latter. 43

Figure 31: Design storm rainfall accumulation for a 24-hour event for 6 return periods, using the NOAA Type C distribution. 44

Figure 32: Relationship between 30-minute average radar reflectivity (dBZ) and 30-minute accumulated rainfall across all available rain gages (see Table 9) for Hurricane Matthew. ..47

Figure 33: Atmospheric sounding from the Wallops Island (VA) radiosonde balloon launched at 8PM local time on July 31, 2016. A parcel instability analysis was performed by assuming an inflow air temperature of 82oF and dew point of 75F, yielding the instability shown by the red dashed lines. The stable layer is shown by the green dashed lines..... 48

Figure 34: Base-elevation radar reflectivity scans from the Wakefield (VA) NEXRAD radar taken at 5:24PM and 5:58PM local time..... 49

Figure 35: Accumulated rainfall at the HRSD Ches-Liz Main Flow gage, which was representative of the highest rainfall intensity produced during the July 31 event. 49

Figure 36: (Lines) Hyetographs of rainfall accumulation (left axis) during Tropical Storm Julia. The blue lines show the maximum 6-hour (red circles) and 24-hour (red squares) accumulations across all gages. The orange and brown bars denote areal coverage (right axis; units: km²) of “heavy” and “very heavy” rain, measured using the 40 dBZ and 45 dBZ radar reflectivity thresholds, respectively..... 51

Figure 37: Maximum 24-hour hyetographs (red lines) during Tropical Storm Julia, as compared to the 10-, 25-, 100- and 500-year design storms. The thick red lines denote the two hyetographs (noted as “High” and “Low”) that were used as a “Check Storm” for which data was aggregated into six-minute totals for direct comparison to the design storm.52

Figure 38: Three-hour rainfall intensity during Tropical Storm Julia, compared to the 10-year and 100-year design storm. For reference, the three-hour 10-year intensity from NOAA Atlas 14 is shown by the dotted gray line.53

Figure 39: (Lines) Hyetographs of rainfall accumulation (left axis) during Hurricane Matthew. The blue lines show the maximum 6-hour (red circles) and 24-hour (red squares) accumulations across all the gages. The orange and brown bars denote areal coverage (right axis; units: km²) of “heavy” and “very heavy” rain as measured using the 40 dBZ and 45 dBZ radar reflectivity thresholds, respectively.....55

Figure 40: Maximum 24-hour hyetographs (red lines) during Tropical Storm Matthew, as compared with the 25-, 100- and 500- and 1000-year design storms. The thick red lines denote the three hyetographs (noted as “High,” “Mid,” and “Low”) that were used as a “Check Storm” for which data was aggregated into six-minute totals for direct comparison to the design storm.56

Figure 41: Three-hour rainfall intensity during Hurricane Matthew, compared to the 10-year and 100-year design storm. For reference, the three-hour 10-year intensity from NOAA Atlas 14 is shown by the dotted gray line.56

Figure 42: All-season PMP (in.) for 24-hour 10 mi². Adapted from Schreiner and Riedel (1978; their Figure 20).57

Figure 43: Percent difference of HMR 51 values compared to largest PMP values from all three storm types; 24-hour 10 square miles. Note that the scale in the legend is specific to the image. Taken from AWA (2015), their Figure 10.12. 58

Figure 44: Snapshot from the Northeast Regional Climate Center’s web-based tool showing changes in the IDF for the New York City area.....65

LIST OF TABLES

Table 1: Summary of meteorological analysis of all 24-hour rainfall events exceeding the one in two-year recurrence interval (3.7 inches) between 1946 and 2016 using the Norfolk Airport (“Norfolk”) OR Oceana Naval Station (“Virginia Beach”) rain gage data. A double-line border is used to separate events into decades..... 6

Table 2: NA-CORDEX experiments used for this analysis. All simulations were conducted using 11km resolution modeling and RCP8.5 scenario boundary conditions. 23

Table 3: Peaks-Over-Threshold accumulation, or “hit”, rate of days exceeding two-year (3.7 inches) and five-year (4.7 inches) using the Norfolk Airport gage compared to the bias corrected model data, and four model average. Units are number of days per decade. 28

Table 4: Summary of P-F curve changes between the modeled historical climate (after bias correction), and mid-term and long-term model projections. For the projections, bold values indicate when the uncertainty bands are statistically distinguishable from the historical period at the 90% confidence level. Note that the Historical Modeled Value is NOT based on NOAA Atlas 14. 31

Table 5: NA-CORDEX experiments used for this analysis. All simulations were conducted using 44km resolution modeling and both RCP4.5 and RCP8.5 scenario boundary conditions.33

Table 6: Same as Table 4 except using for the RCP4.5 scenario using 44-km models. For the projections, bold values indicate when the uncertainty bands are statistically distinguishable from the historical period at the 90% confidence level. Note that the Historical Modeled Value is NOT based on NOAA Atlas 14.....37

Table 7: Same as Table 4 except adding the results from the 44-km model projections using the RCP8.5 scenario. Bold values indicate when the uncertainty bands are statistically distinguishable from the historical period at the 90% confidence level. Note that the Historical Modeled Value is NOT based on NOAA Atlas 14. 38

Table 8: Summary of P-F curve changes between the historical, mid-term and long-term periods using the PDS method (compare to Table 4, which is based on AMS). For the projections, bold values indicate when the uncertainty bands are statistically distinguishable from the historical period at the 90% confidence level. NOAA Atlas 14 estimates are added for reference. Note that the Historical Modeled Value is NOT based on NOAA Atlas 14. 41

Table 9: Summary of rain gages used in the analysis. Total event rainfall is shown for Hurricane Matthew and Tropical Storm Julia in units of inches. 46

Table 10: Summary of precipitation intensity and return period estimates for the July 31, 2016 event..... 50

Table 11: Summary of precipitation intensity and return period estimates for Tropical Storm Julia..... 51

Table 12: Summary of precipitation intensity and return period estimates for Hurricane Matthew.....54

Table 13: Fractional PMP estimates for each of the three events considered in this study.....59

Table 14: Recommended Precipitation-Frequency curve values at key return periods, based on a 20% increase of NOAA Atlas 14..... 70

ACRONYMS

AMS	Annual Maximum Series
CMIP	Coupled Model Intercomparison Project
CoCoRaHS	Community Collaborative Rain, Hail and Snow Network
COOP	Cooperative Observer Program
CREAT	Climate Resilience Evaluation and Awareness Tool
DCR	Virginia Department of Conservation and Recreation
EPA	Environmental Protection Agency
FEMA	Federal Emergency Management Agency
FHWA	Federal Highway Administration
GAGES II	Geospatial Attributes of Gages for Evaluating Stream Flow
GCM	Global Climate Model
GEV	Generalized Extreme Value
HRSD	Hampton Roads Sanitation District
HUC	Hydrologic Unit Code
IPCC	Intergovernmental Panel on Climate Change
NA-CORDEX	North American Coordinated Regional Modeling Experiment
NEXRAD	Next Generation Doppler radar
NOAA	National Oceanic and Atmospheric Administration
NRCS	Department of Agriculture’s Natural Resources Conservation Service
NWS	National Weather Service
PDS	Partial Duration Series
P-F	Precipitation-Frequency
PMP	Probable Maximum Precipitation
POT	Peaks-Over-Threshold
RAWS	Remote Automatic Weather Systems
RCP	Representative Concentration Pathway
SWMM-CAT	Storm Water Management Model Climate Adjustment Tool
US	United States
USACE	U.S. Army Corps of Engineers
USGS	United States Geological Survey
VB	Virginia Beach
WBAN	Weather-Bureau-Army-Navy

INTRODUCTION

Analysis of historical trends in observed rainfall have indicated increases in heavy rainfall occurrence across the entire contiguous United States. Figure 1, from the 3rd National Climate Assessment (NCA; Melillo et al. 2014) report, shows the percent change in the occurrence of 1% daily rainfall, using the 1958-1988 period as the baseline. Although increases in heavy rainfall frequency have been observed across the entire US, particularly strong changes have been documented in the Northeast, Southeast and Upper Mississippi River valley regions. The implications of Figure 1 are especially noteworthy for the Northeast and Mid-Atlantic regions, but it is difficult to use such regionally aggregated results for local-scale decision support.

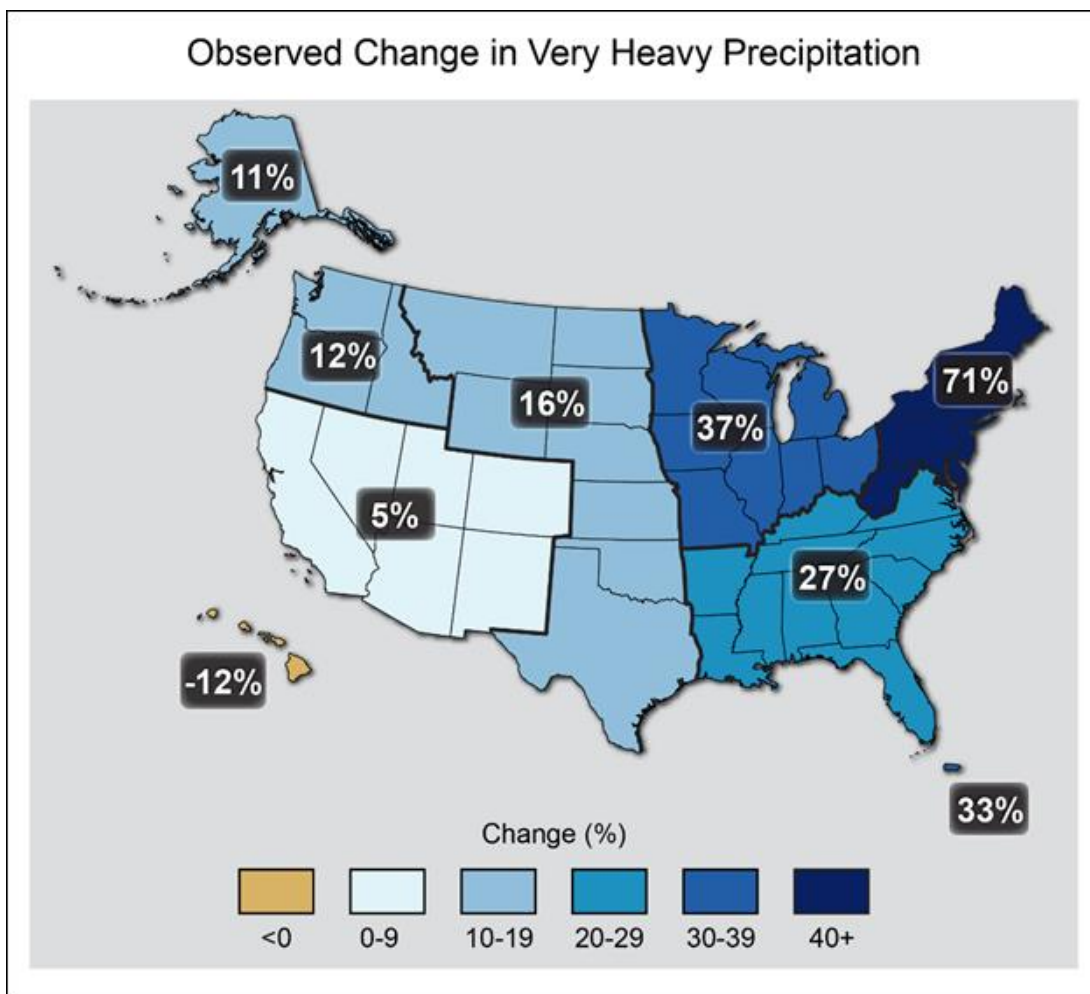


Figure 1: Observed change in very heavy precipitation events (i.e. downpours, the heaviest 1% of annual rainfall events). Source is 3rd National Climate Assessment, <http://nca2014.globalchange.gov/report/our-changing-climate/heavy-downpours-increasing>.

In this document, we perform a comprehensive investigation of heavy rainfall trends and probable maximum precipitation within the Virginia Beach (hereafter, “VB”) area. In Chapter 1, we consider only historical data and perform gage-level, local-level and regional-level analyses. Frequency and intensity changes are considered separately to increase confidence in the analysis.

In Chapter 2, we investigate future projections of heavy rainfall using relatively high-resolution simulations based on the Intergovernmental Panel on Climate Change (IPCC) Coupled Model Intercomparison Project, Phase 5 (CMIP5). CMIP5 was used to inform the IPCC’s 5th Assessment Report on expected climate change impacts across the world. Significant peer-reviewed literature has suggested that increases in heavy rainfall are likely for the VB area (Wehner, 2013; Prein et al. 2016). However, these studies were regionally-aggregated. Our goal in this study is to corroborate or provide dissenting evidence for the immediate VB area.

Chapter 3 performs a comprehensive evaluation of three heavy rainfall events that were responsible for flooding in the City of Virginia Beach during 2016. The main objective was to determine how observed rainfall amounts compared to the area’s precipitation-frequency curve for a variety of durations. A secondary objective was to compare the rainfall temporal distribution with that of the currently used design storm, the NOAA Type C storm. The final objective was to evaluate how each event compared to the region’s Probable Maximum Precipitation (PMP) estimates.

Finally, Chapter 4 provides a review of rainfall design guidance, as related to non-stationarity and future conditions. A succinct summary of existing Federal and state guidance documents is provided reviewed along with a summary of limited telephone interviews.

Our intent is to make findings as relevant as possible for engineering applications. Thus, we frequently use methods involving rainfall Annual Maximum Series (AMS), which is the root of design-rainfall analyses such as NOAA Atlas 14. Our analysis is focused almost exclusively on the 24-hour duration event, which accurately captures the extent of most flood-prone rainfall events in the area.

Conclusions from each of the Chapters are summarized at the end of the document.

CHAPTER 1: HISTORICAL ANALYSIS

Climatology

The City of Virginia Beach is located in extreme southeast Virginia, where the climate can be described as humid subtropical. Because snow represents less than 2% of VB’s yearly precipitation, “precipitation” and “rainfall” will hereafter be used interchangeably. Average annual precipitation is about 46 inches and is relatively well distributed throughout the year. Each month of the year averages at least 3 inches of rainfall, though the wettest months of the year are from June through September due to the influence of diurnal thunderstorm activity and tropical disturbances with Atlantic Ocean origin.

Analysis of heavy rainfall in the VB area reveals significant seasonality that is not reflected when considering only average statistics. The 24-hour precipitation-frequency curve for VB is shown in Figure 2, as reproduced from NOAA Atlas 14 Volume 2, Version 3 (Bonnin et al., 2006). This curve, using data through 2013, shows that five-year 24-hour rainfall is 4.7 inches (range of 4.3 to 5.2 when incorporating uncertainty), 25-year 24-hour rainfall is 7.0 inches (range of 6.3 to 7.7), and 100-year rainfall is 9.4 inches (range of 8.4 to 10.3). However, as shown in Figure 3, the chance of experiencing heavy rainfall is significantly skewed towards the June–October period. For example, the chance of experiencing a two-year 24-hour event is about 13 times higher in September as compared to April.

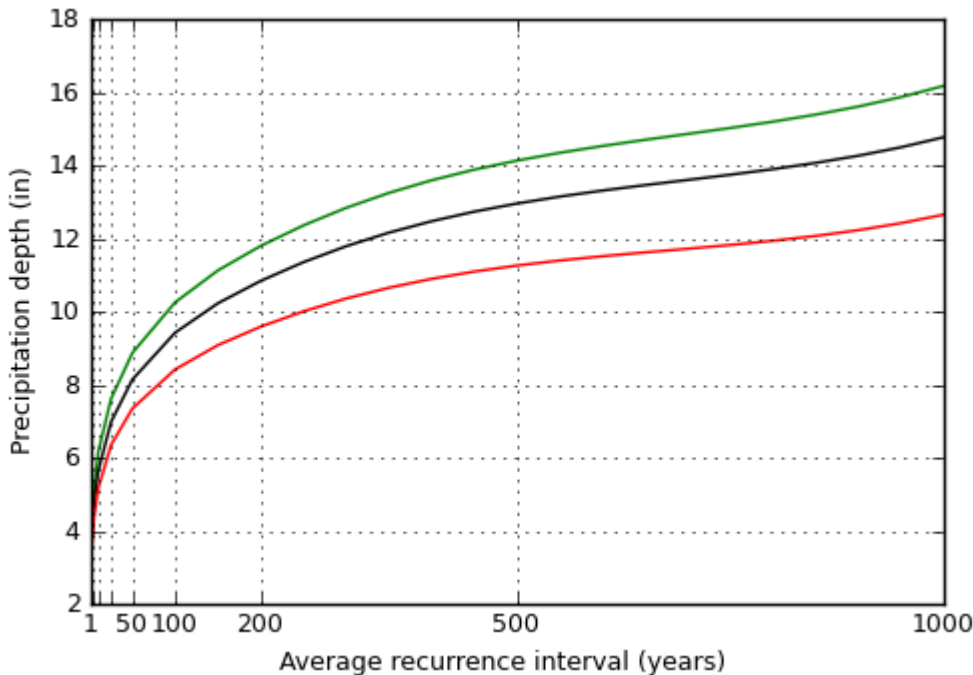


Figure 2: NOAA Atlas 14 precipitation-frequency curves for 24-hour rainfall for a location near VB. The black curve is the “most likely” estimate, while the green and red curves denote the high and low bounds using the 90% confidence level.

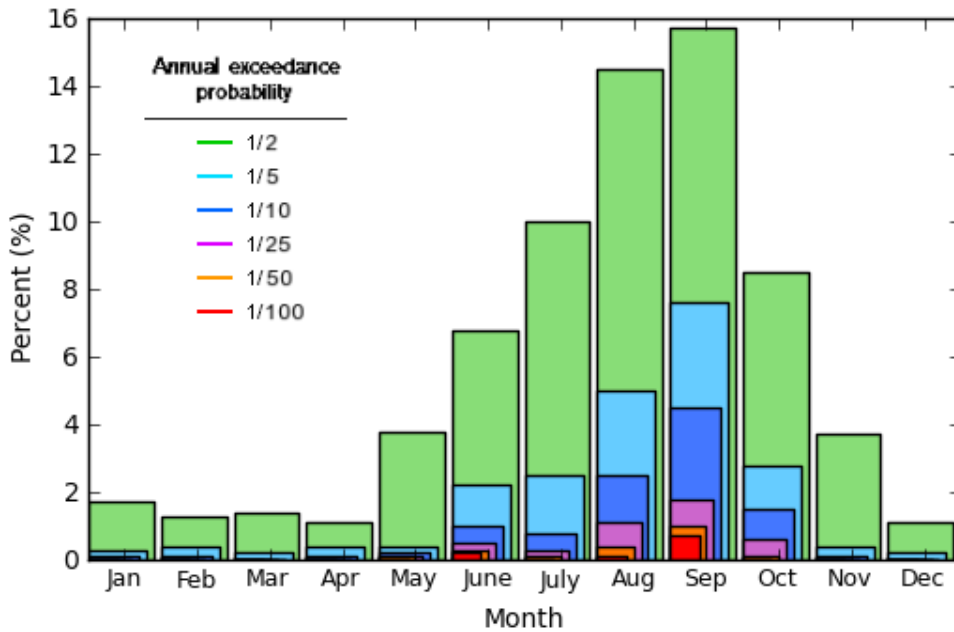


Figure 3: Seasonality analysis for 24-hour precipitation for a location near VB. The percent chance of observing an event exceeding the indicated threshold is shown for the 2-, 5-, 10-, 25- 50- and 100-year recurrence interval. Note that the late summer and fall months show the highest probabilities of occurrence.

To gain a deeper understanding of VB’s heavy rainfall climatology, we performed a meteorological analysis of each event over the past 70 years that produced at least 3.7 inches of rainfall over a 24-hour period at *either* the Norfolk or VB long-record rain gages. This value corresponds to roughly the one in two-year (50% chance) event. For each of the 53 identified events, we noted the 24-hour and 72-hour rainfall at both gages and performed two additional classifications. First, we noted whether the event was Tropical (or Extra-tropical) or Non-tropical in origin (e.g. Nor’easter or stationary front). Note that an Extra-tropical classification indicates the event had some direct connection to the Tropics, but was not officially classified as a tropical storm or hurricane at the time of influence. Second, we subjectively assessed whether the immediate VB area was under the maximum event accumulation, or “Bullseye”, of the regional rainfall field produced by the event. The Bullseye classification was meant to inform whether or not VB experienced a worst-case scenario outcome from the event. Note that each event’s worst-case scenario is dependent on the atmospheric processes available for its formation, and there is large event-to-event variability in worst-case scenarios. Results are shown in Table 1.

Of the 53 events, 17 were classified as Tropical, 5 as Extra-tropical and 31 as Non-tropical. It is worth noting that 12 of the 17 Tropical events have occurred since 1998, which equates to an average of about two events every three years. In comparison, there was a *total* of five Tropical events over the 1946-1997 period, which equates to an average of one event every ten years.

This is important because Tropical events cause higher rainfall amounts: at the Norfolk gage, the mean 24-hour amount across all Tropical events was 4.99 inches, the Extra-tropical mean was 4.31 inches and the Non-tropical mean was 3.65 inches. Furthermore, Tropical events have accounted for the five highest 24-hour accumulations at the Norfolk gage. Thus, the results in Table 1 show that one reason for apparent increase in heavy rainfall in the VB area has been due to a recent active stretch of Tropical-related events. An unanswered question raised by this analysis is whether this is due to climate change or chance. This was not investigated by the current study.

Table 1 shows another noteworthy result regarding the occurrence of “Bullseye” events: of the 53 events, 24 were identified as Bullseye hits and 29 were classified as non-Bullseye. This implies that over the period of record (1946-present) every other event was a Bullseye. However, since 2003, 11 of 13 events were classified as Bullseye hits. The significance of this is similar to the Tropical versus Non-tropical classification: at the Norfolk gage, the mean 24-hour rainfall for Bullseye events is 4.98 inches while non-Bullseye events average 3.44 inches. Thus, Table 1 implies that VB has seen an abnormally high number of Bullseye events over approximately the past 15 years, resulting in an anomalously high rate of “worst-case scenario” type outcomes that were less frequent earlier in the gage record. This has also contributed to the apparent increase in heavy rainfall intensity. There is no basis for attributing this to climate change, and a coincidence, or simple “bad-luck” explanation is alternatively proposed. Thus, overall, the meteorological analysis shown in Table 1 suggests that the increased occurrence of both Tropical and Bullseye events has unquestionably contributed to higher rainfall intensity in the past two decades, while discounting climate change as the major factor, though it is likely a secondary contributor to an increase in rainfall for any given event.

Gage-Level Stationarity Assessment

Design rainfall, such as NOAA Atlas 14, is typically developed using rain gage data. Such data is often referred to as “point” data because it measures the rainfall at a single, localized point in space (for example, a typical rain gage has a surface area of less than 1 ft²). The benefit of conducting a gage-level stationarity analysis is that data is consistent and, given a long record length such as that seen in the VB area, the gage provides many observation points from which statistical significance can be inferred.

Table 1: Summary of meteorological analysis of all 24-hour rainfall events exceeding the one in two-year recurrence interval (3.7 inches) between 1946 and 2016 using the Norfolk Airport (“Norfolk”) OR Oceana Naval Station (“Virginia Beach”) rain gage data. A double-line border is used to separate events into decades.

Event	Date	Norfolk		Virginia Beach		Origin	Bullseye
		1-day	3-day	1-day	3-day		
1	11/21/1952	3.31	4.09	4.18	5.31	Non-tropical	No
2	8/13 - 8/14, 1953	3.46	6.28	6.05	10.78	Tropical	Yes
3	8/17/1953	2.00	2.00	4.14	4.14	Non-tropical	No
4	9/27/1953	2.67	2.75	3.93	4.02	Extra-tropical	No
5	8/12/1955	4.47	4.62	3.85	4.01	Tropical	Yes
6	8/19/1957	2.97	3.22	5.09	5.29	Non-tropical	No
7	9/17/1957	1.63	1.99	5.01	5.17	Non-tropical	No
8	6/2/1959	1.47	1.59	4.80	4.83	Non-tropical	No
9	9/28/1959	6.48	6.80	2.34	2.58	Non-tropical	No
10	10/24/1959	3.71	4.19	1.75	2.03	Non-tropical	No
11	8/5/1961	4.45	4.87	0.36	0.56	Non-tropical	No
12	10/3/1962	3.30	4.12	5.97	7.27	Non-tropical	No
13	6/2/1963	5.76	7.64	3.96	5.33	Non-tropical	Yes
14	9/15/1963	4.98	5.30	2.83	3.26	Non-tropical	Yes
15	8/31 - 9/1, 1964	7.41	11.71	9.84	14.14	Tropical	Yes
16	9/13/1964	4.73	4.80	3.41	3.49	Extra-tropical	No
17	7/30/1966	3.70	3.70	3.01	3.05	Non-tropical	No
18	1/8/1967	3.74	3.80	1.55	1.56	Non-tropical	Yes
19	8/24/1967	3.81	4.76	0.05	1.25	Non-tropical	No
20	3/17/1968	2.94	3.15	4.09	4.30	Non-tropical	No
21	7/27/1969	4.72	7.07	1.95	3.29	Non-tropical	No
22	9/30/1971	3.49	6.48	3.75	6.68	Tropical	No
23	9/2/1972	1.16	1.21	4.09	4.12	Extra-tropical	No
24	7/26/1974	3.81	3.90	3.18	4.21	Non-tropical	Yes
25	7/9/1976	0.56	0.56	4.09	4.12	Non-tropical	Yes
26	9/5/1979	4.31	4.60	3.85	3.85	Tropical	Yes
27	8/15/1980	4.13	4.13	4.28	4.30	Non-tropical	Yes
28	8/12/1986	0.73	1.69	5.29	8.34	Non-tropical	No
29	7/11/1990	1.07	1.62	5.88	6.63	Non-tropical	No
30	8/24/1990	4.32	5.01	1.47	2.49	Non-tropical	No
31	4/20/1991	5.86	5.92	3.06	3.07	Non-tropical	Yes
32	6/22/1991	1.66	1.86	4.55	4.67	Non-tropical	No
33	3/2/1994	3.78	4.38	2.78	3.49	Non-tropical	No
34	2/4/1998	4.75	5.18	6.05	6.35	Non-tropical	No
35	8/27/1998	3.77	6.88	2.93	3.39	Tropical	No
36	9/15/1999	5.03	6.81	NA	NA	Tropical	Yes
37	10/17/1999	6.23	7.29	NA	NA	Tropical	Yes

Table 1, continued: Summary of meteorological analysis of all 24-hour rainfall events exceeding the one in two-year recurrence interval (3.7 inches) between 1946 and 2016 using the Norfolk Airport (“Norfolk”) OR Oceana Naval Station (“Virginia Beach”) rain gage data. A double-line border is used to separate events into decades.

Event	Date	Norfolk		Virginia Beach		Origin	Bullseye
		1-day	3-day	1-day	3-day		
38	6/16/2001	4.39	4.51	4.48	4.55	Tropical	No
39	9/16/2002	3.79	3.96	1.45	1.45	Non-tropical	No
40	10/11/2002	3.45	3.61	5.33	5.40	Tropical	No
41	9/18/2003	4.02	4.02	2.12	2.15	Tropical	Yes
42	8/14/2004	3.72	5.75	2.66	3.73	Tropical	Yes
43	6/14/2006	4.06	4.06	NA	NA	Extra-tropical	Yes
44	9/1/2006	8.93	10.22	NA	NA	Extra-tropical	Yes
45	11/12/2009	4.90	7.71	6.96	10.56	Non-tropical	Yes
46	7/29/2010	4.64	4.64	3.58	3.58	Non-tropical	No
47	9/30/2010	7.85	8.90	3.57	4.25	Tropical	Yes
48	8/27/2011	7.92	8.19	NA	NA	Tropical	Yes
49	10/28 - 10/29, 2012	3.87	6.25	4.78	9.54	Tropical	Yes
50	9/8/2014	3.05	4.78	5.13	6.66	Non-tropical	Yes
51	7/31/2016	6.98	7.55	1.41	1.85	Non-tropical	No
52	9/20 - 9/21, 2016	3.93	9.35	3.92	6.97	Tropical	Yes
53	10/8/2016	7.44	9.24	7.70	7.70	Tropical	Yes

For this analysis, we selected the Norfolk Airport rain gage (GHCN USW00013737), which contains no more than nine missing days in any given year since 1946. A secondary gage, the Diamond Springs gage (GHCN USC00442368), is located less than one mile from the Norfolk Airport gage and was used to extend the data through 1911.

Figure 4 shows the time series of the Annual Maximum Series (AMS) of daily rainfall data for the Norfolk gage, alone. The mean value is 3.6 inches, though the data is heavily skewed with a strong right tail. The 10th and 90th percentile of the AMS is 2.2 and 5.9 inches, respectively, reiterating the significant skew due to rare, but high amounts. A linear trend fit to the time series shows a statistically significant positive trend with a magnitude of about 1.98 inches per century. Visual inspection of Figure 4 also clearly indicates the presence of low-frequency variations with a period of approximately 50 years. For example, note the occurrence of multiple high peaks in the late 1950s and 1960s, followed by a relative lull in the 1980s, during which no events above five inches were observed, followed by a resurgence in the late 1990s through the present.

As the flooding threat is not restricted to the highest-intensity AMS events, we also investigate changes in rainfall frequency using the Peaks-Over-Threshold (POT) approach. Figure 5 shows the resulting time series of annual POTs using a threshold of 1.25 inches per day. This value was selected because it results in an adequate number of events per year from which statistical significance can be assessed. Later in the analysis, a POT method using accumulated event occurrence is explored for the one in two-year and one in five-year event intensity. The mean value in Figure 5 is 7.7 days per year, though a positive trend is apparent. A linear trend fit to the time series again shows a statistically significant positive trend with a magnitude of 4.3 days per century, implying a strong increase given that this is more than 50% of the mean value. This slope is significant at the 95% confidence level. Thus, the results of Figures 4 and 5 show robust increases in both the intensity and frequency of heavy rainfall at the Norfolk Airport gage since 1946.

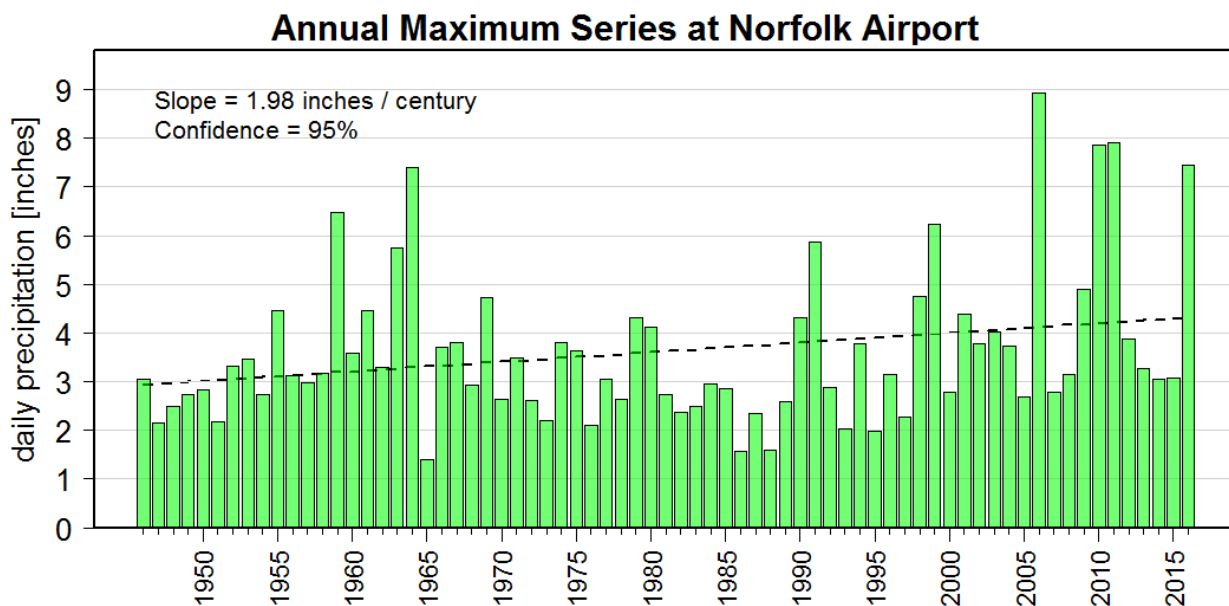


Figure 4: Annual Maximum Series of daily rainfall at the Norfolk Airport rain gage.

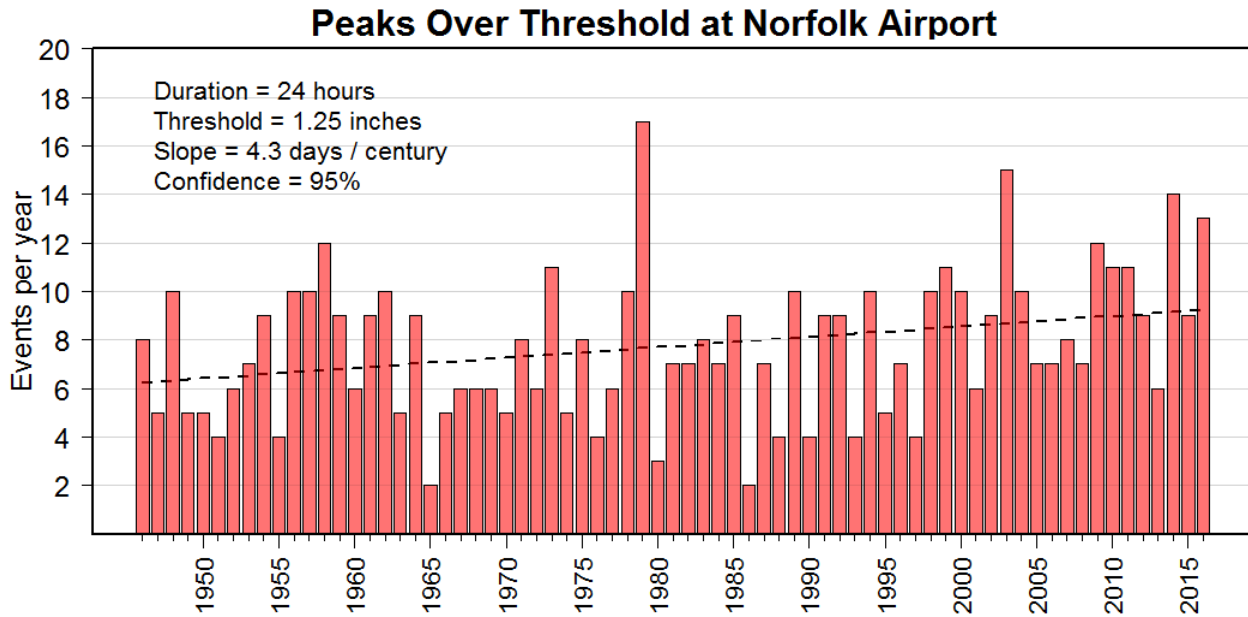


Figure 5. Same as Figure 4 except for annual daily rainfall events exceeding 1.25 inches.

Since heavy rainfall statistics can be extremely sensitive to the length of the data record, a longer record provides more confidence if a trend is detected. To extend the Norfolk Airport record length, we used the nearby Diamond Springs gage. This gage was in service from 1911 through 1980 and thus overlapped with the Norfolk Airport gage for 34 years. However, a scatter plot of AMS between the two gages (Figure 6, left panel) shows a surprising amount of spread. This was determined to be caused by a difference in the observation time at the two gages. To correct this issue, hourly data is needed, but this is not available at the Diamond Springs gage. Another method of correcting the timing issue is to use longer durations such as the 48-hour rainfall totals. As shown in the right panel of Figure 6, using the 48-hour AMS shows a near one to one relationship between the two gages and thus was used to extend the record length.

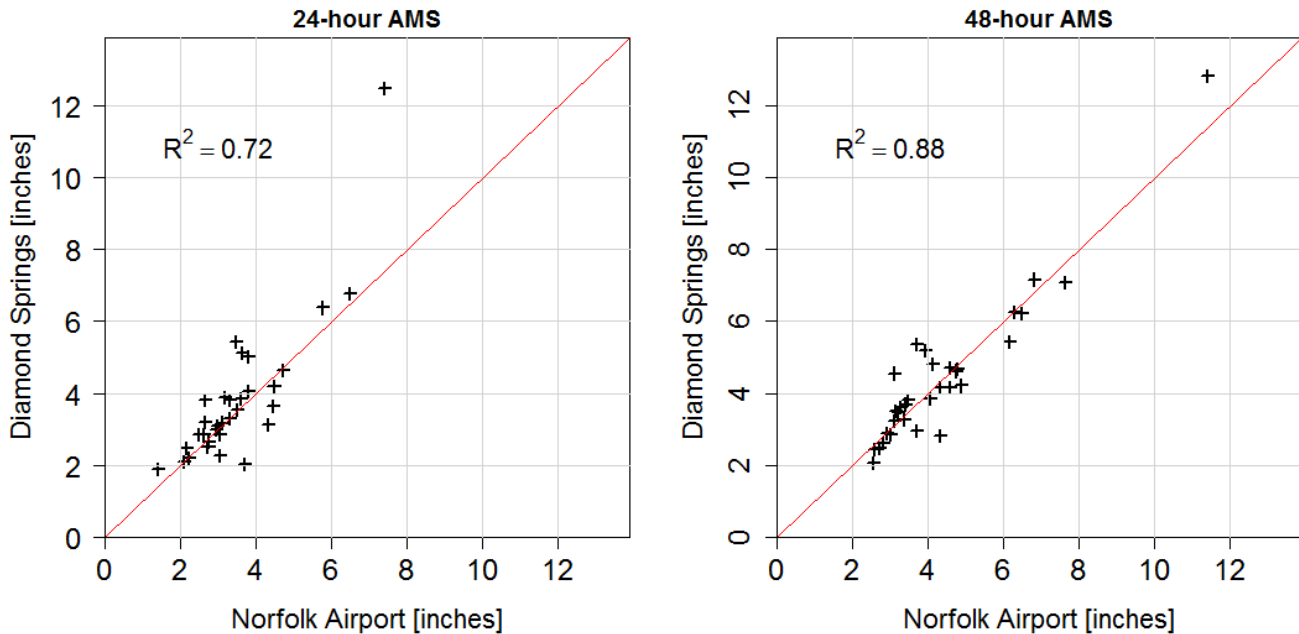


Figure 6: Scatter plot and R-squared value correlating AMS at the Diamond Springs (y-axis) and Norfolk Airport (x-axis) gages using the 24-hour (left) and 48-hour (right) durations.

Figure 7 shows the 48-hour AMS when combining the Norfolk Airport and Diamond Springs gages (hereafter, “blended” Norfolk gage). The blended record was created by first finding Diamond Springs’ AMS values, and then superseding them with the Norfolk Airport value (though the order of this operation could be switched with no effect on the final result). Although the Diamond Springs gage data is available through 1911, there were many years with insufficient record coverage (defined as ten or more missing days per year) as seen by the gaps in Figure 7. Nonetheless, the blended Norfolk record continues to show a positive trend in AMS intensity. However, the slope is now lower at 1.3 inches per century (though still statistically significant at the 95% confidence level), compared to nearly 2 inches per century in Figure 4. Thus, a comparison of Figures 4 and 7 suggests that there has been a recent acceleration in the AMS trend, a portion of which may be due to climate change. Appendix A shows that climate modeling of the historical record indicates that, at least for temperature data, an anthropogenic-forced climate began to differ from a natural climate in the mid-1980s, or about 30 years prior to the current study. Thus, of the 71 qualifying years of the Norfolk Airport AMS (Figure 4), almost 50% of the record can be expected to be influenced by climate change. Meanwhile, the Norfolk blended record, at 106 years in length, is only expected to be influenced by climate change for 30% of its observations. This would explain the weaker trend in Figure 7 compared to Figure 4, though it is essential to stress that the trend in Figure 7 is still statistically significant.

48-hr Annual Maximum Series at Norfolk [2 gage blend]

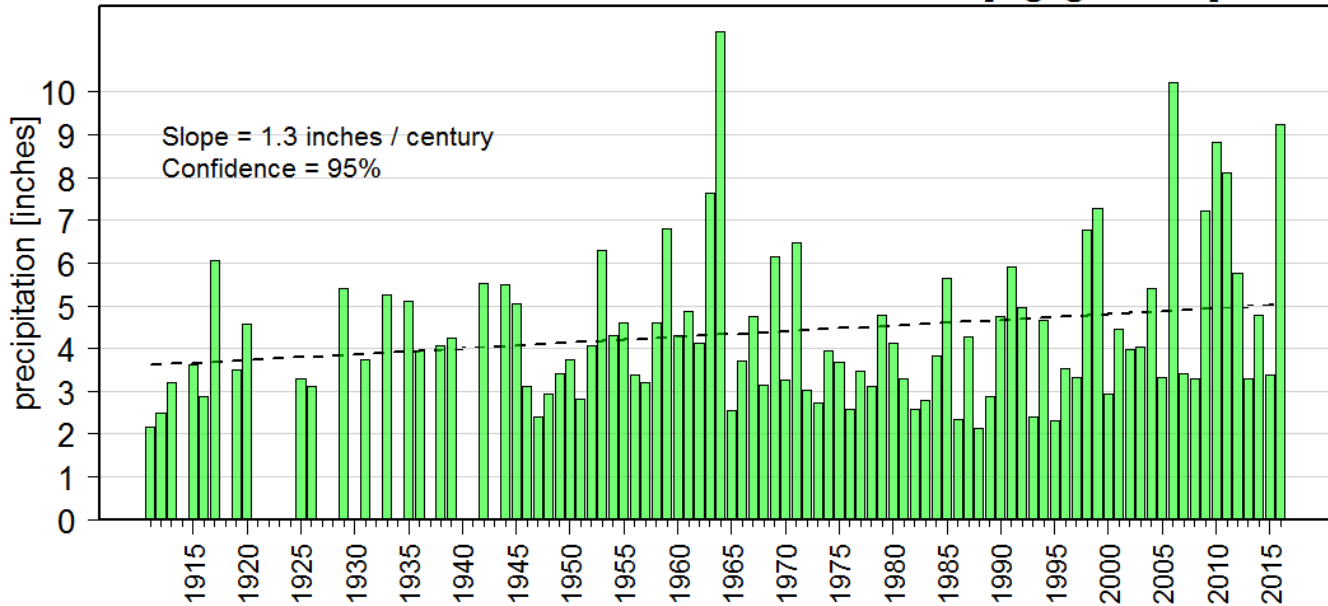


Figure 7: Trend in the 48-hour AMS at the blended Norfolk gage (combining Norfolk Airport and Diamond Springs rain gage data).

Figure 8 shows the annual POT series and trend at the blended Norfolk gage when using a 48-hour duration and a threshold of two inches. Similarly, to Figure 5, this value was used to provide an adequate number of events per year even though not all events will cause a flood risk. Additionally, as in Figure 5, a visual inspection suggests a clear upward trend, which is confirmed using a linear regression. However, the linear trend, with a magnitude of 1.9 days per century, is only significant at the 88% confidence level. Thus, when interpreting only data from the Norfolk Airport gage (Figures 4, 5), the trends in AMS and POT would appear overstated compared to a longer-term record at this location. This does not diminish the fact, however, that AMS and POT are still found to increase, though the overall significance was more robust for AMS than for POT.

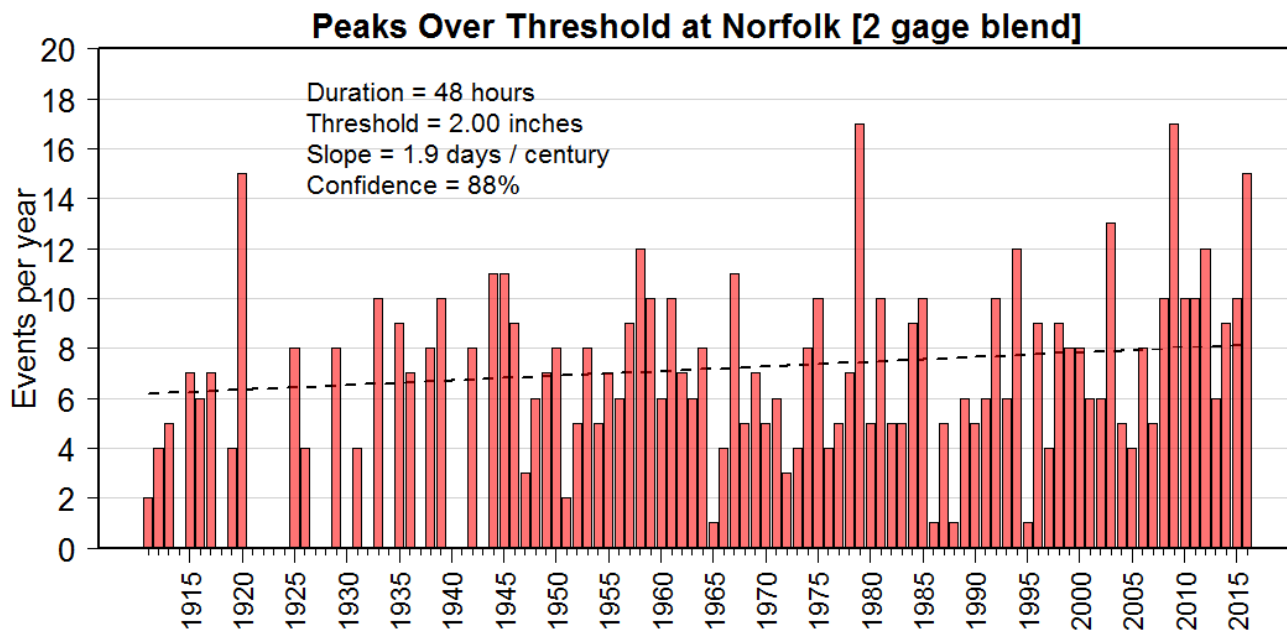


Figure 8: Same as Figure 7 except for annual 48-hour Peaks-Over-Threshold, with a threshold of two inches.

Local-Level Stationarity Assessment

The benefit of conducting gage-level stationarity analysis, as was shown in the previous section, is its simplicity in assessing results. However, a notable limitation is that a gage-level analysis does not directly inform the flood threat since flooding is more closely tied to rainfall volume versus a point amount. We have leveraged the availability of an increasing number of quality-controlled rain gage observations to briefly investigate this topic by conducting a “local-level” rainfall analysis.

Figure 9 shows the method used for the local-level analysis. First, a radius of interest centered on VB was selected. A radius of 60 miles was used in order to capture all storms that either hit VB or were in very close proximity. Next, we accessed all available quality-controlled rain gages within the radius of interest. This included data from Cooperative Observer Program (COOP), Remote Automatic Weather Systems (RAWS), Weather-Bureau-Army-Navy (WBAN) and Community Collaborative Rain, Hail and Snow Network (CoCoRaHS) observational networks. Finally, we calculated the AMS value of daily rainfall across *all gages* regardless of missing data. In addition to tracking the AMS, we also noted the number of contributing gages for each year’s AMS, as well as the aggregate area covered by gages, which we termed “coverage area”. To calculate the latter statistic, we subjectively gave each gage a five-mile radius of influence and then tracked the union of all contributing gages’ coverage areas. This measure was meant mainly for informational purposes. Figure 9 shows the overlapping coverage area

for all available gages during 2015, when the gage count was highest. Figure 10 shows the results of the analysis.

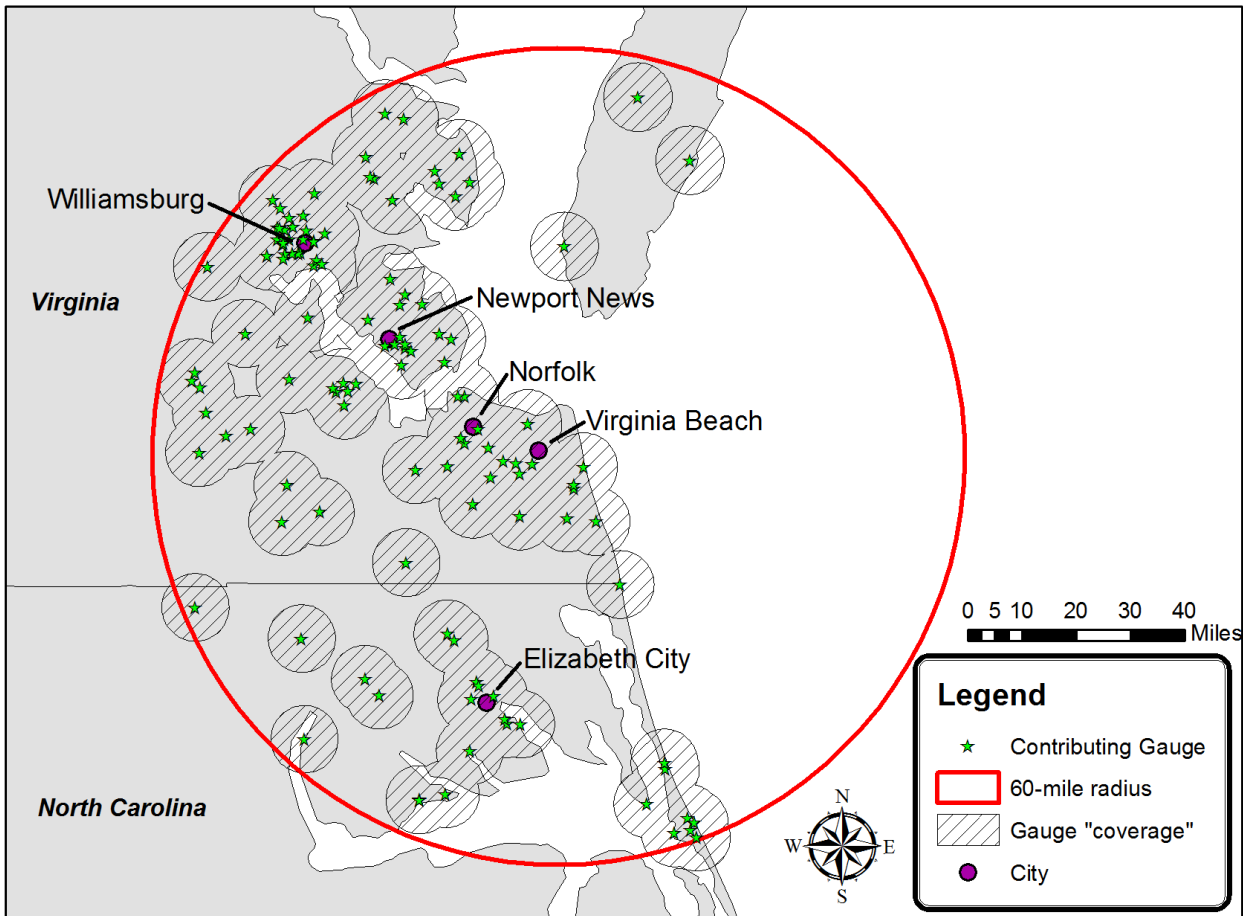


Figure 9: Method used for conducting a “local-level” rainfall analysis. This shows the qualifying gages during 2015, along with their “coverage” area.

In Figure 10a, we see that by including all gages within the 60-mile VB radius of interest, we can now extend the 24-hour AMS record back through 1869 (though as Figure 10b shows, only 1 gage is available from 1869 through 1892 for this analysis). The most notable result from Figure 10a is that there has been a tremendous increase in 24-hour AMS at the local level. A trend line fit to this analysis shows a positive slope exceeding 3.0 inches per century, and is statistically significant at the 99% confidence level. However, a major complication in fitting a simple trend line is that there has also been a large build-up of quality controlled stations. In other words, heavy rainfall events have become better sampled, which alone could cause an increase in values regardless of whether or not other factors such as climate change are present.

Figure 10b shows three main time periods at which the gage network sharply increased. First, in 1893, four rain gages were added to the original gage providing a total of five gages. Next, starting around 1940, the gage count again increased from about six to more than 20 by 1950. A notable increase in the AMS intensity was associated with this, simply from better monitoring of the area. The final, and most dramatic increase in gage count started around 2000 when contributing gages increased from about 15 to over 100 in 2015 [see Figure 9 for 2015 gage “coverage area”]. This was due to the expansion of the CoCoRaHS network. Another notable increase in AMS in the area has been associated with this increase. For example, of eight AMS values exceeding ten inches since 1869, seven have occurred since the “CoCoRaHS-era” started in the late 1990s.

As Figure 10c shows, there has been an associated increase in the collective gage “coverage area. Figure 9 shows that in 2015, the coverage area, which is the union of each gage’s assigned five-mile radius, now covers over 70% of the land area with the 60-mile radius of interest. As more gages are added, the coverage area will eventually approach 100%, slowing the rate of AMS increases due to gage inflation. However, it is very difficult to speculate when this may happen or what portion of the three-inch per century trend in Figure 10a arises due to gage inflation. This would require the partitioning of each gage’s contribution, which is difficult to ascertain due to various gage data lengths.

While the 60-mile radius used in Figure 10a may be too wide to be of direct influence for VB, repeated analyses with radiuses of 25 miles and 15 miles (by the time we limit the radius of interest to 15 miles, we are now at scale of the Lynnhaven watershed, which is of direct interest to VB), displayed similar results: that inclusion of all gages shows higher trends than assessments that only consider the Norfolk Airport and Diamond Springs gages. Thus, the salient take-away from Figure 10 is that when expanding the AMS analysis outside of the standard protocol of using one rain gage, rainfall recurrence statistics rapidly change. Stated differently, what is termed a 100-year at the Norfolk Airport gage becomes a 1 in 50-year event for a 15-mile radius of interest, and 1 in 35-year event for a 60-mile radius of interest. It is very likely that the factors driving the increasing trend in Figure 10a include both gage inflation and climate change. Although we cannot separate the two, both inform the flood risk in the VB region, and are thus important for understanding how design rainfall standards may need to be adjusted.

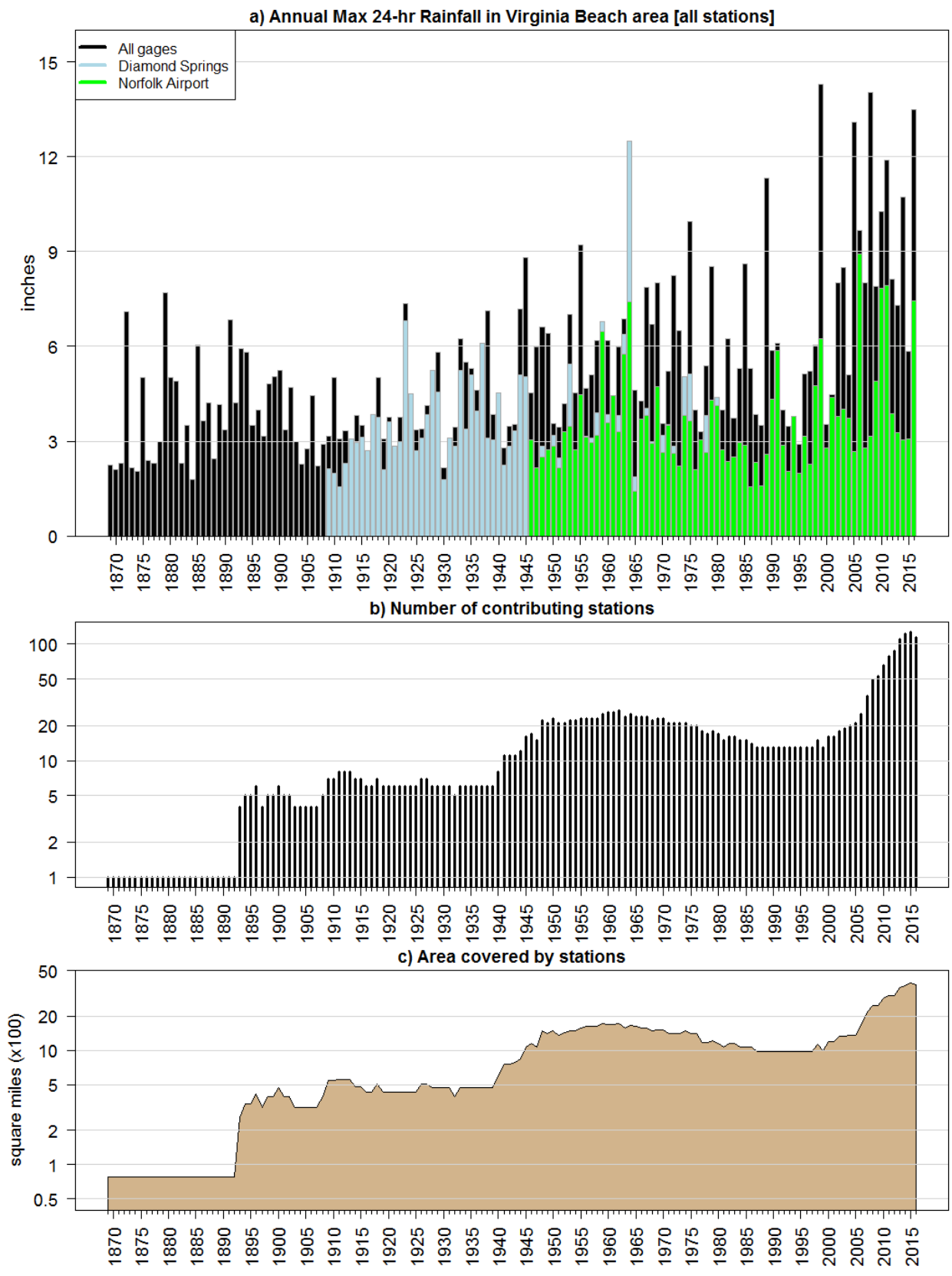


Figure 10: Results of local-level rainfall analysis.

Regional-Level Stationarity Assessment

The chief limitation of the local-scale analysis is that many of the gages can be simultaneously impacted by the same storm, thus causing correlation among gages to become an obstacle when assessing the significance of heavy rainfall trends. To overcome this issue, we further expanded the analysis to a “Regional-Level.” We subjectively defined such a region, hereafter, the “VB Climate Region,” as an area in which heavy rainfall statistics are broadly consistent with those of VB. One way to infer the spatial extent of such an area is to look at the regional variations in extreme precipitation intensities. Figure 11 shows the variation in the 100-year 24-hour (100Y-24H) event, a commonly used event for design and planning purposes. For VB, this value is 9.4 inches, with a range of 8.4 to 10.3 inches when accounting for uncertainty at the 90% confidence level (Bonnin et al. 2006). On a regional-level, it is seen that amounts of eight- inches or greater parallel the entire eastern Atlantic seaboard from central Florida through Massachusetts. This is likely due to the fact that the entire region is prone to land falling Atlantic tropical cyclones that recurve along the US Atlantic coast and follow various routes north and northeastward. This was already confirmed when looking at

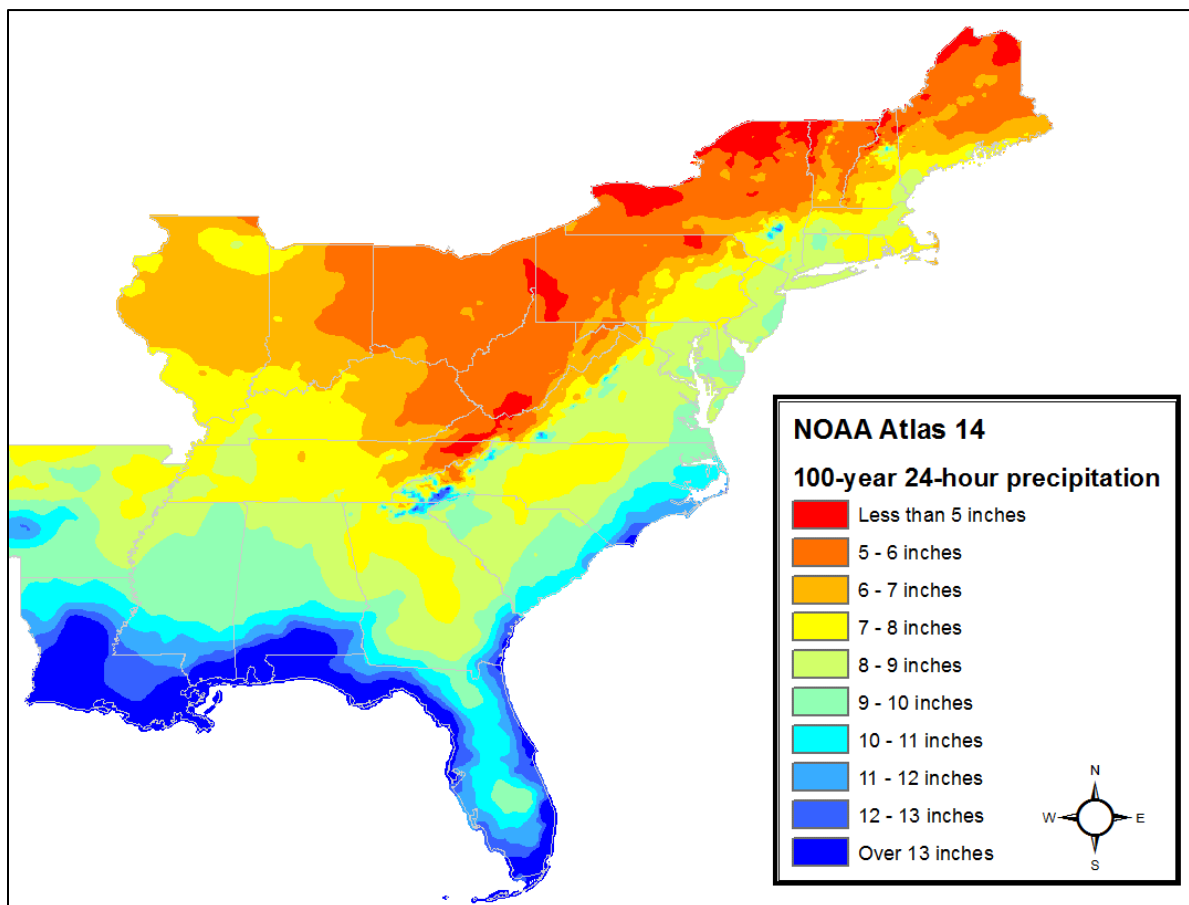


Figure 11: Estimates of 100-year 24-hour precipitation across the eastern United States.

the seasonality of heavy rainfall events in VB (Figure 3). Note that the distinct maximum during the late summer and fall months (Figure 3) is consistent with the climatology of Atlantic tropical cyclone activity. A simple way to capture these areas with a common climate is to include all rain gages within about 250 km (156 miles) of the Atlantic coast line. Other pockets of eight-inch or greater 100Y-24H magnitudes are seen farther inland, but this is likely due to enhancement from topographic features such as the Blue Ridge Mountains. Such processes are not relevant for VB heavy rainfall events and thus, these regions are not included in the analysis. Note that the Regional-Level analysis differs from the Local-Level analysis by using only long-record gages, which can better inform climate change-related impacts.

We accessed daily rainfall records from gages belonging to the GHCN. Gages were selected based on the following criteria:

- Located within VB “climate region” – roughly 250 km (156 miles) from Atlantic Ocean coastline;
- Years with more than nine days of missing data were excluded;
- The last qualifying year was 2007 or later (see Appendix A); and
- At least 60 qualifying years of data.

The criteria above yielded 175 qualifying gages as shown in Figure 12.

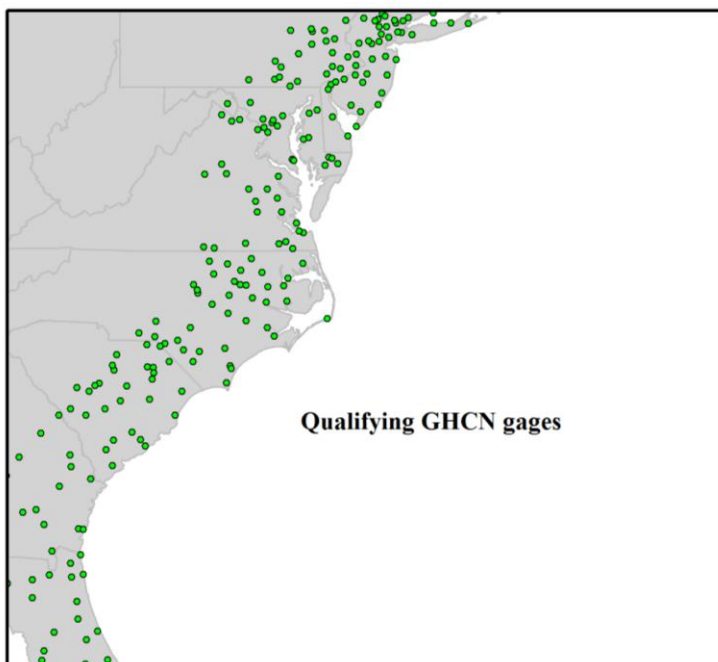


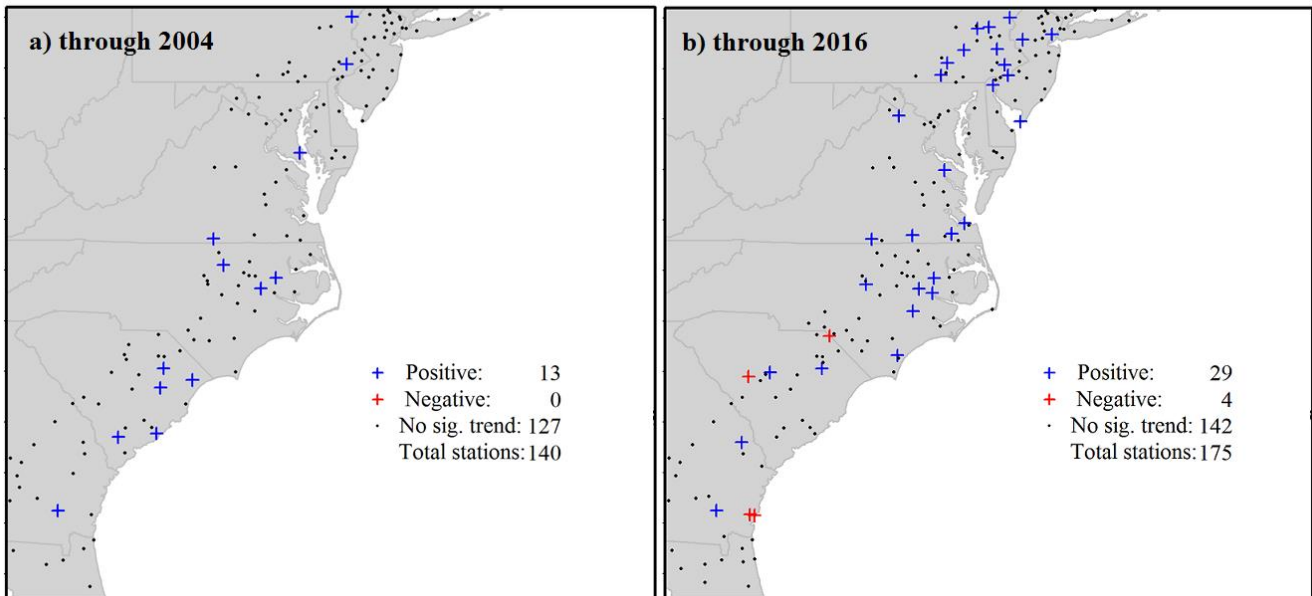
Figure 12: A total of 175 qualifying, long-record GHCN gages were used for the historical analysis.

In a similar approach to the gage-level analysis, we investigated heavy rainfall trends using three tests:

1. Trends in Annual Maximum Series to investigate changes in *intensity* – similar to the gage-level analysis presented earlier, but instead of showing the time series at each gage, we simply noted whether the trend was statistically significant (positive and negative trends were characterized separately) at the 95% confidence level. Statistical significance is based on calculating the Spearman correlation between the year and the AMS. The Spearman method was preferred over the Pearson method because the former is less sensitive to very rare but extreme events that can strongly affect the Pearson correlation. Trends are considered significant if they exceed the 95% confidence level.
2. Trends in Peaks-Over-Threshold using the same 24-hour duration and threshold of 1.25 inches per day. Similar to (1), we were only interested in whether the trend is significant at the 95% confidence level. A similar Spearman correlation test as in (1) is used to calculate significance.
3. Changes in the 99th percentile of the rainy-day distribution. This was assessed by finding the 99th percentile over the 1985-2015 period and finding the percent change from the 99th percentile over the 1954-1984 time period. For additional perspective, we also tabulated this percent change for the 70th percentile (corresponding to a light/moderate rainfall event), which allowed us to determine whether the entire rainfall distribution is changing, or just a portion of it. For example, peer-reviewed literature has suggested that heavy precipitation events are projected to be more sensitive to climate change than light and moderate events (e.g. Prein et al., 2016).

AMS values are increasing across the region, indicating non-stationarity well beyond a level allowed simply by chance, as illustrated by Figure 13. Figure 13b shows the trend in the daily AMS using qualifying gages and data through 2016. The AMS measures the highest daily rainfall observed during the calendar year. Of 175 qualifying stations, 33 stations (19%) show significant trends. Using the 95% significance level, we would only expect 18 stations to show significant trends, simply by chance. More importantly, of the 33 stations with a significant trend, 29 show positive trends. Again, by chance, we would only expect nine stations to show positive trends. Interestingly, the Figure 13a shows the analogous AMS trend, but restricted to data through 2004. In that case, only 13 of 140 qualifying gages show trends (all 13 being

Annual Maximum Series



Peaks Over Threshold

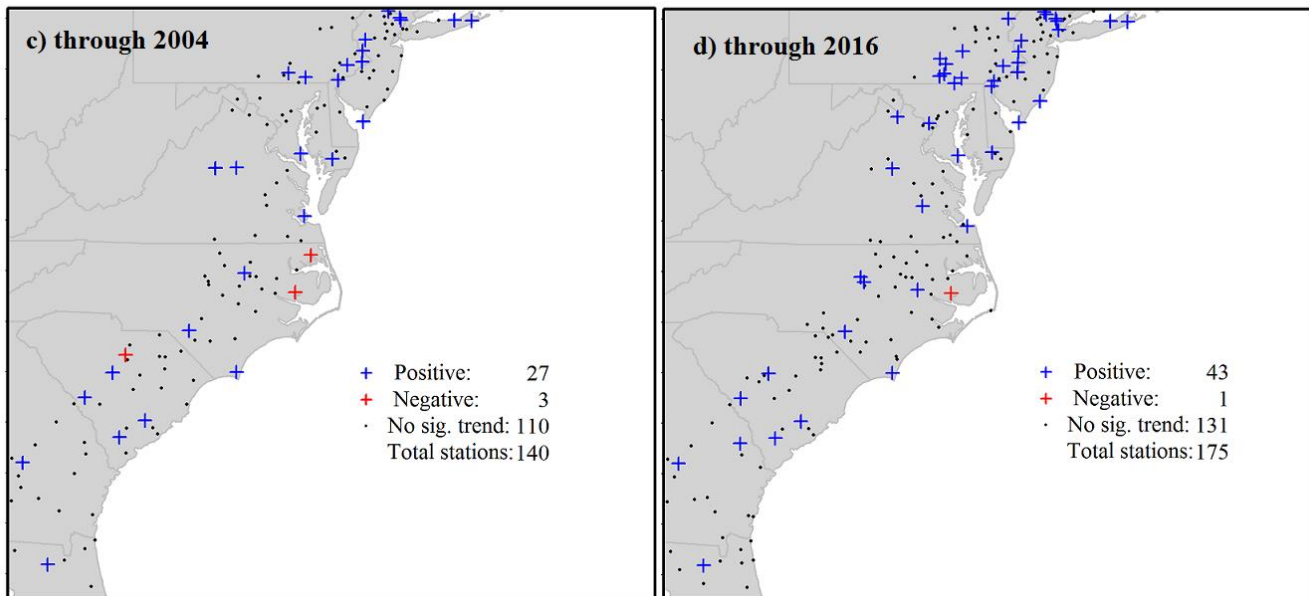


Figure 13: Trends in Annual Maximum Series (a and b) and Peaks Over Threshold (c and d). Panels (a) and (c) restrict data to 2004, while panels (b) and (d) use values through 2016. Peaks-Over-Threshold time series are calculated using number of annual days exceeding 1.25 inches at each gage. The legend shows the number of statistically significant trends at the 95% confidence level.

positive). Although this is still a statistically significant result, the non-stationarity signal is much weaker through 2004 compared to 2016. This may be due to the increasing effect of climate change given that 2016 contains a longer portion of the record that is affected by global warming (see Appendix A). This result supports the need for routine updates to rainfall design guidance in order to account for such changes.

To infer about non-stationarity regarding heavy rainfall *frequency*, Figure 13 panels (c) and (d) show the analogous result of the Peaks-Over-Threshold trend test. Results are similar to the AMS trends, though with an even stronger signal indicating the presence of non-stationarity. Of 175 qualifying gages, 44 (25%) show a statistically significant trend with 43 showing a *positive* trend, which is higher than can be expected by chance alone. Figure 13c shows the result of limiting the data record to 2004 for the POT analysis, in which case 27 of 140 (19%) qualifying gages show statistically significant positive trends. Although the impact of a shorter record is not quite as stark for the POT as it is for the AMS, there is nevertheless a significant increase in the number of gages experiencing positive trends.

Collectively, Figures 13 shows that heavy rainfall frequency and intensity are increasing broadly across the Mid-Atlantic and Northeast states, which is a more robust conclusion than if only one of these measures were true. Furthermore, this regional analysis corroborates the gage-level and local-level analyses presented earlier, implying that the changes are not strictly limited to the VB region. Climate change is expected to affect heavy precipitation across the eastern United States in the future, and the results presented thus far suggest that this is likely already the case.

Figure 14 shows the change in the distribution of rainy day rainfall on a regional level. The 99th and 70th percentiles were used to capture heavy rainfall and light/moderate rainfall, respectively. At Norfolk, these percentiles correspond to a 24-hour accumulation of about 2.7 and 0.3 inches, respectively. Figure 14a shows the percent change in the 99th percentile. This analysis continues to show strong non-stationarity, with many more gages experiencing an increase in the 99th percentile. Of the 175 qualifying gages, 73 (42%) show an increase in the 99th percentile intensity with 52 showing substantial increases of 15% of greater. This is much greater than the 27 (15%) gages that show decreases in the 99th percentile. A particularly interesting result is found in Figure 14b, which assesses the percent change in the 70th percentile of daily rainfall (measuring days with light rainfall intensity). In this case, there are about as many gages seeing increases as decreases. Similar results are found when using the 50th, 60th and 80th percentiles. Collectively, Figure 14 implies that while the higher end rainfall events are getting wetter, this does not apply for the rest of the distribution. This result has also

been hypothesized in literature as an impact of climate change on precipitation (e.g. Prein et al. 2016).

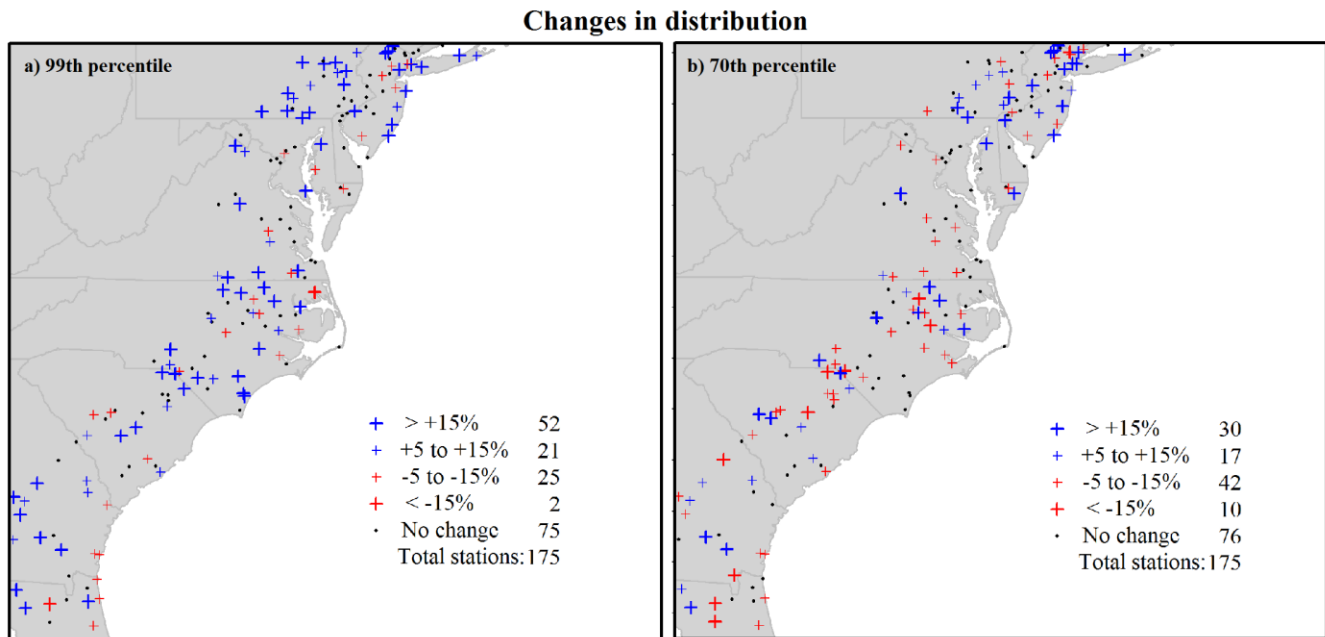


Figure 14: Regional analysis of changes in the (a) 99th and (b) 70th percentile of rainy day (i.e. dry days are excluded) rainfall. At Norfolk, the 99th percentile is about 2.7 inches per day and is representative of heavy rainfall events, while the 70th percentile is about 0.3 inches per day and is representative of light rainfall events. The legend provides a summary of the number of gages that fall in each category.

Regarding Figures 13 and 14, it is important to note that even though not all gages show a statistically significant increase, this does not negate the argument for non-stationarity. Heavy rainfall events are rare, implying that their statistics can be volatile, particularly for shorter periods of time. The regional approach used here is essential to combating the low sample size issue by including more non-correlated events across similar climate regions. However, if climate change is indeed playing a major role in driving an increase in heavy rainfall frequency, we would expect to see a continued increase in the number of gages with statistically significant findings.

CHAPTER 2: FUTURE PROJECTION

Overview

To investigate future projections of heavy rainfall events in the VB region, we used data from the IPCC's CMIP5 modeling experiments. However, using raw Global Climate Model (GCM) data would be insufficient for informing regional and local-scale rainfall due to the coarse resolution of the data (Hayhoe, 2010). Thus, we used output from the North American Coordinated Regional Modeling Experiment (NA-CORDEX; Castro et al. 2015). NA-CORDEX is a set of medium- to high-resolution regional climate model (RCM) simulations that use boundary conditions from the CMIP5 GCMs. NA-CORDEX simulations were accessed for both RCP4.5 (medium emission) and RCP8.5 (high emission) scenarios. Two analyses were completed. An initial analysis used only simulations based on the RCP8.5 scenario. The rationale for this was that if a strong signal was found for RCP8.5, it may warrant consideration of other scenarios. On the contrary, assuming a linear sensitivity of precipitation to climate change, if no significant changes were found for RCP8.5, then it is unlikely that other scenarios would show significant changes either.

A strong increase in heavy precipitation was indeed found for the RCP8.5 scenario. Thus, a secondary analysis was completed to incorporate the RCP4.5 scenario. Figure 15 shows that the RCP4.5 scenario implies about half the amount of radiative forcing (and roughly speaking, temperature increase) as RCP8.5, though this ratio decreases slightly towards the end of the 21st century. One notable complication between the initial and secondary analysis is that the former was done using higher resolution (11 km; 7 mi) model output whereas the latter used medium resolution (44 km; 28 km) output because no higher resolutions simulations were available. The important implication is that the secondary analysis had to re-create the RCP8.5 analysis to test for consistency between the different model resolutions. Below, each analysis is described separately, followed by a discussion comparing results from both analyses.

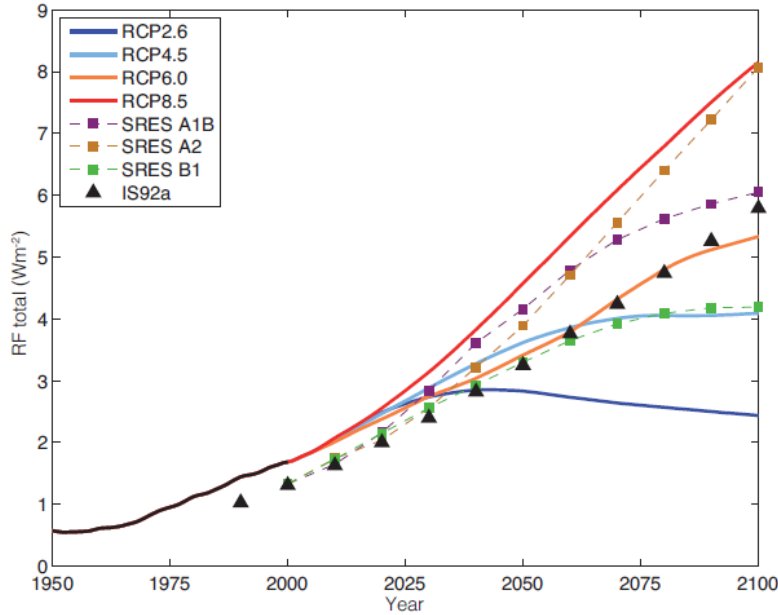


Figure 15: Historical and projected total anthropogenic RF ($W m^{-2}$) relative to preindustrial (about 1765) between 1950 and 2100. Source: Reproduced from Cubasch et al. (2013), their Figure 1.15.

RCP8.5 Analysis (11 km model resolution)

Table 2 shows the four RCMs accessed for this analysis. Each simulation had a horizontal resolution of about 11 km, which is roughly an order of magnitude higher than the Global Climate Models (GCMs) contributing to the CMIP experiment. This allows for a substantially more realistic representation of heavy precipitation processes across the VB region.

Table 2: NA-CORDEX experiments used for this analysis. All simulations were conducted using 11km resolution modeling and RCP8.5 scenario boundary conditions.

Modeling Agency Responsible for Global Climate Model	Global Climate Model (Boundary)	Regional Climate Model
Canadian Centre for Climate Modeling and Analysis (Canada)	CanESM2	CanRCM4
Geophysical Fluid Dynamics Lab (United States)	GFDL-ESM2M	RegCM4
Geophysical Fluid Dynamics Lab (United States)	GFDL-ESM2M	WRF
Met Office Hadley Centre (United Kingdom)	HadGEM2-ESM	RegCM4

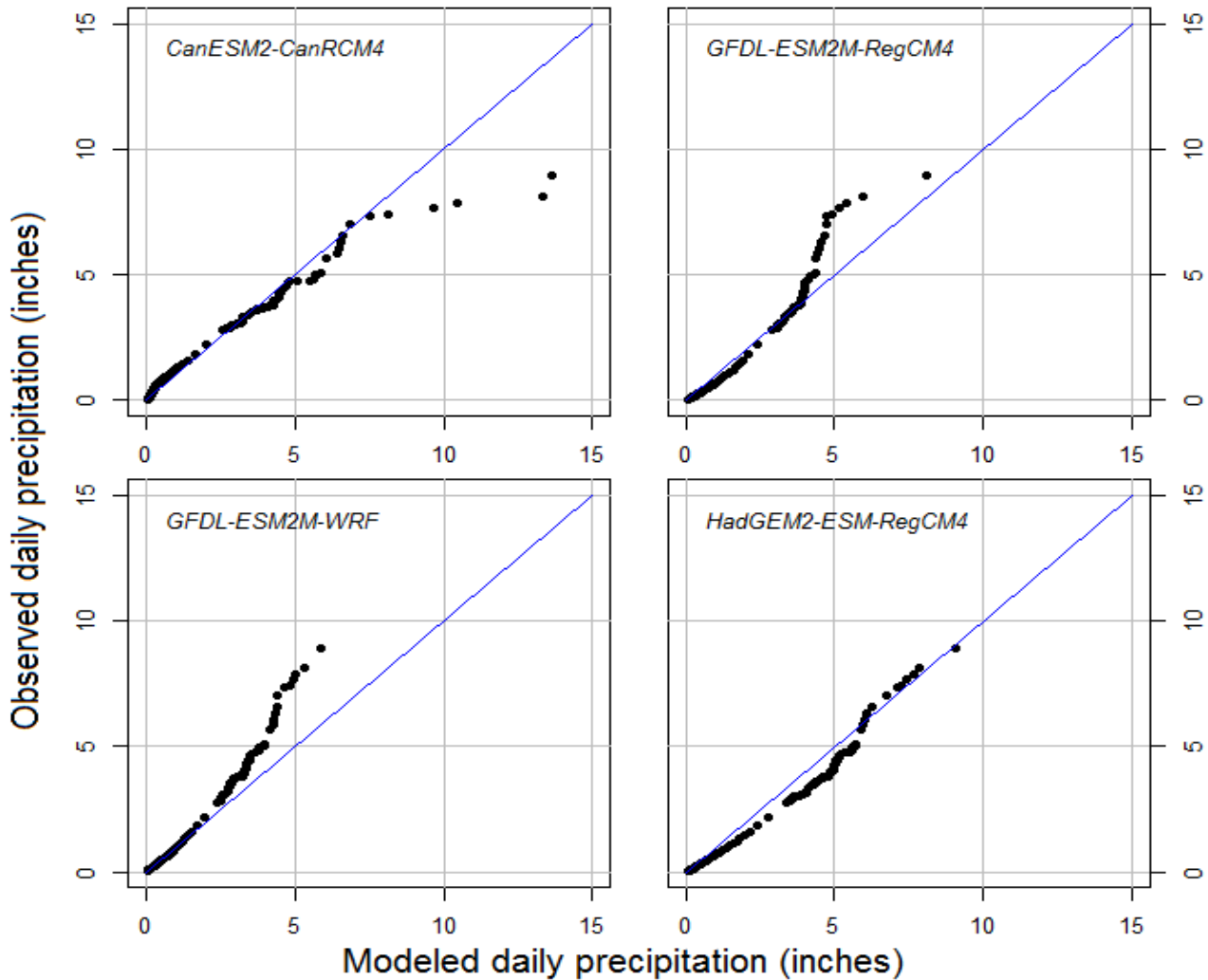


Figure 16: Quantile-quantile maps comparing observed daily precipitation of historical 11-km model simulations.

We accessed daily model output of precipitation over the 1950-2100 period. The 1950-2005 period was termed a “historical hindcast” where observed greenhouse gas forcing was used, whereas the 2006-2100 period was forced by RCP8.5 emissions. The first step to assessing future rainfall was to compare model climatology with the Norfolk gage over the historical period. Figure 16 shows that three of the four models contained either wet or dry biases compared to observations, while the HadGEM2-ESM-RegCM4 model was nearly unbiased throughout the period of record. We used Figure 16 to perform a bias correction through quantile mapping (Themeßl et al. 2011). For this procedure, the model daily rainfall amount is first converted into a quantile (quantile increment was 0.005) and the mapped to its analogous quantile using the observed Norfolk rain gage data. Note that this both corrects the precipitation amount and adjusts the wet and dry days to match the Norfolk climatology.

In order to determine future rainfall amounts, the raw model data for the 2006-2100 period was corrected using the same quantile mapping transfer function. Thus, **the key assumption is that the future quantile-quantile relationship is identical to the past** (Themeßl et al. 2011). However, in situations where future modeled rainfall exceeded the highest value over the historical modeled period, the quantile-quantile ratio of the highest historical modeled value was applied. In practice, this was only noted to happen on, at most, ten different future days for any given model simulation.

After bias-correcting the model data, we investigated two properties of model simulated heavy rainfall: its frequency using the Peaks-Over-Threshold approach, and its intensity using the Annual Maximum Series. A notable end-result from the latter analysis was the creation of Precipitation-Frequency (P-F) curves for the VB region. The bias correction procedure allowed our projected P-F curves to be directly comparable to current (NOAA Atlas 14) guidance for an easy interpretation of the impact of climate change on design rainfall. Bias corrected Annual Maximum Series from each model can be found in Appendix D.

Peaks-Over-Threshold (POTs)

Figures 17 and 18 show the results of the POT analysis of future model projections for the 24-hour duration, using thresholds of a one in two-year (3.7 inches) and one in five-year (4.7 inches) event, respectively, as inferred from the NOAA Atlas 14 guidance for Norfolk (see Figure 2). This presentation is slightly different from the earlier presented results because it does not show annual totals, but instead a running total of all events. Note that, in an effort to focus on only flood-prone events, the thresholds considered here are higher than the 1.25 inches shown in Figure 5. However, similar results were seen for a variety of thresholds including 1.25 inches. We refer to the slope of the lines in Figures 17 and 18 as the POT “hit rate” because it signifies how many events occur over a given period of time. Roughly speaking, we expect a hit rate of about 0.5 per year for a one in two-year event and 0.2 per year for a one in five-year event. However, due to the significant variability in occurrence, there can be long stretches where the hit rate appears to vary significantly from its expected value. In practice, this can be particularly striking for less frequent events. For example, note that in Figure 18, the Norfolk Airport gage from the mid-1960s to the early 1990s does not indicate a single precipitation event that exceeded the 24-hour one in five-year threshold.

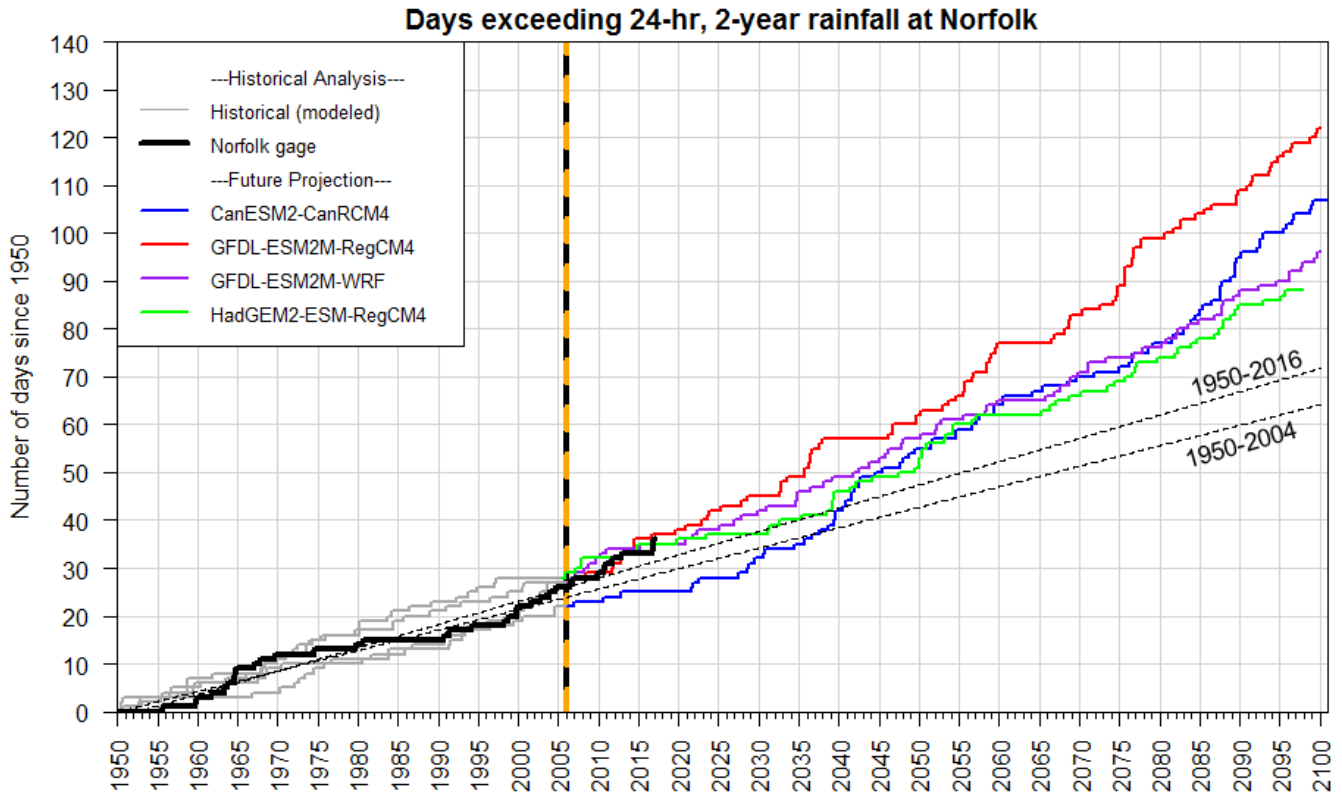


Figure 17: Accumulation of POT exceeding the 24-hour two-year rainfall (3.7 inches).

There are several important findings in Figure 17 and 18. First, note that the historical modeled POT accumulations are consistent with those observed at the Norfolk gage. This shows that the bias correction technique was effective and that the model-simulated heavy rainfall frequency matches the observed climatology. Note in Figure 17 that through 2005, there were about 29 total one in two-year events, which is close to the expected value for that 55-year period of record. Similar results are seen in Figure 18 through 2005, the observed tally at Norfolk was similar to modeled historical results, despite the prolonged stretch of non-occurrence during the 1965-1990 period.

Another important result in Figures 17 and 18 is that the observed slope, or hit rate, of POT occurrence has increased when comparing the 1950-2004 period with the 1950-2016 period. This is similar to what was observed regionally in Figure 13 (c and d), except with a specific focus on the Norfolk Airport gage. Thus, it appears that climate change is already increasing heavy rainfall occurrence in the VB area.

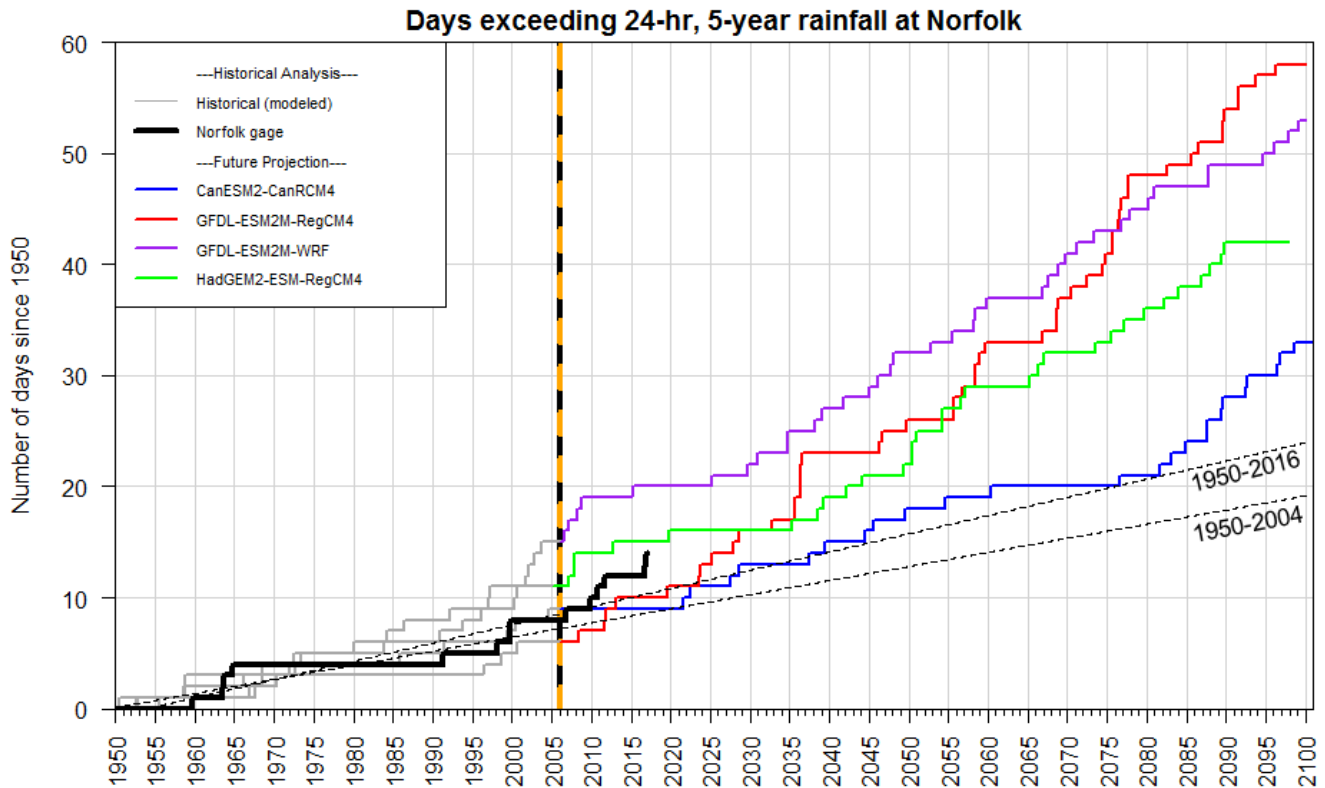


Figure 18: Same as Figure 17 except for 24-hour, five-year rainfall.

The main goal in Figures 17 and 18 is to ascertain how *future* POT hit rates will behave. Both figures show robust increases in the number of one in two- and one in five-year intensity events, suggesting a continuation or acceleration of recently observed increases in POT. Although significant variability is found across the four models, all show hit rates above the 1950-2016 level.

Table 3 presents a summary of Figures 17 and 18. The two-year event hit rate is expected to increase from a present-day model average value of about 4.6 days per decade (1950-2005 observed value is 4.3) to 8.8 by 2045 and 9.0 by 2075. Some uncertainty is seen with these estimates, as several models show robust increases by 2045 with slower increases, or even steady rates, thereafter. However, this is attributed to the variability in heavy rainfall statistics, and it is argued that the four-model average, which shows an increase from 2045 to 2075, is more meaningful. Regarding the five-year rainfall hit rate, strong increases are projected from a present-day model average value of about 1.6 (1950-2005 observed value is 1.2) to 4.3 in 2045 and 4.7 in 2075. Again, there is some uncertainty around these numbers, but all models point to increased POT hit rates in the future.

Table 3: Peaks-Over-Threshold accumulation, or “hit”, rate of days exceeding two-year (3.7 inches) and five-year (4.7 inches) using the Norfolk Airport gage compared to the bias corrected model data, and four model average. Units are number of days per decade.

Data type	2-year rainfall hit rate			5-year rainfall hit rate		
	Historical	2045	2075	Historical	2045	2075
Norfolk gage	4.3	---	---	1.2	---	---
Can-ESM2-CanRCM4	3.4	10.8	9.7	1.4	2.8	2.5
GFDL-ESM2M-RegCM4	5.0	9.1	12.1	0.7	5.6	7.7
GFDL-ESM2M-WRF	4.5	7.5	7.5	2.3	4.6	4.6
HadGEM2-ESM-RegCM4	5.7	7.9	6.8	2.2	4.1	3.9
Model Average	4.6	8.8	9.0	1.6	4.3	4.7

Precipitation-Frequency Curve

NOAA Atlas 14 uses a Generalized Extreme Value (GEV) distribution for fitting the Precipitation-Frequency (hereafter, P-F) curve for the VB region (see Table 4.5.1 in Bonnin et al. 2006). Figure 19 compares the fit of historical modeled AMS (with the 90% uncertainty band) to the Norfolk Annual Maximum Series (AMS) of the daily precipitation data. The GEV captures the essence of the empirical AMS, though a deviation is seen for events in the 8 to 25-year return period range. We also tested the Pearson Type 3, Generalized Logistic and Generalized Normal distributions and found that the GEV provides as good of a fit as any of the other three; thus, we found no reason to deviate from the GEV, especially given its use in NOAA Atlas 14. The main point from Figure 19 is that historical modeled data can be used interchangeably with the observed P-F curve, and thus lends confidence to preparing a projected P-F curve using modeled future conditions.

Projected P-F curves were developed for the mid-term (centered on 2045) and long-term (centered on 2075) periods. Each P-F curve was calculated using a 40-year window of data around the centered data. In other words, the 2045 curve was calculated using 2026-2065 data, and the 2075 curve was calculated using 2056-2095 data. Due to the bias correction method, each model’s precipitation distribution was statistically indistinguishable from the other models (this was confirmed using the Kolmogorov-Smirnov test). Thus, all four model time series were concatenated into one long (160 year) time series before creating the P-F curve, which allows for a reduction in the P-F curve uncertainty band, especially for higher return periods. The P-F curve was calculated by fitting a GEV distribution to the AMS time series of this concatenated record. In addition to fitting the GEV, a Monte Carlo sensitivity study was developed by randomly sampling the 160-year record 1,000 times (allowing for

replacement). The uncertainty bands in Figures 20 and 21 show the 5th to 95th percentile range, equivalent to a 90% confidence level.

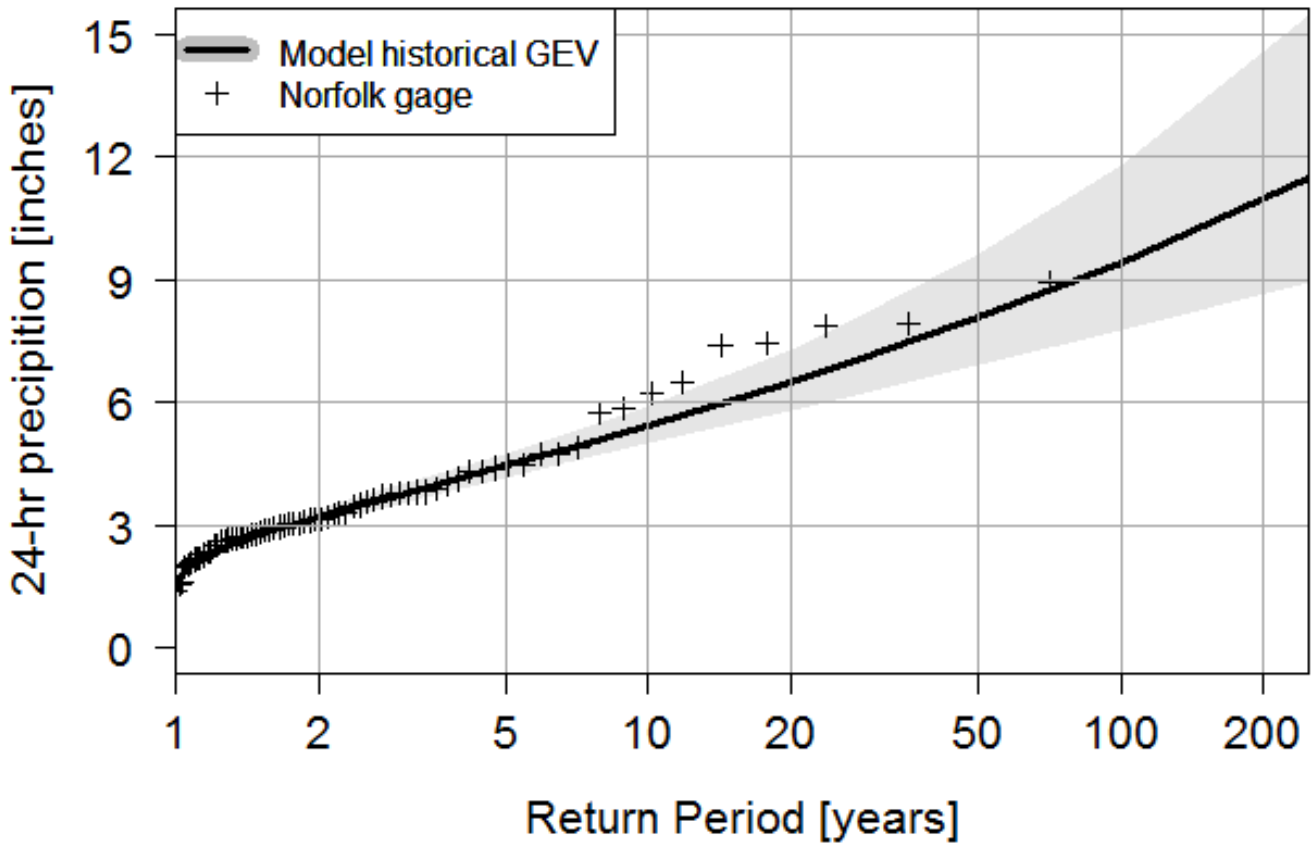


Figure 19: Historical modeled GEV (black line), with a 90% uncertainty band, compared to empirical estimates using 24-hour AMS from the Norfolk Airport.

Figures 20 and 21 show the projected P-F curves for the mid-term [2045] and long-term [2075] periods, respectively. Projected P-F curves are higher than the historical curve across all return periods for both the 2045 and 2075 periods. However, due to increasing uncertainty for less frequent events, a statistically significant separation is limited through up to the ten-year event in the 2045 projection and up to the 20-year event in the 2075 projection. Nonetheless, the main conclusion is that future heavy rainfall is expected to have higher intensity than current heavy rainfall.

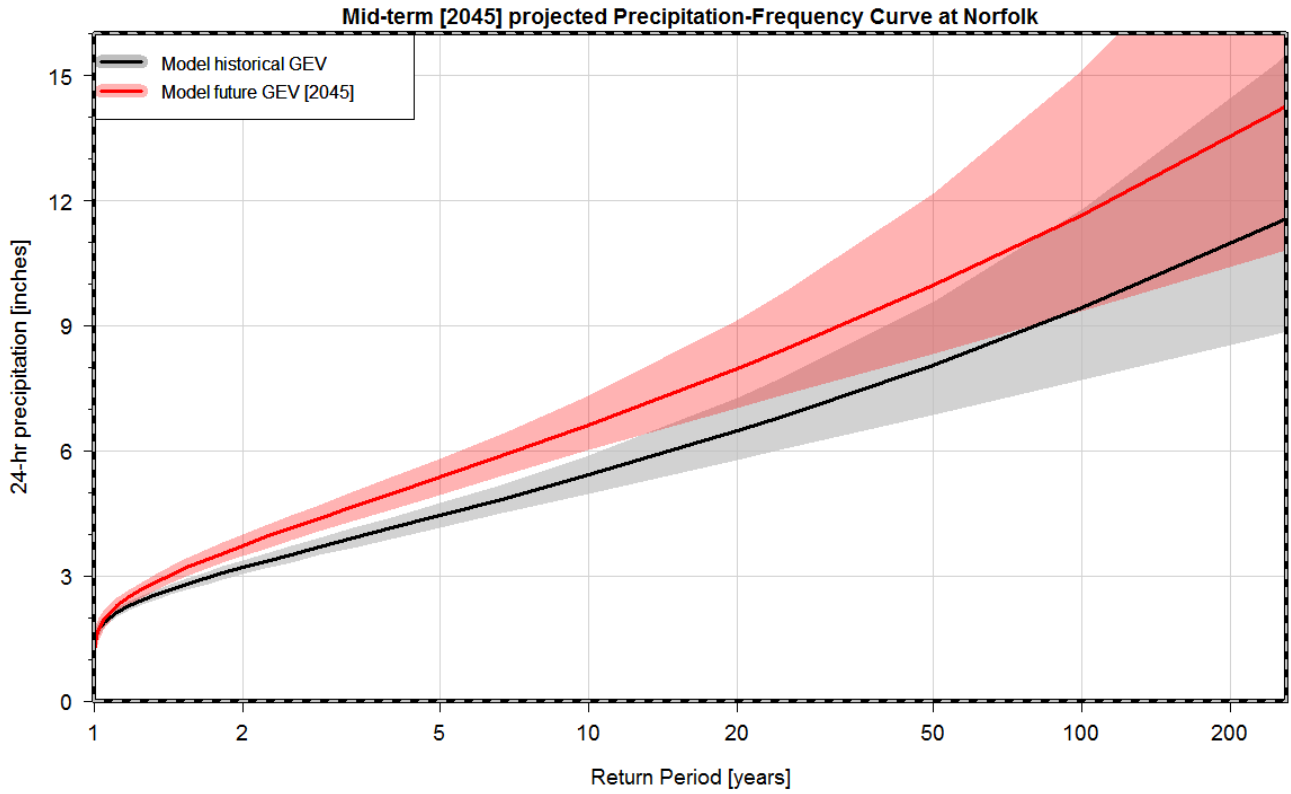


Figure 20: Precipitation-Frequency curve centered on 2045 (orange) compared to the historical curve (black and gray).

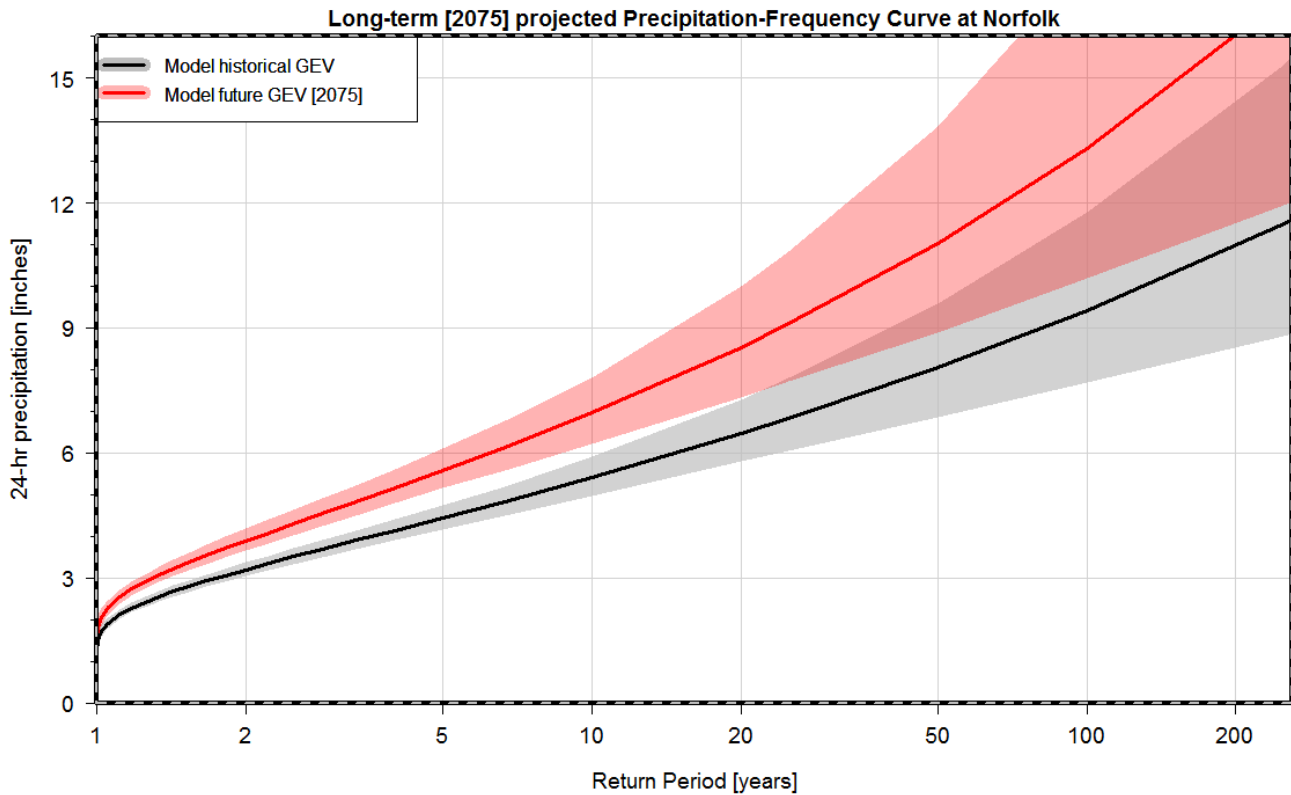


Figure 21: Same as Figure 20 except for the long-term period centered on 2075.

Table 4 summarizes Figures 20 and 21, and provides a comparison to historical P-F curve values for key return periods. For the mid-term projection, despite a slight and statistically insignificant decrease in the one-year event rainfall, increases of 17-24% are expected across all return periods. Once again, note that, due to increasing uncertainty (fewer samples) at lower frequency events, return periods higher than the 20-year cannot be distinguished as statistically different at the 90% confidence level. Nonetheless, the “most likely” outcome still suggests sizeable increases that may be meaningful for design standards. For the long-term projection, much more significant changes in the range of 21-41% are expected. Events up to the 20-year are statistically significantly higher than the historical period. Thereafter, uncertainty rapidly increases, though “most likely” changes still show significant increases.

It is important to stress that this investigation of future precipitation projections is preliminary. For example, one important omission is a characterization of model heavy rainfall according to its process (such as the historical analysis in Table 1). Figure 22 shows the seasonality of Annual Maximum Series of 24-hour rainfall in the models (right 4 columns) compared to the Norfolk Airport gage. Note that in observations, a distinct late summer and early fall peak is observed (also see Figure 3) due to the influence of tropical-related rainfall.

Table 4: Summary of P-F curve changes between the modeled historical climate (after bias correction), and mid-term and long-term model projections. For the projections, bold values indicate when the uncertainty bands are statistically distinguishable from the historical period at the 90% confidence level. Note that the Historical Modeled Value is NOT based on NOAA Atlas 14.

Return Period (yr)	Modeled Historical Value (in)	Mid-term [2045]		Long-term [2075]	
		Value (in)	% change	Value (in)	% change
1	1.4	1.3	-8%	1.7	+21%
2	3.2	3.7	+17%	3.9	+22%
5	4.4	5.4	+21%	5.6	+25%
10	5.4	6.6	+22%	7.0	+28%
20	6.5	8.0	+23%	8.5	+32%
50	8.0	10.0	+24%	11.0	+37%
100	9.4	11.7	+24%	13.3	+41%

Also, note that in general all models with the possible exception of the CanESM2-CanRSM4, lack this kind of seasonality and instead place too much emphasis on heavy rainfall during other months. In particular, the GFDL-ESM2M-WRF has a near minimum during the summer with a peak during the winter months presumably associated with Nor’easter type storms. Figure 22 does not imply that modeled precipitation is inaccurate, but it does suggest that models are not fully reproducing Atlantic tropical cyclone activity, and in turn may be placing a larger emphasis on Non-tropical events as the source of AMS precipitation. A deeper analysis

of this issue would require full model fields such as three-dimensional geopotential height and moisture. At the time of this report, only the temperature and precipitation fields were available.

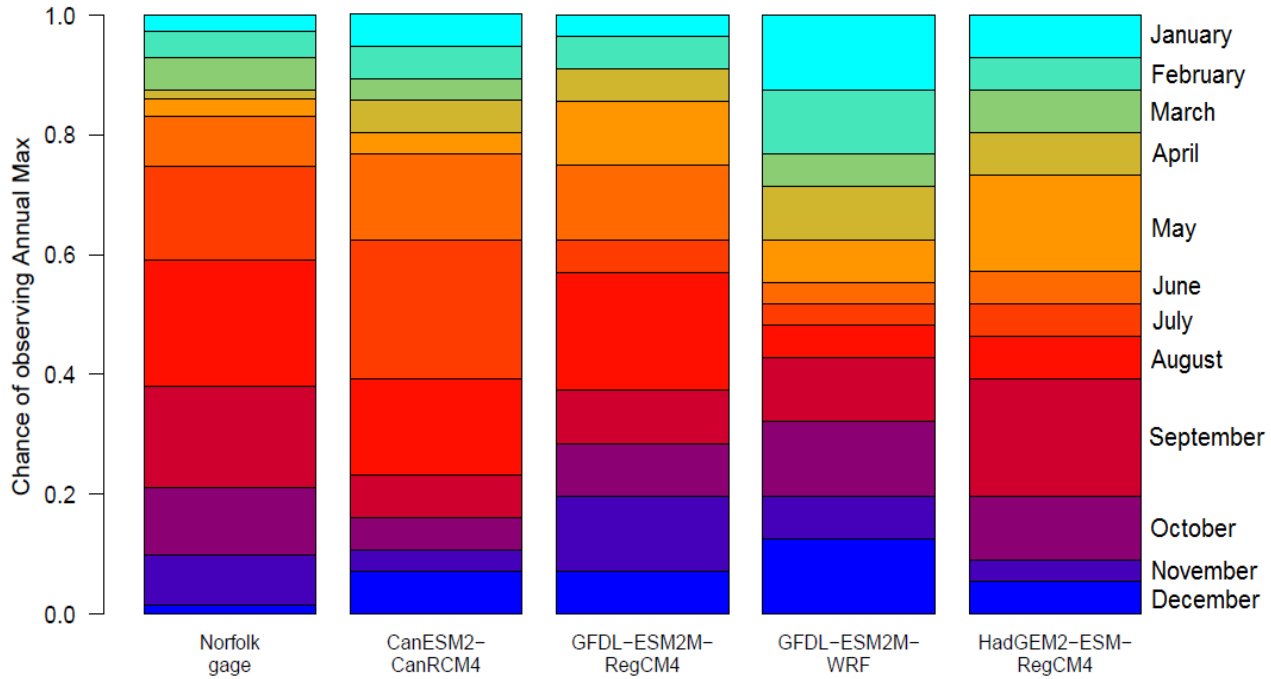


Figure 22: Seasonality of AMS occurrence, by month, for the Norfolk gage (left column) and the four RCMs contributing to the future projections (right four columns).

RCP4.5 and RCP8.5 Analysis (44km model resolution)

In the previous section, it was found that significant increases in heavy precipitation are expected for the RCP8.5 scenario. In this section, a complementary analysis is done using the intermediate RCP4.5 scenario. Table 5 shows the models that were used in this analysis, which used model simulations conducted at 44-km resolution (recall the 11-km simulations were not available for RCP4.5). Note that not all of the models used in the 11-km analysis were available for the 44-km analysis.

Table 5: NA-CORDEX experiments used for this analysis. All simulations were conducted using 44km resolution modeling and both RCP4.5 and RCP8.5 scenario boundary conditions.

Modeling Agency Responsible for Global Climate Model	Global Climate Model (Boundary)	Regional Climate Model
Canadian Centre for Climate Modeling and Analysis (Canada)	CanESM2	CanRCM4
Canadian Centre for Climate Modeling and Analysis (Canada)	CanESM2	CRCM5
Canadian Centre for Climate Modeling and Analysis (Canada)	CanESM2	RCA4
European Centre for Medium-Range Weather Forecasts (United Kingdom)	EC-Earth	HIRHAM5
Max Planck Institute (Germany)	MPI-ESM-MR	CRCM5

The methodology for this analysis followed closely that presented for the RCP8.5 (11-km) analysis in the previous section. As the main objective of the study was design guidance only the P-F curves were investigated; however, all conclusions are expected to apply to projections in Peaks Over Thresholds. First, historical simulations of daily precipitation were bias-corrected using the Norfolk Airport rain gage. The quantile-quantile relationships are shown in Figure 23.

Note that unlike for the 11-km simulations, which did not have a systematic bias, the 44-km model simulations all underestimate heavy precipitation. Nonetheless, after bias-correction, simulations of the historical period match the Norfolk distribution closely (not shown). Fitting a GEV distribution to bias-corrected Annual Maximum Series closely reproduces the Atlas 14 estimate (not shown, but see Figure 19). Future projections are bias corrected using the relationships established in Figure 23, similar to the 11-km RCP8.5 analysis. All model time series are then concatenated into a single long time series before fitting a GEV to the future projections using a 40-year window centered on 2045 and 2075, as in the 11 km RCP8.5 analysis. Four resulting curves are shown in Figures 24 through 27, showing the 2045 and 2075 estimates for the RCP4.5 and RCP8.5 scenario. Bias corrected Annual Maximum Series from each model can be found in Appendix D.

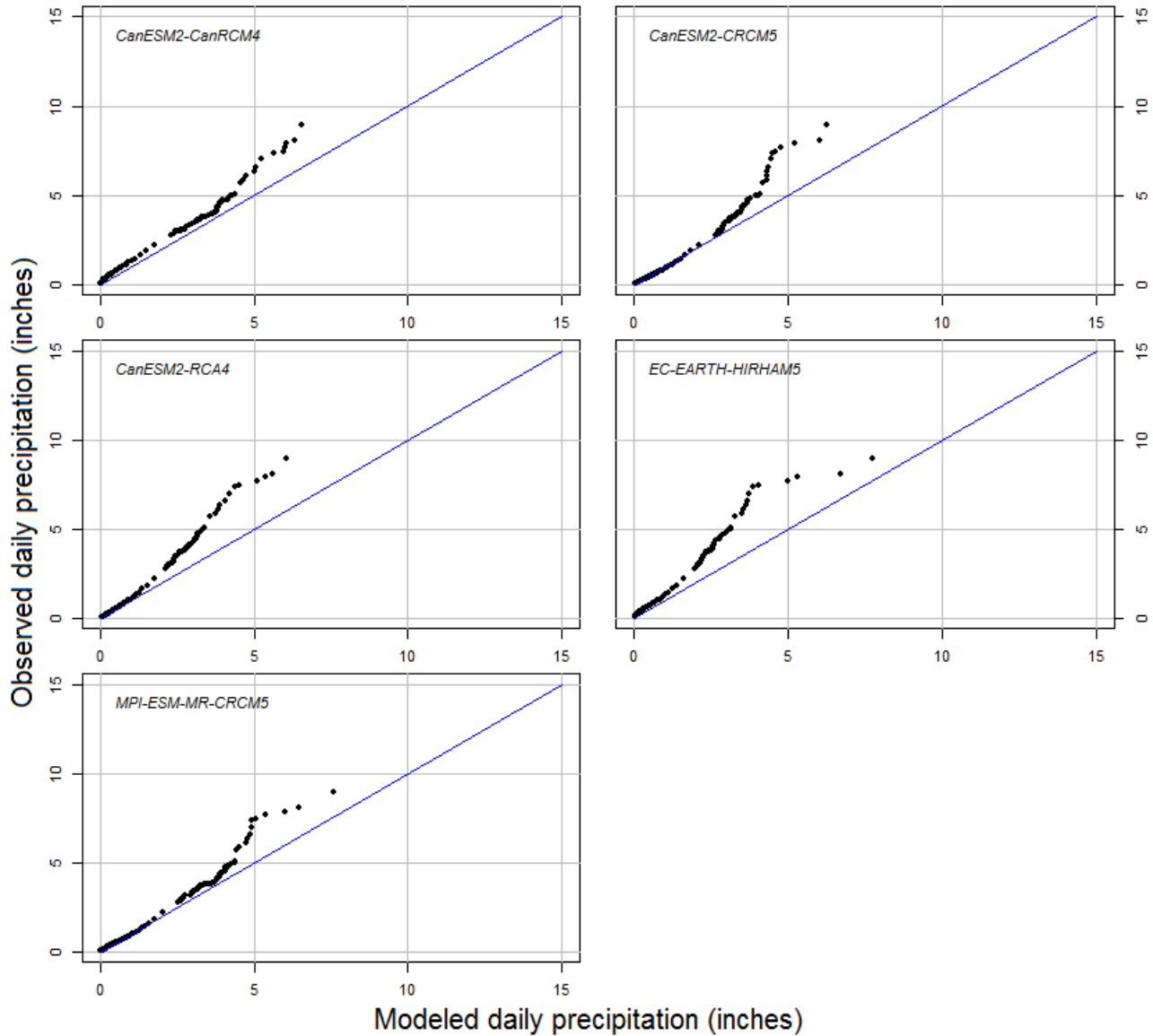


Figure 23: Quantile-quantile maps comparing observed daily precipitation of historical 44-km model simulations.

As shown in Figures 24 for the mid-term (2045) RCP4.5 scenario, there is a notable increase the rainfall up through the 1- in 2-year event. However, the remaining portion of the curve is nearly indistinguishable from the historical analog. A nearly identical result is seen in Figure 25 for the long-term (2075) RCP4.5 scenario. The fact that there is little dependence on timeframe in the RCP4.5 scenario is likely due to the radiative forcing profile seen in Figure 15. Note that after about 2050, the radiative forcing is nearly constant, which can be taken to imply that if there was no sensitivity through 2050, there may not be any sensitivity thereafter.

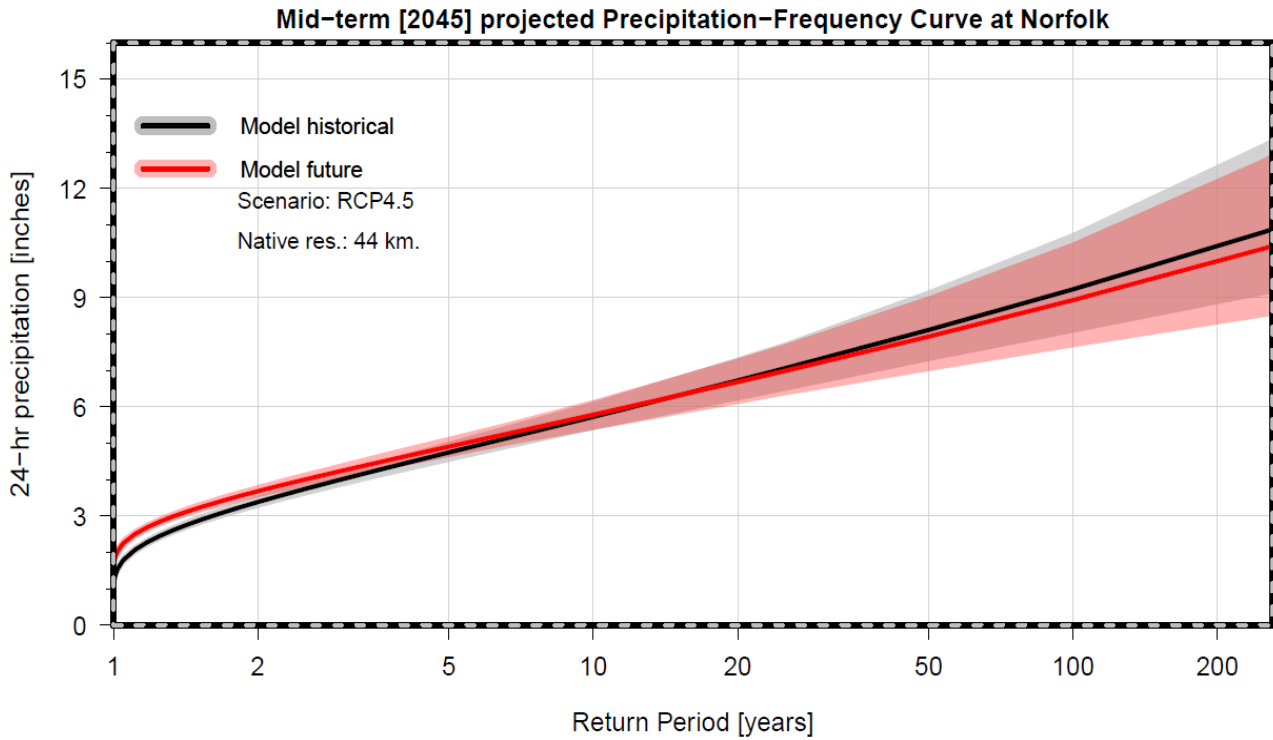


Figure 24: Precipitation-Frequency curve centered on 2045 (red) compared to the historical curve (black and gray) using the 44-km model simulations for the RCP4.5 scenario.

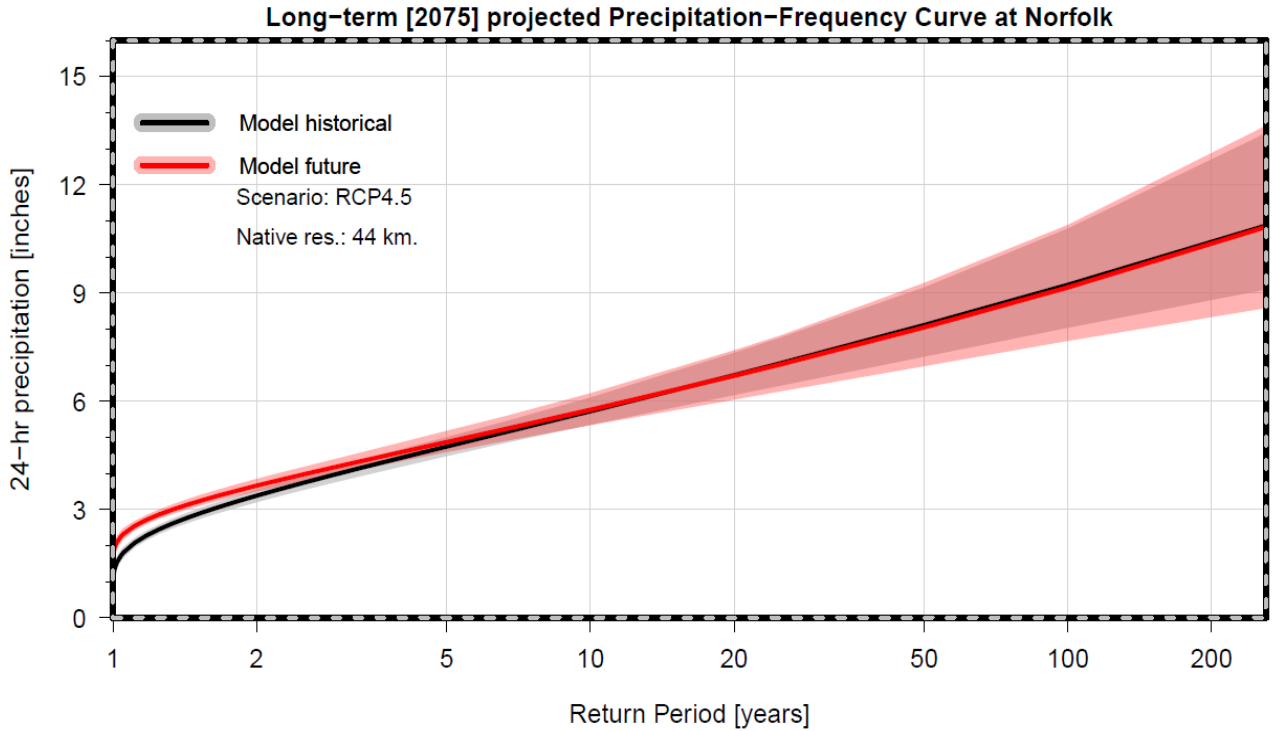


Figure 25: Same as Figure 24 except centered on 2075.

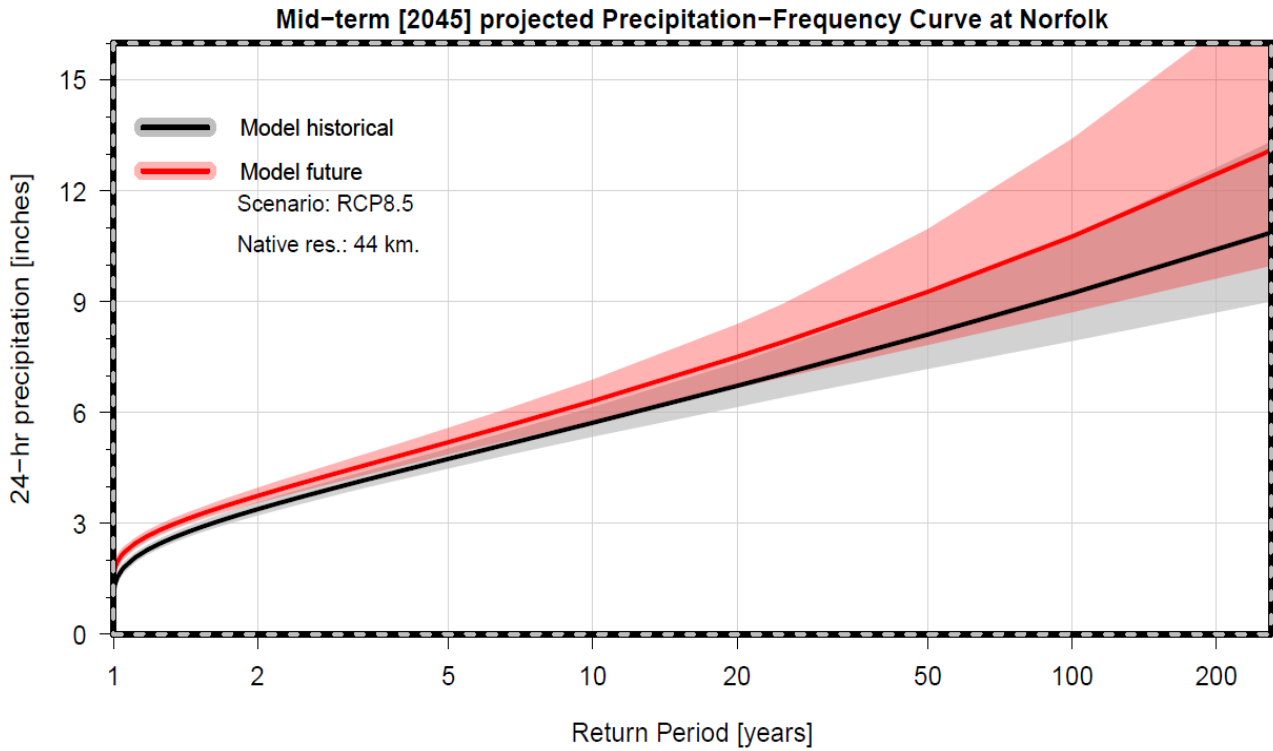


Figure 26: Precipitation-Frequency curve centered on 2045 (red) compared to the historical curve (black and gray) using the 44-km model simulations for the RCP8.5 scenario.

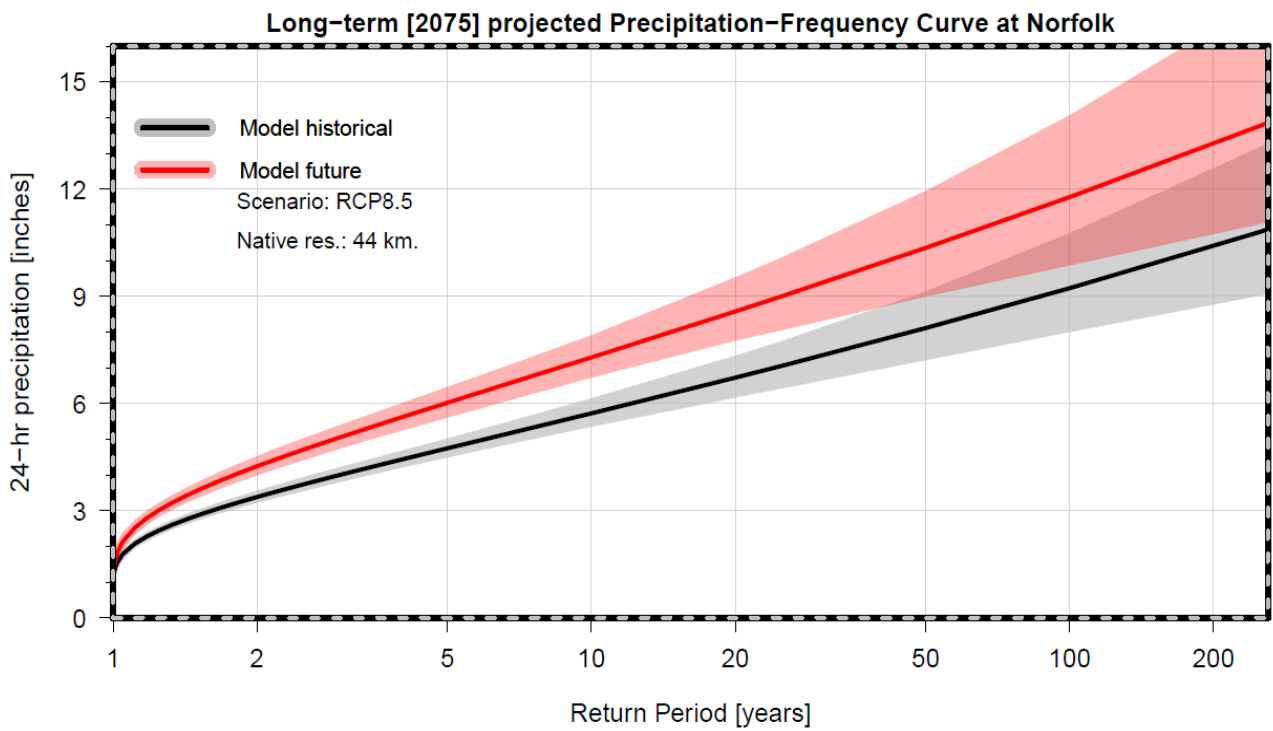


Figure 27: Same as Figure 26 except centered on 2075.

In consistency with the findings using the 11-km models (RCP8.5 scenario), Figure 26 and 27 show increases across the entire P-F curve for the RCP8.5 scenario of the 44 km models; however, a few differences are noted. First, the increase by 2045 (Figure 26) is not as large as that of the 11-km models (compare Figure 26 with Figure 20). Second, the most pronounced increases, especially by 2075 occur in the more frequent events, whereas the less frequent events such as the 50 and 100-year events show smaller changes using the 44-km results compared to the 11-km

Tables 6 and 7 provide summaries of the changes in the Precipitation-Frequency curve based on the 44-km model simulations. The RCP4.5 scenario (Table 6) shows increases of about 15-20% in the 1-year and 2-year events, with little to no change for less frequent events, regardless of the timeframe. Meanwhile, the RCP8.5 scenario (Table 7) shows similar changes as RCP4.5 in the shorter-term projection, but increases up to 36% in the 2-, 5-, 10-, and 20-year event amount.

One complication that has not been investigated is the significance of the differences in the bias correction relationships in Figures 16 and 23. It was shown in Figure 22 that the 11-km simulations show notable errors in the seasonality of the Annual Maximum Series occurrence, presumably due to the underrepresentation of tropical cyclones. It is hypothesized that this may be further aggravated with the coarser resolution 44-km models. One recommendation for future research is to compare the dynamical forcing responsible for heavy rainfall events, which would help explain (i) the need for bias correction and (ii) differences in bias correction between the 11-km and 44-km models.

Table 6: Same as Table 4 except using for the RCP4.5 scenario using 44-km models. For the projections, bold values indicate when the uncertainty bands are statistically distinguishable from the historical period at the 90% confidence level. Note that the Historical Modeled Value is NOT based on NOAA Atlas 14.

Return Period, yr	Modeled Historical Value (in).	Mid-term [2045]		Long-term [2075]	
		Value, in.	% change	Value, in.	% change
1	1.4	1.6	+14%	1.7	+21%
2	3.2	3.7	+16%	3.7	+16%
5	4.4	4.9	+11%	4.9	+11%
10	5.4	5.8	+7%	5.8	+7%
20	6.5	6.7	+3%	6.7	+3%
50	8.0	7.9	-1%	8.0	0%
100	9.4	8.9	-5%	9.2	-2%

Table 7: Same as Table 4 except adding the results from the 44-km model projections using the RCP8.5 scenario. Bold values indicate when the uncertainty bands are statistically distinguishable from the historical period at the 90% confidence level. Note that the Historical Modeled Value is NOT based on NOAA Atlas 14.

Return Period, yr	Modeled Historical Value, in.	Mid-term [2045]				Long-term [2075]			
		Value, in.	% change	Value, in.	% change	Value, in.	% change	Value, in.	% change
1	1.4	1.6	+14%	1.3	-8%	1.2	-16%	1.7	+21%
2	3.2	3.7	+16%	3.7	+17%	4.2	+31%	3.9	+22%
5	4.4	5.2	+18%	5.4	+21%	6.0	+36%	5.6	+25%
10	5.4	6.3	+17%	6.6	+22%	7.3	+35%	7.0	+28%
20	6.5	7.5	+15%	8.0	+23%	8.6	+32%	8.5	+32%
50	8.0	9.3	+16%	10.0	+24%	10.4	+30%	11.0	+37%
100	9.4	10.8	+15%	11.7	+24%	11.8	+26%	13.3	+41%
		44 km		11km		44km		11km	

Comparing RCP scenarios

A comparison of Figures 24-25 with 26-27 (and Tables 6 and 7) disclaims the assumption that precipitation in the Virginia Beach area responds linearly in a warming climate. Although there is a statistically significant 14-21% increase in the 1-year and 2-year rainfall amounts under the RCP4.5 scenario, there is little change for less frequent events such as the 10-year event. Thus, from the standpoint of design guidance, the RCP4.5 scenario does not suggest a need to update engineering practices.

On the other hand, the RCP8.5 scenario, regardless of both model resolution and what model is being considered (see Appendix D), shows strong increases across the entire P-F curve. However, there is some disagreement between which part of the curve will change the most. The higher resolution simulations suggest a stronger increase for the less frequent events like the 100-year, which is projected to increase by 41% using the 11 km simulations but only 26% in the 44 km simulations. Meanwhile, the medium resolution simulations suggest a stronger increase in the mid-range events such as the 5- and 10-year event, where increases above 30% are projected by 2075.

Limitation of Using Annual Maximum Series

The historical PF values in the previous analyses (Tables 4, 6, 7; Figures 20, 21, 24, 25, 26, 27), which were derived from a distribution fit to model simulations, compared very favorably with NOAA Atlas 14 for the 10, 25, 50 and 100 year return periods. However, underestimates are noted for the 1 and 2 year return periods, particularly severe for the former.

In a discussion with the City on October 5, 2017, it was hypothesized that the underestimates for the 1 and 2 year return periods are due to the use of Annual Maximum Series (AMS) to develop the precipitation-frequency estimates. Briefly, the reasoning is that AMS only uses one value per year, necessarily implying that it will dismiss potentially high rainfall amounts that did not exceed the annual maximum but may have qualified as an AMS during many other years. It was further hypothesized that the underestimate issue could be improved or resolved using Partial Duration Series (PDS), which uses the rainfall amount regardless of when it occurred (note that NOAA Atlas 14 actually uses PDS data for PF curve estimation). This is confirmed in Figure 28, below, which shows a comparison of PDS and AMS values at the Norfolk Airport gage. Note that the two are nearly identical for return periods of 10 years and greater. Meanwhile, deviations arise for more frequent return periods.

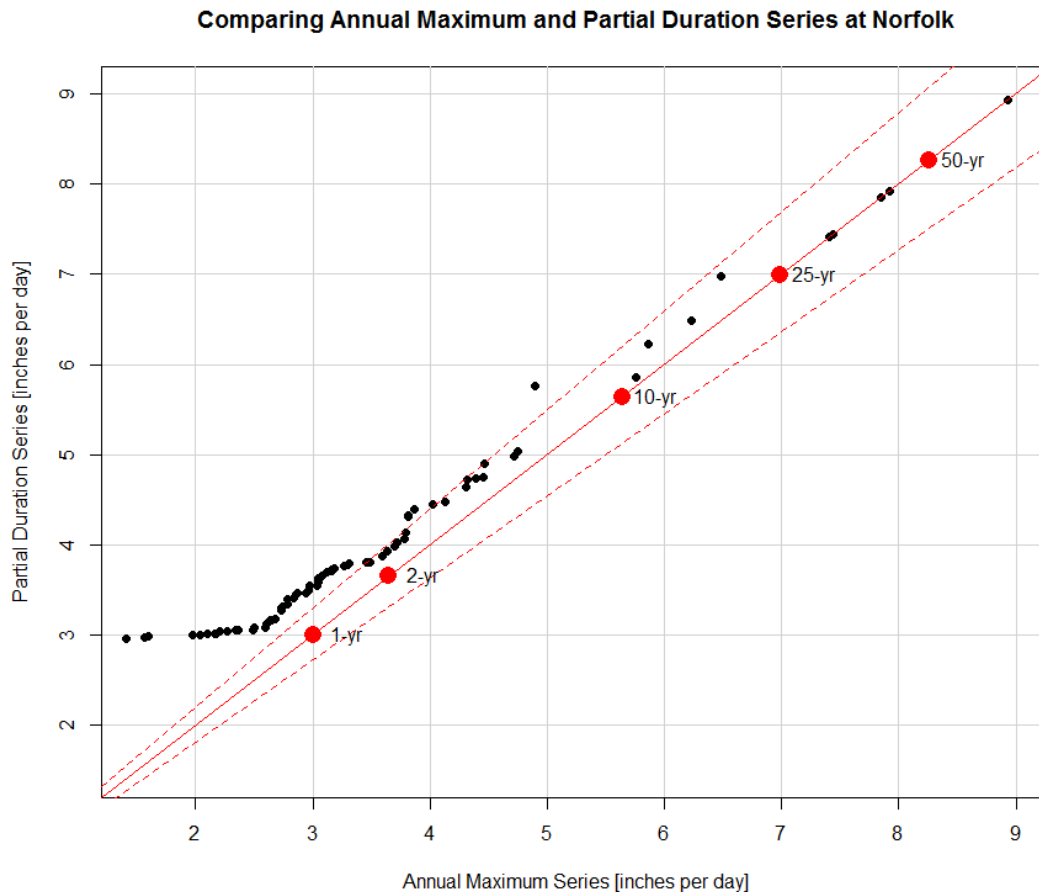


Figure 28: Comparisons of the AMS and PDS estimates at the Norfolk Airport rainfall gage.

As expected, using the PDS approach to recreate the PF curves results in a significant improvement for the 1 and 2 year return periods. Figure 29 shows the updated “Mid-term”

projection based on the 11-km model simulations. When compared to Figure 20, the most notable change is at the 1 and 2 year return periods (there are changes at the 200 year return period, but these are insignificant given the large uncertainty range at that frequency).

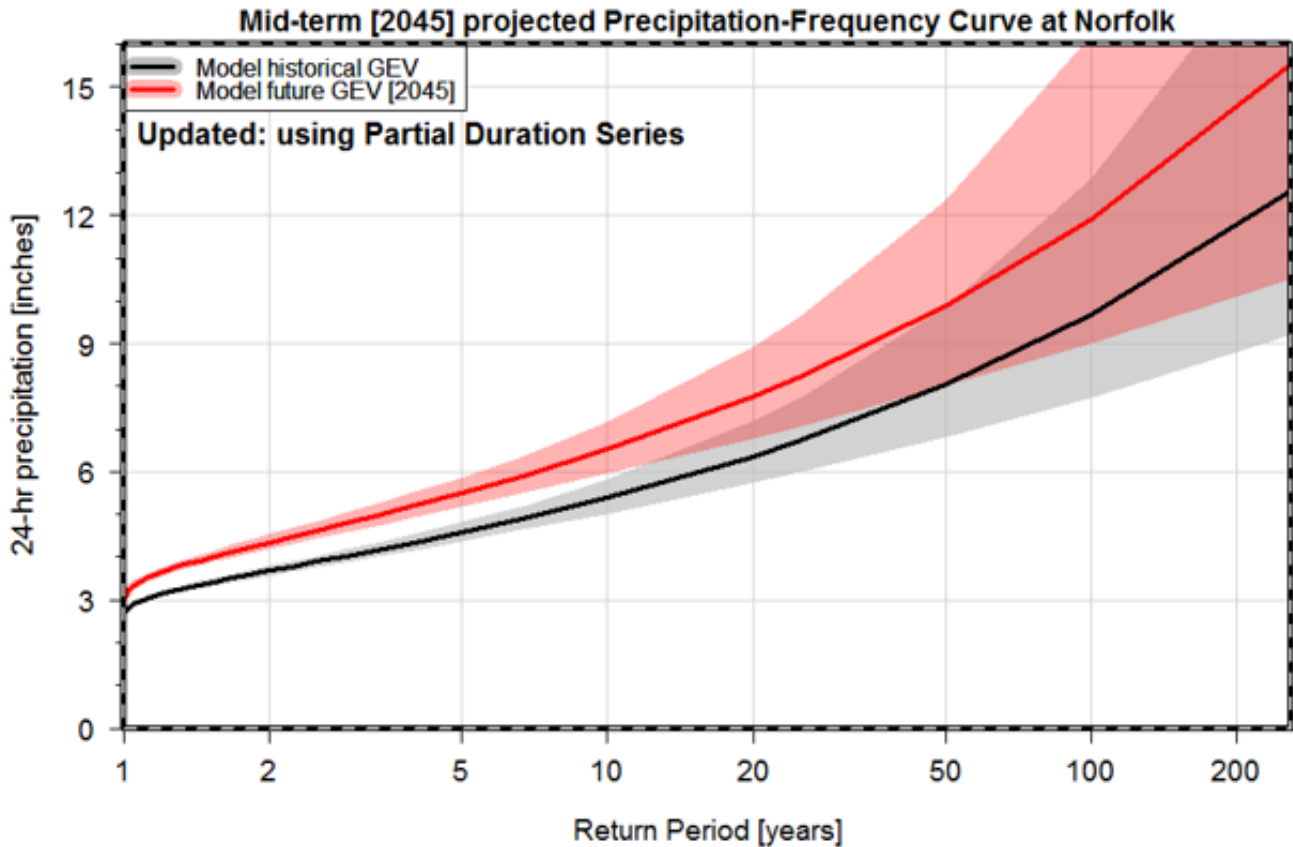


Figure 29: Precipitation-Frequency curve centered on 2045 (orange) compared to the historical curve (black and gray) using the PDS method. This should be compared to Figure 20, which was based on the AMS method.

Table 8 shows a re-creation of Table 4 (i.e. using the RCP8.5 11-km resolution simulations), except using Partial Duration Series. There are two notable changes. The historical estimate of the 1 year return period event has increased markedly from 1.4 to 2.7 inches. Although this is still 10% lower than the Atlas 14 value used by the City, given the rest of the curve, this can be accepted as a reasonable measure of baseline, historical conditions. Likewise, the 2 year return period estimate has increased from 3.2 to 3.7 inches, and is now almost identical to Atlas 14. Secondly, with the exception of the 1 year return period, the percent change between the historical and projected values is now insensitive to the return period. Although the projected increase for the 1 year return period event value are lower than the rest of their respective curves, we cannot find peer reviewed study results that would support a separate recommendation for the more frequent events. **Thus, based on the results herein and previous discussions with the City, we recommend a constant**

20% increase in design rainfall guidance across the entire precipitation-frequency curve.

Table 8: Summary of P-F curve changes between the historical, mid-term and long-term periods using the PDS method (compare to Table 4, which is based on AMS). For the projections, bold values indicate when the uncertainty bands are statistically distinguishable from the historical period at the 90% confidence level. NOAA Atlas 14 estimates are added for reference. Note that the Historical Modeled Value is NOT based on NOAA Atlas 14.

Return Period (yr)	NOAA Atlas 14 (in)	Historical Modeled Value (in)	Mid-term [2045]		Long-term [2075]	
			Value (in)	% change	Value (in)	% change
1	3.00	2.7	3.0	+11%	3.2	+19%
2	3.65	3.7	4.4	+19%	4.6	+24%
5	4.72	4.6	5.5	+20%	5.9	+28%
10	5.64	5.4	6.5	+20%	7.1	+31%
20	6.53	6.4	7.8	+22%	8.5	+33%
50	8.26	8.0	9.9	+24%	10.9	+36%
100	9.45	9.7	11.9	+23%	13.2	+36%

CHAPTER 3: CHECK STORM ANALYSIS AND COMPARISON WITH PROBABLE MAXIMUM PRECIPITATION

Background

At least three 100-year rainfall events affected the City of Virginia Beach during 2016 (see Figure 30 for a spatial view of event rainfall totals). The first occurred during the evening of July 31, when the city had over 6 inches of rainfall in a period of less than three hours, with the heaviest precipitation occurring across the northern part of the city. The second event took place over a 72-hour stretch starting on September 19, during which Tropical Storm Julia and its moisture feed generated numerous rounds of moderate-to-heavy rainfall. The final, and most severe event occurred during a 24-hour period starting on October 8 when Hurricane Matthew's rainfall bands moved across the region.

Flooding was observed in the city during each event, and some parts experienced flooding during all three. The intensity and frequency of these events calls into question the presumed rarity of such occurrences. This was covered by Tasks 1 and 2 of this project, which also investigated future rainfall projections to quantify how these levels of rainfall are predicted to change.

This task has three main objectives: First, through a comprehensive analysis of each event's rainfall intensity and temporal distribution, we seek to determine duration-frequency estimates to gain an understanding of the timescale(s) over which the heavy rainfall occurred. Our second objective builds on this, and we assess how the intensity and distribution of the observed rainfall compares with local design rainfall, which is used for engineering purposes. Next, we evaluate how the observed events compared to Probable Maximum Precipitation (PMP) estimates for the region.

The chapter is organized as follows: First, we introduce the design rainfall currently being employed by the City of Virginia Beach. We then provide an in-depth summary of each of the three aforementioned heavy rain events, especially in the context of a design storm. The final section provides a discussion of the region's PMP estimates and approximate each event's magnitude as a PMP fraction.

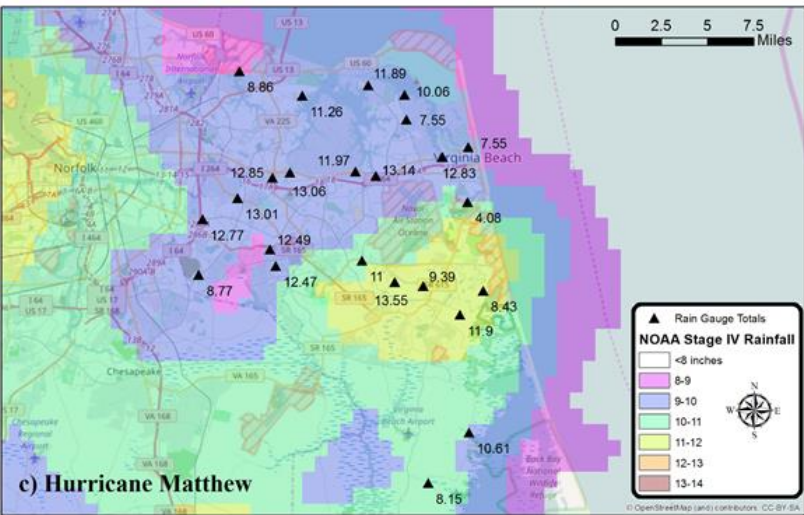
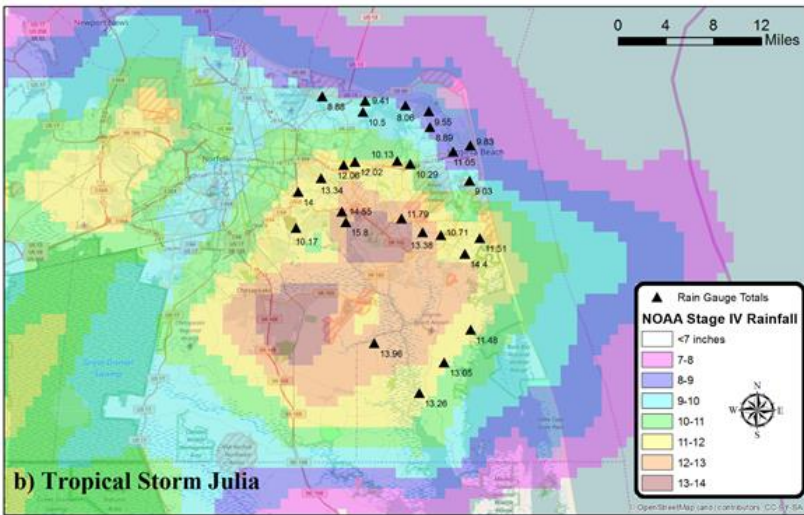
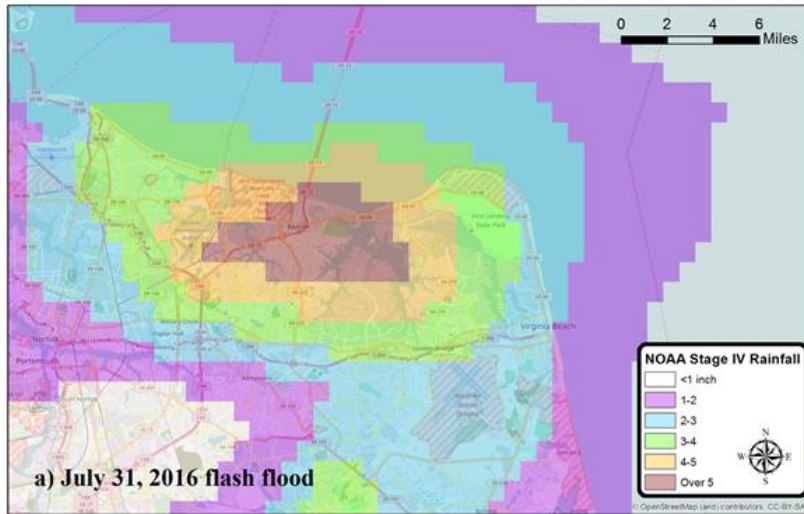


Figure 30: Estimated rainfall totals (color fill) from the NOAA Stage IV gridded precipitation product for (a) July 31, 2016, (b) Tropical Storm Julia and (c) Hurricane Matthew. Individual rain gage totals are overlaid in (b) and (c). Note that gage totals may not exactly match the gridded data due to averaging effects in the latter.

Design Storm

The concept of a “design storm” (used here interchangeably with “design rainfall”) was developed during the 1950s and 1960s to more easily inform runoff volume, especially for municipal engineering applications. The United States Department of Agriculture’s Natural Resources Conservation Service (NRCS; formerly Soil Conservation Service) has been a key agency involved in the development of design rainfall. Of particular importance is their Technical Paper 149 (USDA-SCS, 1973), which described and validated the “Type I” and “Type II” rainfall distributions for use in the United States. The Type II distribution was designated for use in the Virginia Beach region. Design rainfall distributions have been updated since then, mainly to incorporate the significant increase in quality-controlled precipitation data since the 1973 report. Today, the City of Virginia Beach uses the NOAA Type C design rainfall distribution based on the NOAA Atlas 14 Rainfall Atlas (Bonnin et al. 2006; Merkel et al. 2015; M. Bumbaco, personal correspondence). See Appendix B for the NOAA Atlas 14-point precipitation-frequency curve used in this analysis.

Figure 31 shows the rainfall accumulation profile for a variety of 24-hour design storm intensities using the NOAA Type C rainfall distribution. Note that the maximum rainfall *intensity* of a 24-hour design storm, regardless of the duration, is centered on hour 12. Stated differently, the rainfall accumulation is unsteady over the course of the “event” – over 50% of the total accumulation occurs during a two-hour period from hour 11 through hour 13.

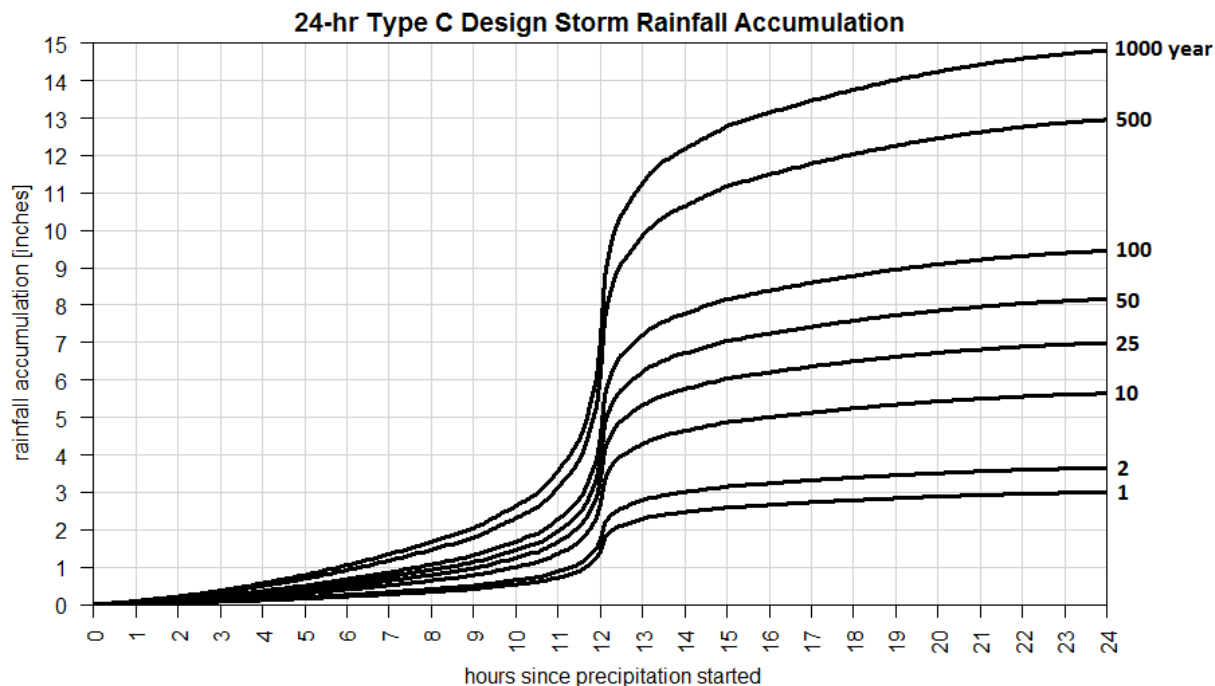


Figure 31: Design storm rainfall accumulation for a 24-hour event for 6 return periods, using the NOAA Type C distribution.

Precipitation data

Two types of data were used for this analysis: rain gage observations, and base-elevation radar reflectivity data from the Wakefield, Virginia Next Generation Doppler Radar (NEXRAD). The goal of this study was not to perform a comprehensive spatial reconstruction of each event; thus, radar data was only used in a supporting role to ensure that there were not areas between gages that received substantially more rainfall than gaged locations, as well as to estimate the area of high rainfall intensity coverage as the event evolved.

Table 9 shows the 28 rainfall gages used for this analysis, all of which were obtained from three sources: the Hampton Roads Sanitation District (HRSD); obtained through the City of Virginia Beach), United States Geological Survey (USGS), and the CoCoRaHS network. The HRSD and USGS gages have a 15-minute temporal resolution, while daily CoCoRaHS reports are typically received every morning. Data from CoCoRaHS gages was manually inspected for quality assurance since they are not officially quality controlled, and all data was deemed physically reasonable. However, given that CoCoRaHS gages only report 24-hour precipitation totals, their data was only used to determine if there were areas not covered by the HRSD and USGS gages that may have received much higher rainfall. We did not find any such instance as, fortuitously, each of the three events considered here was well sampled by at least one gage with high temporal resolution. Figure 30 (b, c) shows the distribution of gages across the Virginia Beach area.

The radar data is used here to approximate the reflectivity-rainfall (Z-R) relationship during Hurricane Matthew as shown in the scatter plot in Figure 32. The blue line shows a qualitatively estimated fit based on consideration of a variety of documented Z-R relationships (Liguori and Rico-Ramirez 2014). Due to the tropical nature of both the Matthew and Julia events, even normally insignificant reflectivities as low as 40 dBZ produced heavy rainfall. For the Matthew and Julia events, we use 40 dBZ (translating to about 0.6 inches in 30 minutes) and 45 dBZ (approximately 1.2 inches in 30 minutes) as the thresholds for areas experiencing “heavy” and “very heavy” rain. It should be reiterated that the radar information was used for qualitative assessment only.

Table 9: Summary of rain gages used in the analysis. Total event rainfall is shown for Hurricane Matthew and Tropical Storm Julia in units of inches.

Gage ID	Source	Latitude (°N)	Longitude (°W)	Matthew (in)	Julia (in)
HRSD MMPS-004 John B. Dey	City of VB	36.898	-76.063	11.89	8.06
HRSD MMPS-093 Ches-Liz Main Flow	City of VB	36.907	-76.164	8.86	8.88
HRSD MMPS-140 Independence	City of VB	36.840	-76.138	12.85	12.06
HRSD MMPS-144 Kempsville	City of VB	36.795	-76.140	12.49	14.55
HRSD MMPS-146 Laskin Rd	City of VB	36.853	-76.005	12.83	11.05
HRSD MMPS-160 Pine Tree	City of VB	36.844	-76.073	11.97	10.13
HRSD MMPS-163 Providence	City of VB	36.814	-76.193	12.77	14.00
HRSD MMPS-171 Shipp's Corner	City of VB	36.788	-76.068	11.00	11.79
HRSD MMPS-185 Lagomar IFM	City of VB	36.769	-75.973	8.43	11.51
HRSD MMPS-255 Virginia Beach PS 606	City of VB	36.772	-76.020	9.39	10.71
HRSD MMPS-256 Virginia Beach PS 472	City of VB	36.779	-76.196	8.77	10.17
HRSD MMPS-281 Mill Landing Rd	City of VB	36.648	-76.016	N/A	13.05
HRSD MMPS-281 Virginia Beach PS 472	City of VB	36.648	-76.016	8.15	N/A
USGS0204288721	USGS	36.827	-76.166	13.01	13.34
USGS0204291317	USGS	36.843	-76.124	13.06	12.02
USGS0204293125	USGS	36.841	-76.057	13.14	10.29
USGS0204295505	USGS	36.859	-75.984	7.55	9.83
USGS0204297575	USGS	36.825	-75.985	4.08	9.03
USGS0204300267	USGS	36.680	-75.984	10.61	11.48
USGS02043269	USGS	36.618	-76.046	11.86	13.26
VA-VBC-13 (Virginia Beach 2.4 N)	CoCoRaHS	36.775	-76.042	13.55	13.38
VA-VBC-21 (Virginia Beach 3.1 ENE)	CoCoRaHS	36.754	-75.991	11.90	14.40
VA-VBC-30 (Virginia Beach 6.0 WNW)	CoCoRaHS	36.785	-76.136	12.47	15.80
VA-VBC-23 (Virginia Beach 10.6 N)	CoCoRaHS	36.892	-76.035	10.06	9.55
VA-VBC-34 (Virginia Beach 9.5 N)	CoCoRaHS	36.877	-76.033	7.55	8.89
VA-VBC-5 (Virginia Beach 5.9 SSW)	CoCoRaHS	36.667	-76.101	N/A	13.96
VA-VBC-22 (Virginia Beach 11.9 NNW)	CoCoRaHS	36.902	-76.112	N/A	9.41
VA-VBC-2 (Virginia Beach 11.2 NNW)	CoCoRaHS	36.892	-76.115	11.26	10.50

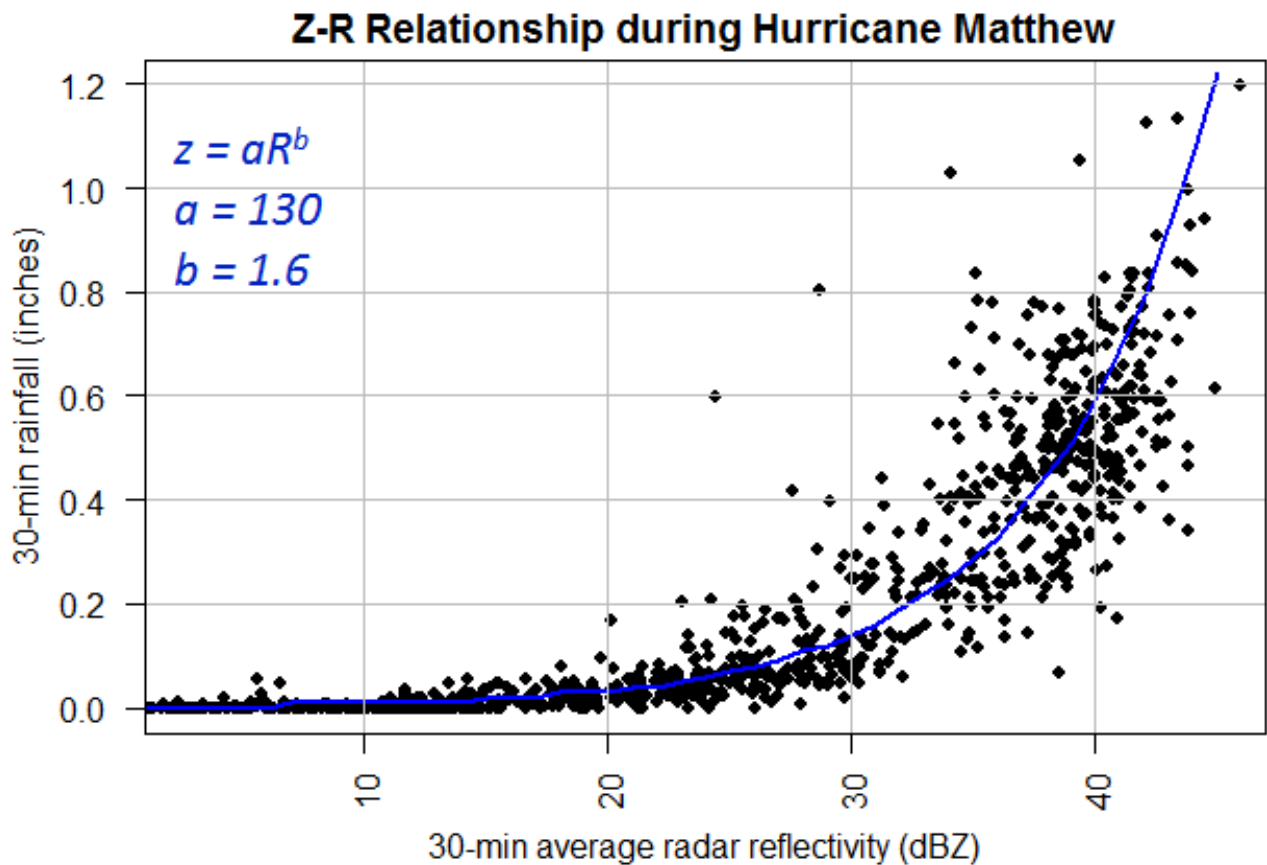


Figure 32: Relationship between 30-minute average radar reflectivity (dBZ) and 30-minute accumulated rainfall across all available rain gages (see Table 9) for Hurricane Matthew.

Event Summaries

July 31, 2016 Heavy Rainfall

The atmospheric dynamics for the July 31 event were not particularly noteworthy. A stationary front was draped across the northern Mid-Atlantic States, with a weak trough seen at the upper levels. Typical summertime thunderstorms were forecasted for the afternoon and evening hours across the region. However, near-surface moisture levels were high: dew point temperatures on the morning of July 31 were in the 72-74°F range, and rose to as high as 77°F in the time immediately before storms moved into the area. An 8PM sounding from Wallops Island shows that a large amount of instability (Convective Available Potential Energy exceeding 1,500 J/kg) was available for thunderstorm formation (Figure 33). Furthermore, directional wind shear was relatively weak in the low- and mid-levels, suggesting storm motion would be less than about 25 mph – this is supportive of heavy rainfall over a given location assuming that a storm can stay intact.

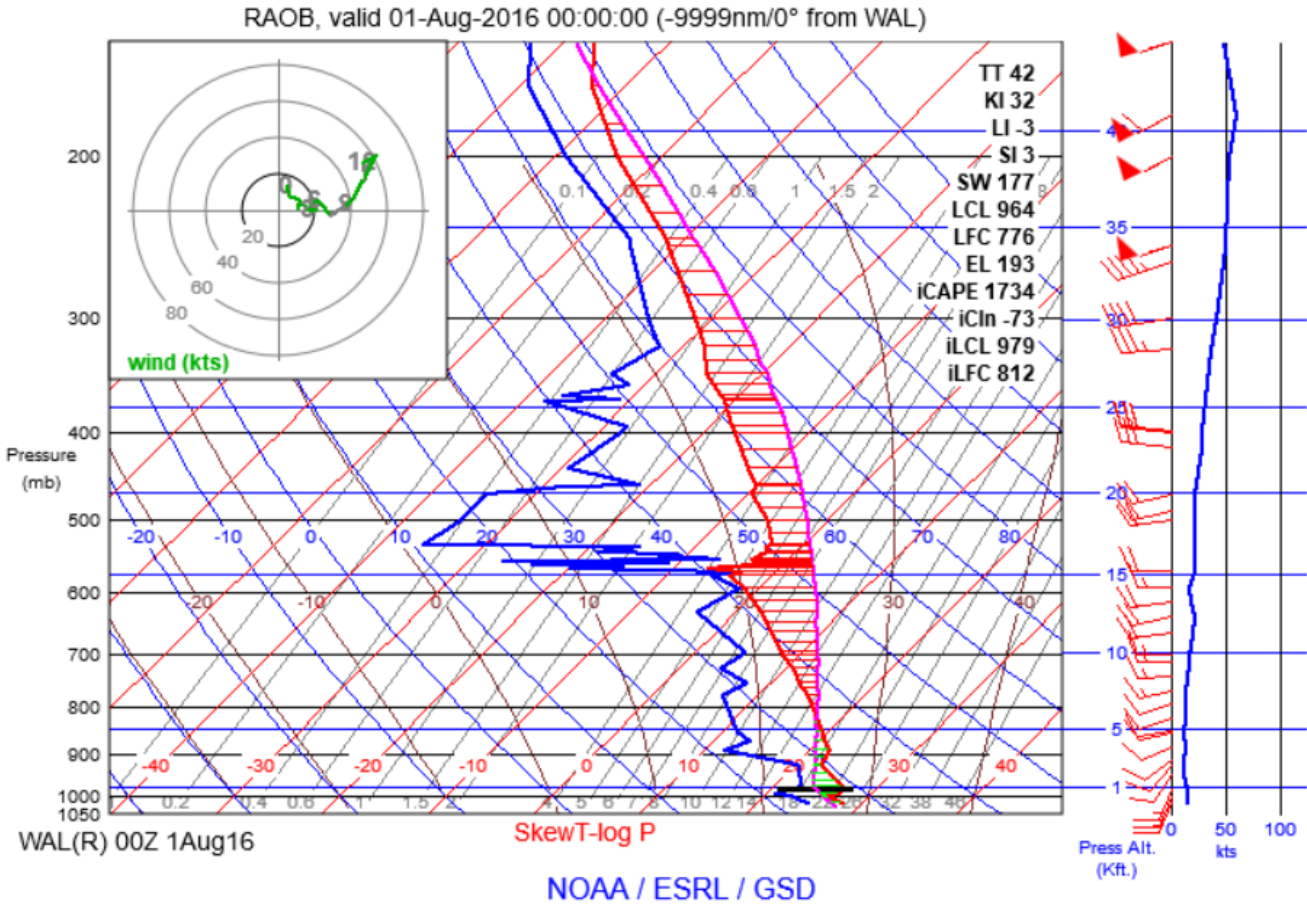


Figure 33: Atmospheric sounding from the Wallops Island (VA) radiosonde balloon launched at 8PM local time on July 31, 2016. A parcel instability analysis was performed by assuming an inflow air temperature of 82oF and dew point of 75F, yielding the instability shown by the red dashed lines. The stable layer is shown by the green dashed lines.

Thunderstorms moved into the Virginia Beach area shortly after 5PM ET as captured by Figure 34, which shows base-elevation radar reflectivity at 5:24PM and 5:58PM local time. Two separate rainfall waves were identified. In the first, a well-defined and isolated storm complex developed along the coastline between Virginia Beach and Norfolk, producing very heavy rainfall for these areas (see the left panel of Figure 34). It is possible that this feature was caused by a localized land-ocean circulation that is physically constrained within some distance of the coastline (the region under this storm received over 5 inches of rainfall, whereas areas further south that received the main storm complex only recorded 4 inches or less). During the second rainfall wave, the main storm complex moved in from the southwest, causing 60-90 minutes of very heavy rainfall across the entire Norfolk-Virginia Beach area.

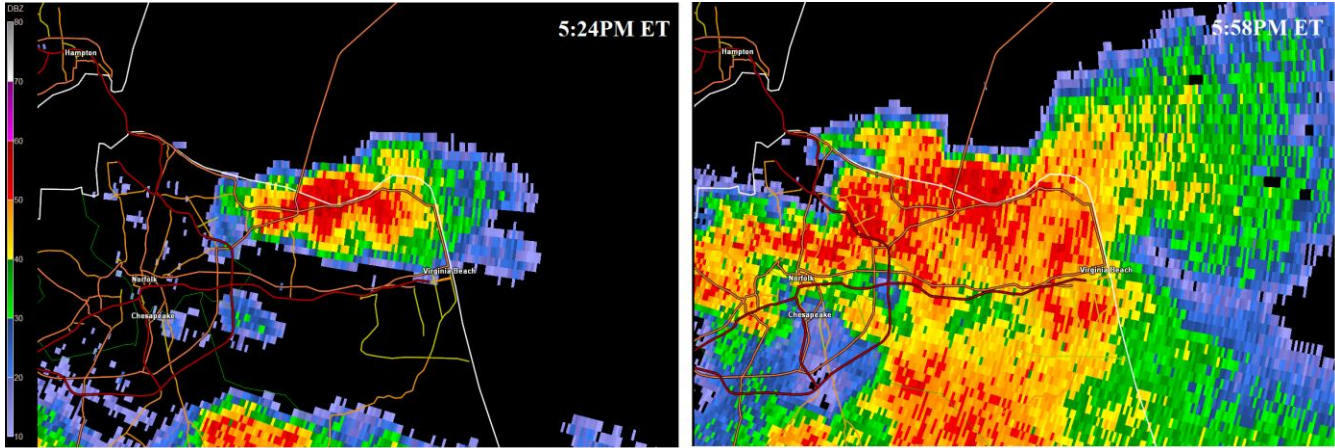


Figure 34: Base-elevation radar reflectivity scans from the Wakefield (VA) NEXRAD radar taken at 5:24PM and 5:58PM local time.

The hyetograph from the HRSD Ches-Liz Main Flow rain gage likely captured the most intense rainfall accumulation for the duration of the storm, shown in Figure 35. Despite the complexity of the radar reflectivity patterns, this gage showed a surprisingly steady accumulation over a period of about two hours (the resolution of this gage is 15 minutes, so it is possible that some variation in intensity would be noted if higher temporal resolution data were available). Nearby CoCoRaHS gages, as well as the Norfolk International Airport gage all confirmed that rainfall approached or exceeded 7 inches in the immediate area of northwest Virginia Beach.

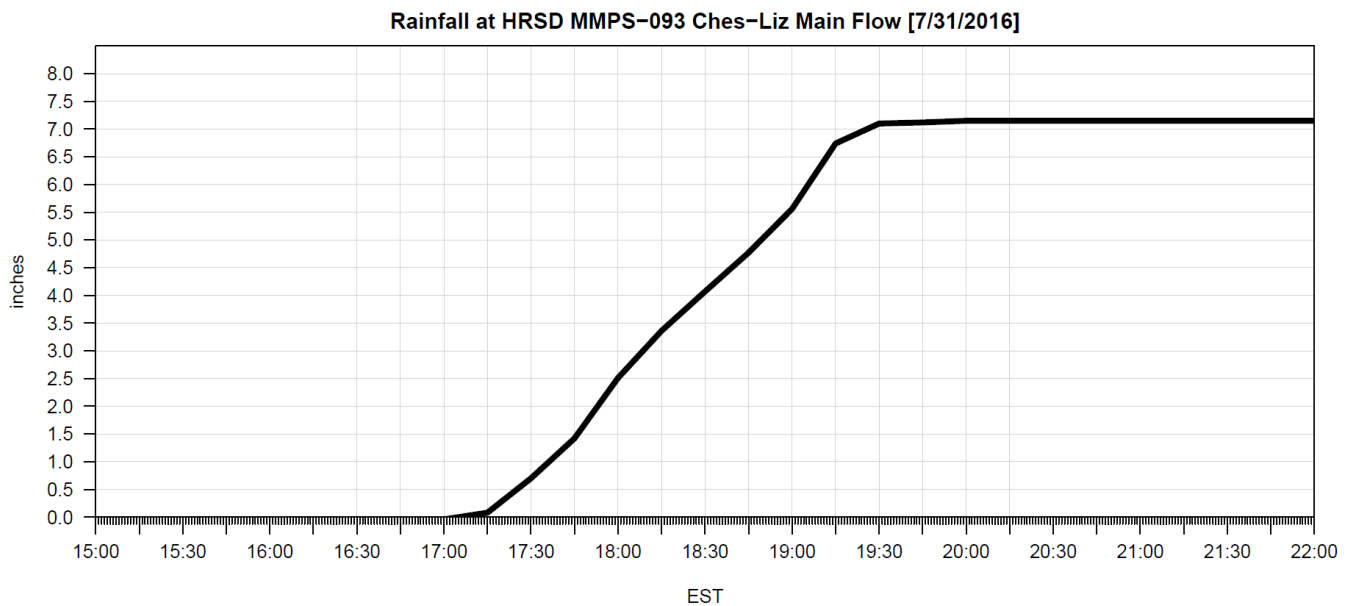


Figure 35: Accumulated rainfall at the HRSD Ches-Liz Main Flow gage, which was representative of the highest rainfall intensity produced during the July 31 event.

Table 10 summarizes the maximum rainfall intensity that occurred during the July 31 event. While the event did produce short-term heavy rainfall rates (for example, 1.18 inches in 15 minutes classifies as a 1 in 5 to 10-year event), it was the longer duration of this rate that made it particularly striking. For example, at the two-hour duration, 6.66 inches of rainfall was observed, which classifies as a 1 in 500 to 1000-year event. Notably, even though almost all of the rainfall fell within a two-hour period, this event still exceeds a 1 in 100-year event at the six-hour duration.

Table 10: Summary of precipitation intensity and return period estimates for the July 31, 2016 event.

Duration	Maximum Rainfall Amount (in)	Estimated Return Period (yr)
15 min	1.18	5-10
30 min	1.97	10-25
1 hour	3.38	50-100
2 hour	6.66	500-1000
3 hour	7.19	500-1000
6 hour	7.19	100-200

Tropical Storm Julia

Tropical Storm Julia (hereafter, “Julia”) affected the Virginia Beach area over a 72-hour period beginning on September 19. Although the storm itself was not particularly strong (with maximum winds topping out at 50 mph), it spent a considerable amount of time slowly drifting off the coastline of the southeast United States. In turn, this allowed for a prolonged fetch of subtropical moisture to be advected into southeastern Virginia. Numerous rounds of tropical-like showers and thunderstorms trekked across Virginia Beach, providing moderate to heavy rainfall. Figure 36 shows a summary of all gage hyetographs across the area (refer to Figure 30b for areal totals across the region). Interestingly, the heaviest shorter-term (six hours or less) rainfall intensity was observed on September 19, well before the main tropical-storm related rain bands moved into the region.

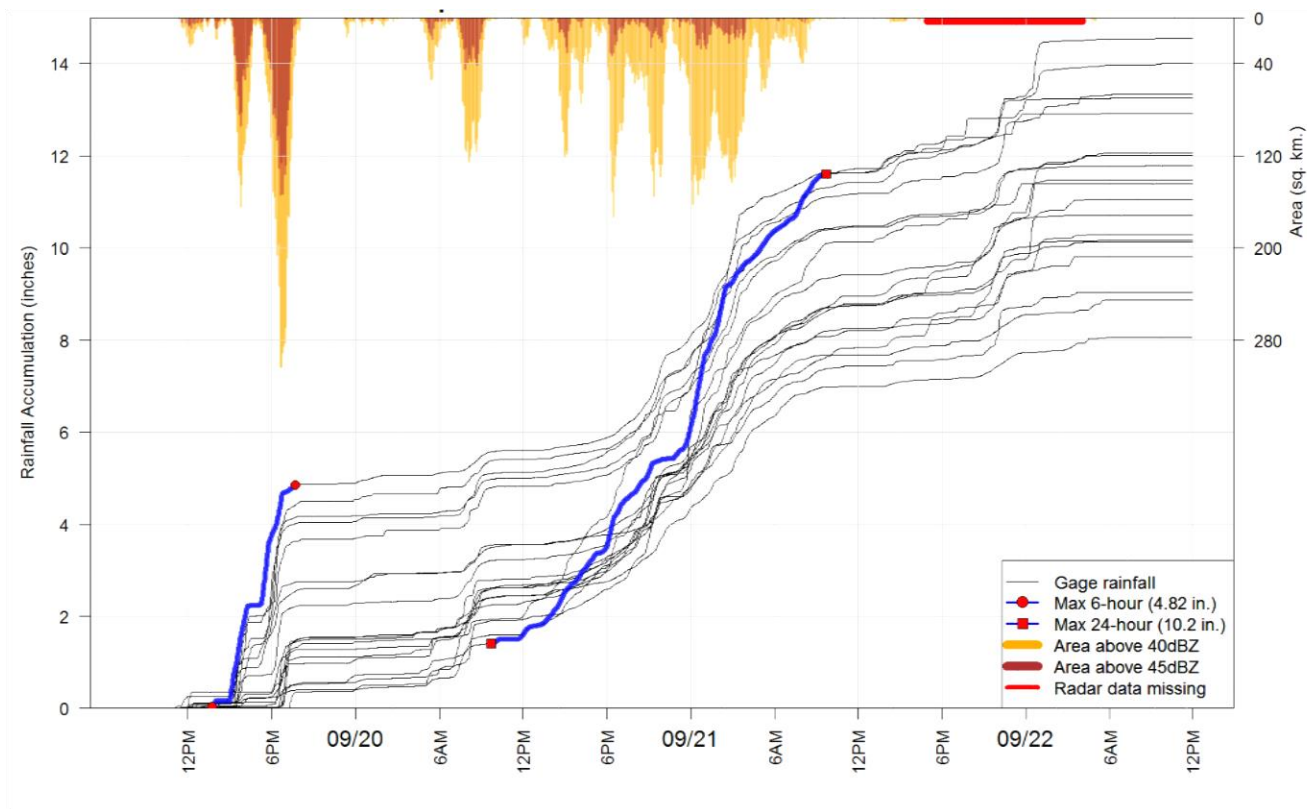


Figure 36: (Lines) Hyetographs of rainfall accumulation (left axis) during Tropical Storm Julia. The blue lines show the maximum 6-hour (red circles) and 24-hour (red squares) accumulations across all gages. The orange and brown bars denote areal coverage (right axis; units: km²) of “heavy” and “very heavy” rain, measured using the 40 dBZ and 45 dBZ radar reflectivity thresholds, respectively.

Table 11 shows a summary of the maximum rainfall amounts across a range of durations. As is typical with storms of tropical origin, it was not the short-term rainfall intensities that caused the highest impacts, but the long duration of the event. For example, the maximum one-hour rainfall rate was about 2.3 inches, which classifies as a 1 in 5 to 10-year event. However, once the duration is increased to 24 hours, parts of the area received over 10 inches, which amounts to a 1 in 100 to 200-year event.

Table 11: Summary of precipitation intensity and return period estimates for Tropical Storm Julia.

Duration	Maximum Rainfall Amount (in)	Estimated Return Period (yr)
30 min	1.64	5-10
1 hour	2.33	5-10
3 hour	3.62	10-25
6 hour	4.82	25-50
24 hour	10.20	100-200
48 hour	12.32	100-200

Figure 37 shows the maximum 24-hour hyetograph from each of the gages compared to several different design storms (10-, 25-, 100- and 500-year event). As previously described, none of the hyetographs mimic the design storm’s distribution due to the relatively disorganized nature of the storm’s precipitation field. A typical tropical storm impacts the region through organized rain bands, which increase in rainfall intensity as one gets closer to the storm circulation. In this case, however, the rainfall processes were driven by single and multi-cell thunderstorms that intermittently produced heavy rainfall. Nonetheless, Figure 37 shows that two gages ultimately tallied rainfall totals that exceeded 1 in 100-year values. Two of the 24-hour maximum hyetographs, labeled as “High” and “Low” in Figure 37, were selected for use as “Check Storms” to compare with design storm distributions. Microsoft Excel spreadsheets that break down each Check Storm’s rainfall accumulation into six-minute periods are also provided. These can be used for direct comparison with a design storm for Hydrologic and Hydraulic (H&H) modeling applications.

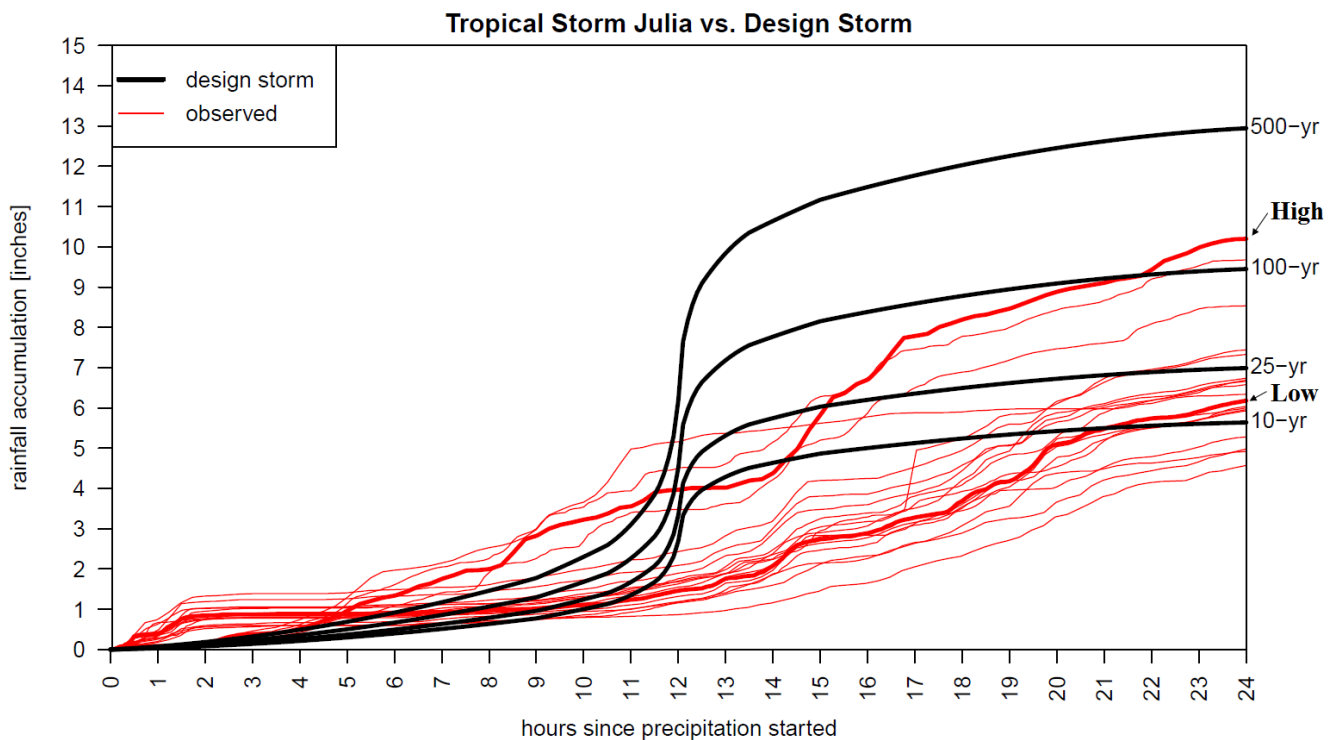


Figure 37: Maximum 24-hour hyetographs (red lines) during Tropical Storm Julia, as compared to the 10-, 25-, 100- and 500-year design storms. The thick red lines denote the two hyetographs (noted as “High” and “Low”) that were used as a “Check Storm” for which data was aggregated into six-minute totals for direct comparison to the design storm.

Figure 38 displays similar analysis to Figure 37, except for rainfall *intensity* at the three-hour duration. Intensities of the 10-year and 100-year storm are shown for comparison. Note that for the 24-hour design storm, the maximum three-hour intensity for any given return period matches the associated value derived by NOAA Atlas 14 (i.e. the dashed gray line in

Figure 38 compared with the peak of the 10-year event; the slight discrepancy may be attributed to selecting a slightly different point estimate than that used for the design storm calculation).

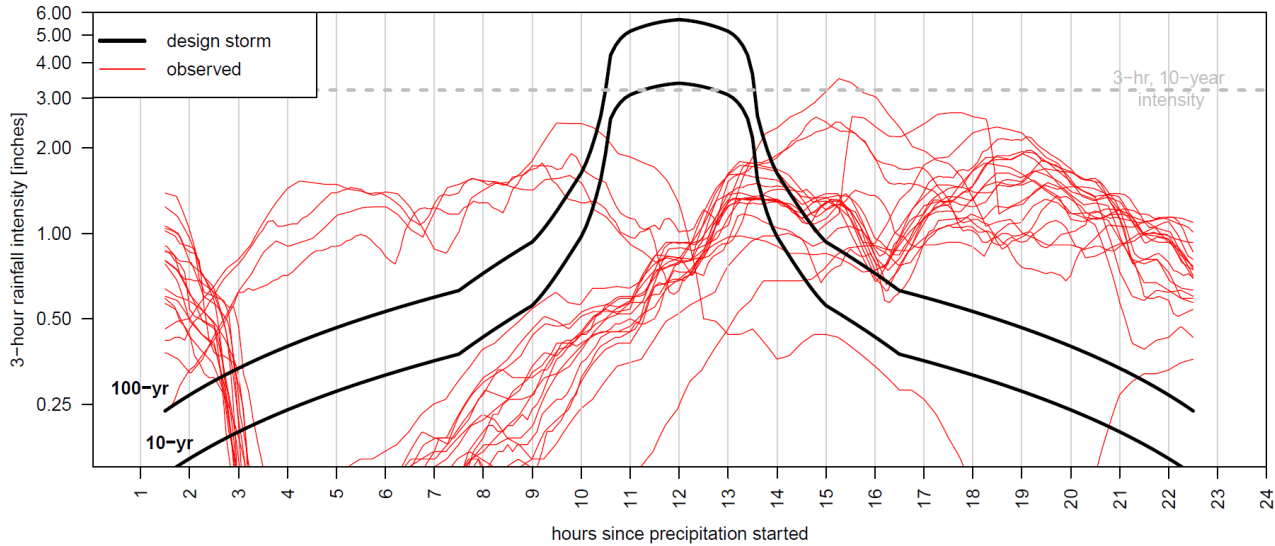


Figure 38: Three-hour rainfall intensity during Tropical Storm Julia, compared to the 10-year and 100-year design storm. For reference, the three-hour 10-year intensity from NOAA Atlas 14 is shown by the dotted gray line.

Collectively, Figure 36, Figure 37, and Figure 38 show that Julia was an exceptionally long-duration event that amounted to rainfall exceeding 1 in 100-year levels at the 24-hour duration and longer. However, shorter-term rainfall intensities were substantially lower than their design storm analogs. It is recommended that the Check Storm hyetographs be compared with design rainfall distributions within local H&H models to determine the durations at which the rainfall threat transitioned into a runoff and flooding threat.

Hurricane Matthew

In contrast to Tropical Storm Julia, Hurricane Matthew (hereafter, “Matthew”) provided one, sustained 12-15 hour period of very heavy rainfall across the Virginia Beach region as it moved northeastward along the coastline of the southeastern United States. Figure 39 shows the hyetograph summary of all rainfall gages. Note that, compared to Julia, there is significantly less spread in both rainfall distribution and intensity. This occurred because Matthew’s rain bands were more organized, as it maintained its structure throughout its effect on Virginia Beach.

Table 12 shows that, as with Julia, Matthew’s short-term rainfall rates were not particularly noteworthy. For example, the maximum 30-minute rainfall was 1.21 inches, and the maximum 60-minute rainfall was 2.11 inches, classifying as 1 in 1 to 2-year, and 1 in 5 to 10-year event, respectively. This was because atmospheric instability was limited across the region, which is common in the vicinity of tropical cyclones. Instead, it is the long duration of the rainfall that caused the vast majority of its impacts. For all durations longer than three hours, Matthew produced rainfall exceeding 1 in 100-year values across large sections of Virginia Beach.

Another important distinction between Matthew and Julia is the heavy rainfall coverage. Note that during Julia, the maximum coverage of the 40dBZ reflectivity (i.e. “heavy” rainfall) was about 280 km² (109 mi²), though this was only briefly observed. Throughout most of the event, that coverage was generally in the 40-120 km² (16-47 mi²) range. During Matthew, however, the maximum “heavy” rainfall coverage approached 420 km² (164 mi²) and stayed above 180 km² (70 mi²) for a period of six or more hours. As shown in Table 12, Matthew’s rainfall exceeded 12 inches at the 12-hour duration, classifying as a 1 in 500 to 1000-year event. This value was even exceeded by over half of the 28 gages used in the analysis. It is also noteworthy that most of the rainfall was coming to an end when the strongest winds began during the early morning hours of October 9 (see Appendix C). Thus, analyzed from the standpoint of joint rainfall-surge effects, Matthew is unlikely to have served as a worst-case scenario; however, it does serve as a reasonable event to test design against for extreme rainfall. Probable coastal water levels could be input as a tailwater boundary conditions in conjunction with the rainfall to address this limitation.

Table 12: Summary of precipitation intensity and return period estimates for Hurricane Matthew.

Duration	Maximum Rainfall Amount (in)	Estimated Return Period (yr)
30 min	1.21	1-2
1 hour	2.11	5-10
3 hour	5.54	100-200
6 hour	8.81	500-1000
12 hour	12.47	>1000
24 hour	13.14	500-1000

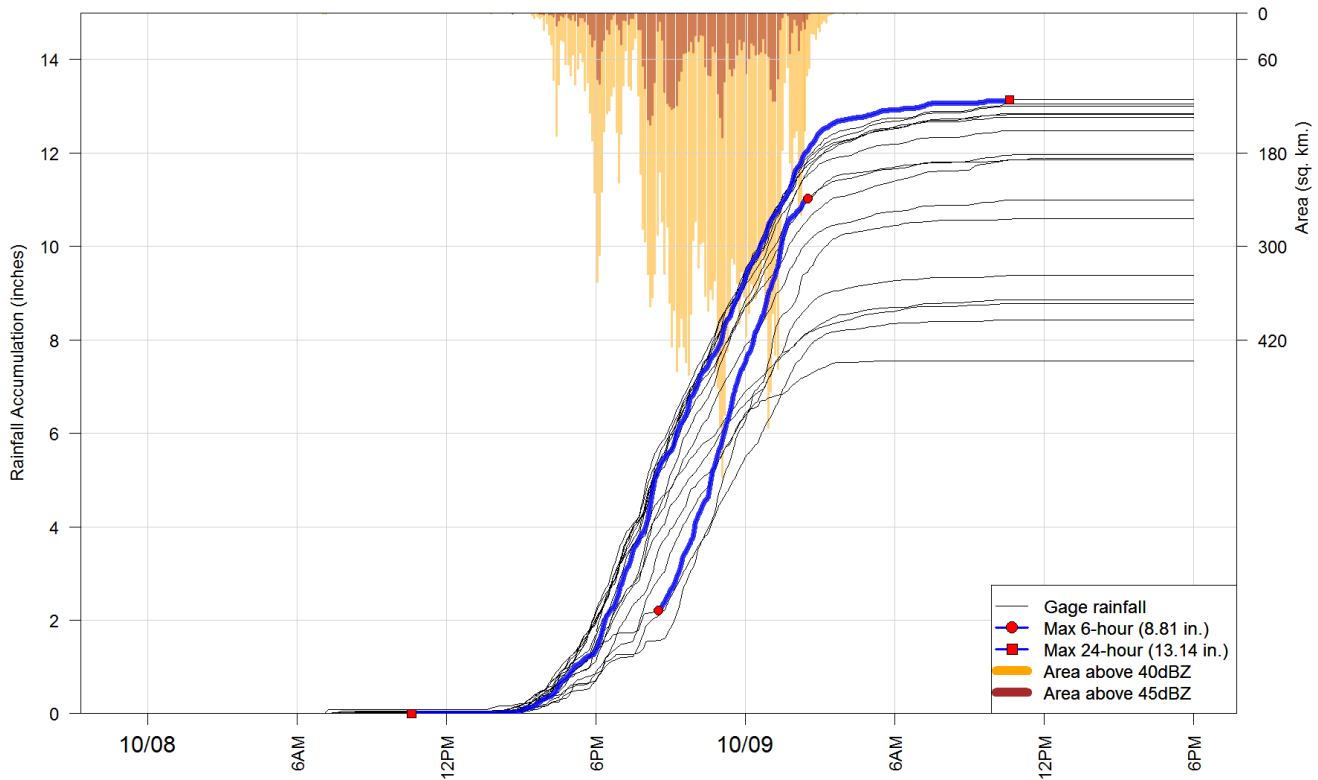


Figure 39: (Lines) Hyetographs of rainfall accumulation (left axis) during Hurricane Matthew. The blue lines show the maximum 6-hour (red circles) and 24-hour (red squares) accumulations across all the gages. The orange and brown bars denote areal coverage (right axis; units: km²) of “heavy” and “very heavy” rain as measured using the 40 dBZ and 45 dBZ radar reflectivity thresholds, respectively.

Figure 40 compares maximum 24-hour hyetographs with a range of design storm hyetographs. Note that the 24-hour duration captured nearly all of the rainfall that occurred during Matthew. One striking conclusion is that Matthew’s rainfall distribution bore little to no resemblance to a design storm due to its steady but long-lasting nature. This can be seen more clearly in Figure 41, which shows rainfall intensity over a three-hour period. Although Matthew will be noted as a 1 in 500-year event at the 24-hour level, its peak three-hour rainfall intensity was significantly longer-lasting than a design storm. Three hyetograph traces were selected as “Check Storms,” corresponding to “High,” “Mid,” and “Low” event-relative rainfall amounts. These are noted on the right y-axis in Figure 40 and have been aggregated into six-minute totals for comparison with a design storm.

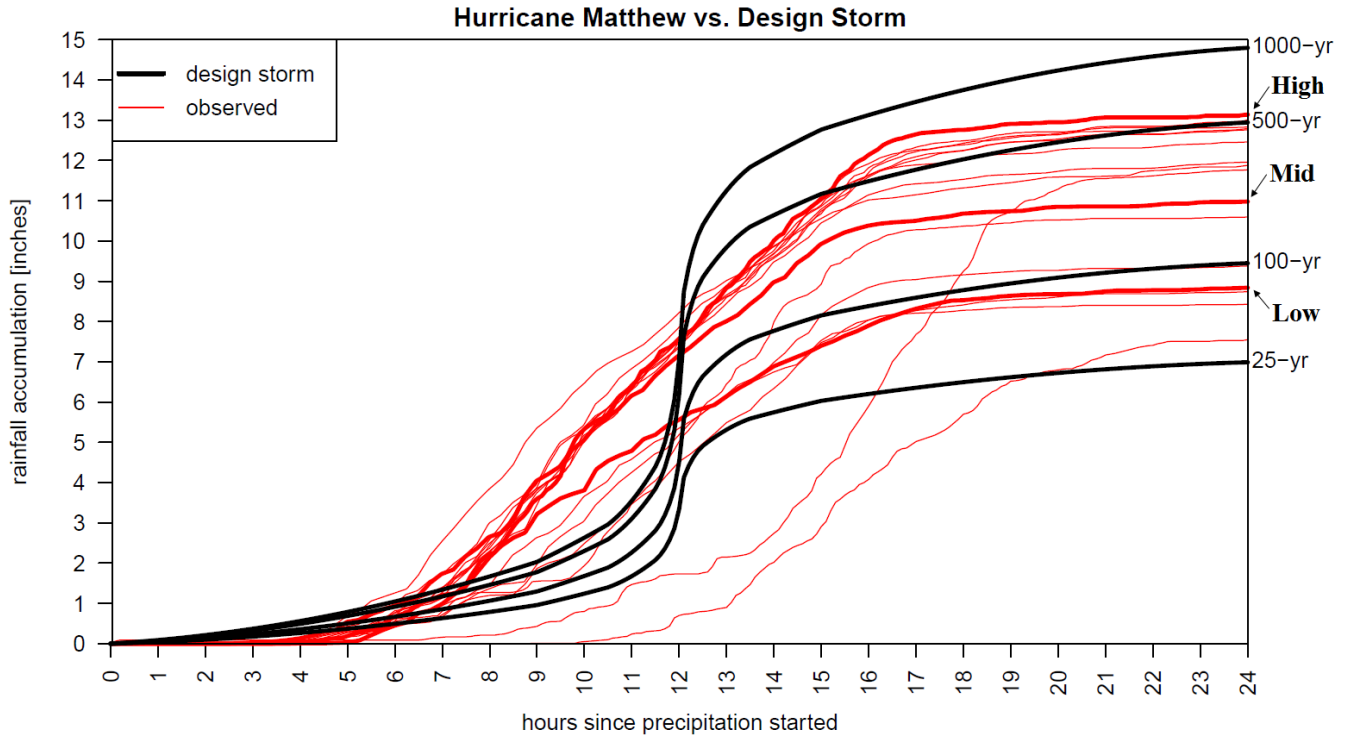


Figure 40: Maximum 24-hour hyetographs (red lines) during Tropical Storm Matthew, as compared with the 25-, 100- and 500- and 1000-year design storms. The thick red lines denote the three hyetographs (noted as “High,” “Mid,” and “Low”) that were used as a “Check Storm” for which data was aggregated into six-minute totals for direct comparison to the design storm.

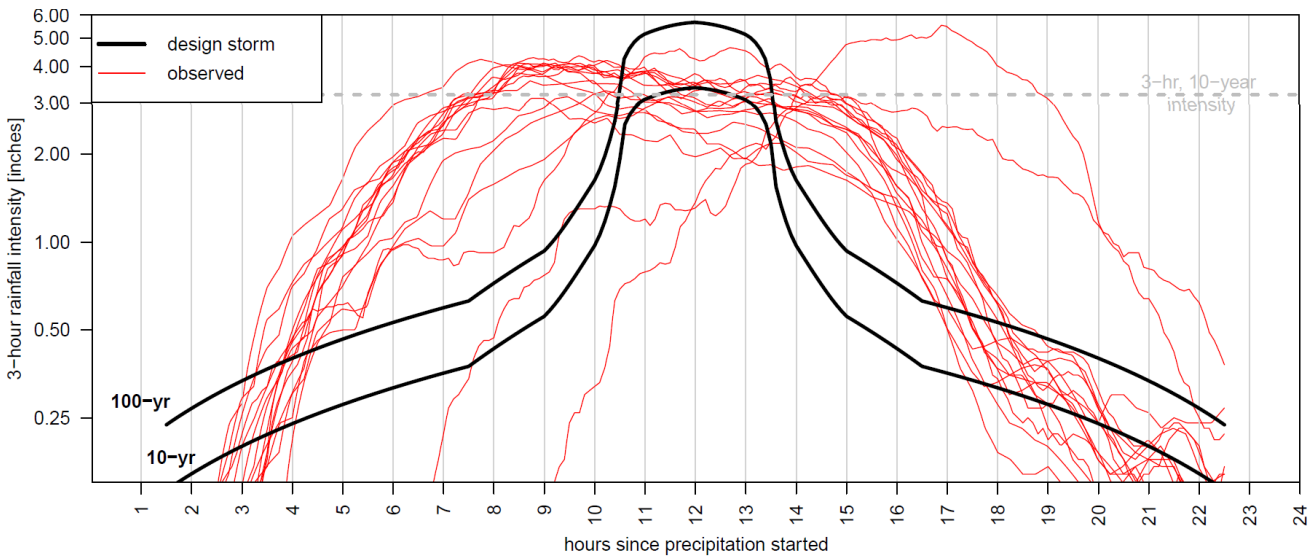


Figure 41: Three-hour rainfall intensity during Hurricane Matthew, compared to the 10-year and 100-year design storm. For reference, the three-hour 10-year intensity from NOAA Atlas 14 is shown by the dotted gray line.

Comparison to Probable Maximum Precipitation

Two main sources of Probable Maximum Precipitation (PMP) estimates have been identified for the Virginia Beach region. The first source is HMR 51 (Schreiner and Riedel, 1978), prepared by the United States Weather Bureau in 1978. Figure 42 shows the 24-hour PMP isopleths for a 10 mi² event, the smallest area considered in that report. For Virginia Beach, the 24-hour PMP value is between 40 and 42 inches, which is at least twice as high as anything observed during Julia or Matthew.

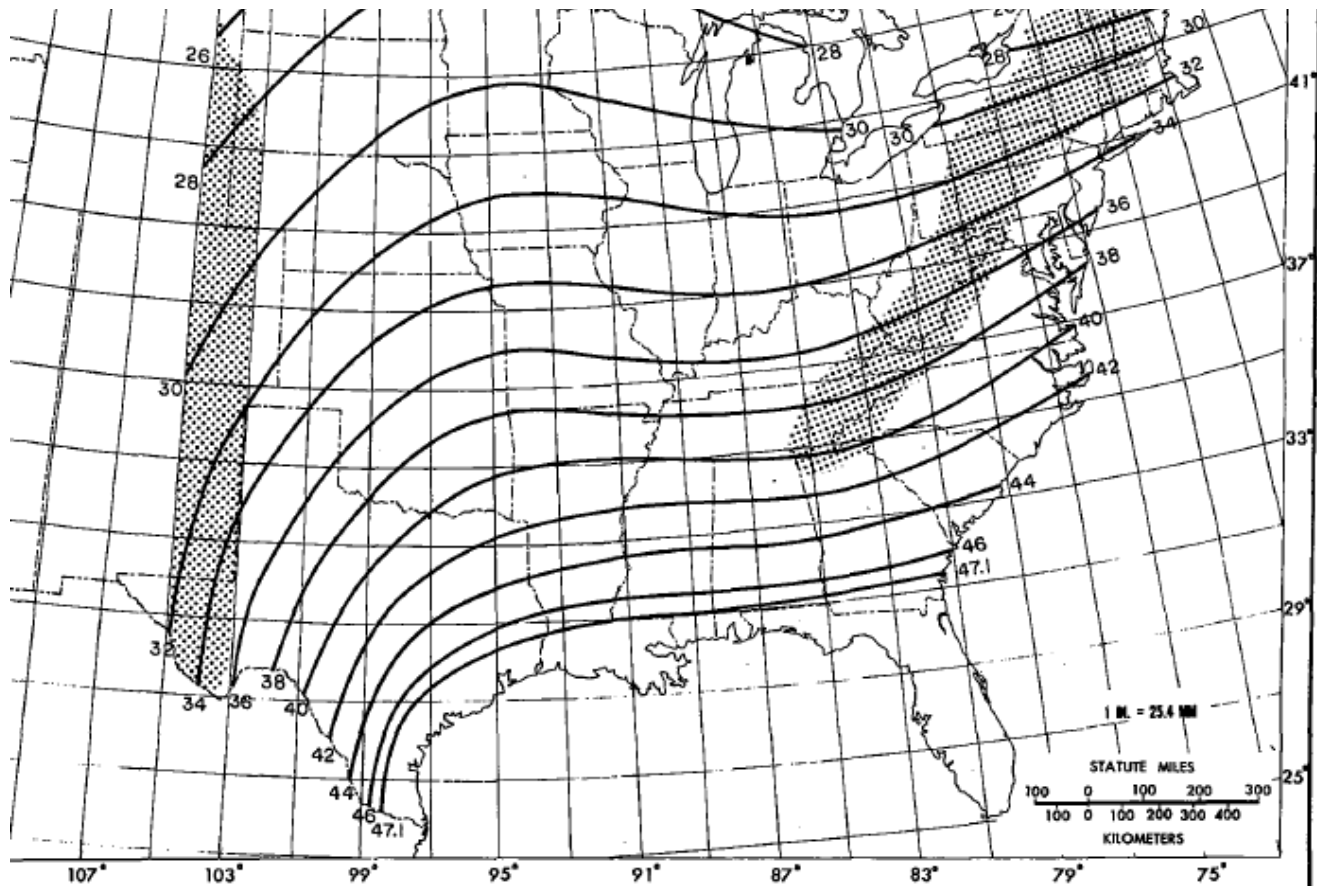


Figure 42: All-season PMP (in.) for 24-hour 10 mi². Adapted from Schreiner and Riedel (1978; their Figure 20).

In 2015, a comprehensive PMP study was completed by Applied Weather Associates (2015) for the Virginia Department of Conservation and Recreation (DCR). While the study found significant reductions in PMP estimates (compared to HMR51) across western parts of Virginia, the estimates for the Virginia Beach area were within approximately 10% of the values developed in HMR51. Figure 43 shows the percent difference between the Virginia DCR study and HMR51.

PMP Comparison to HMR 51 - Percent Difference 24-Hour 10 mi²
Virginia Statewide PMP Study

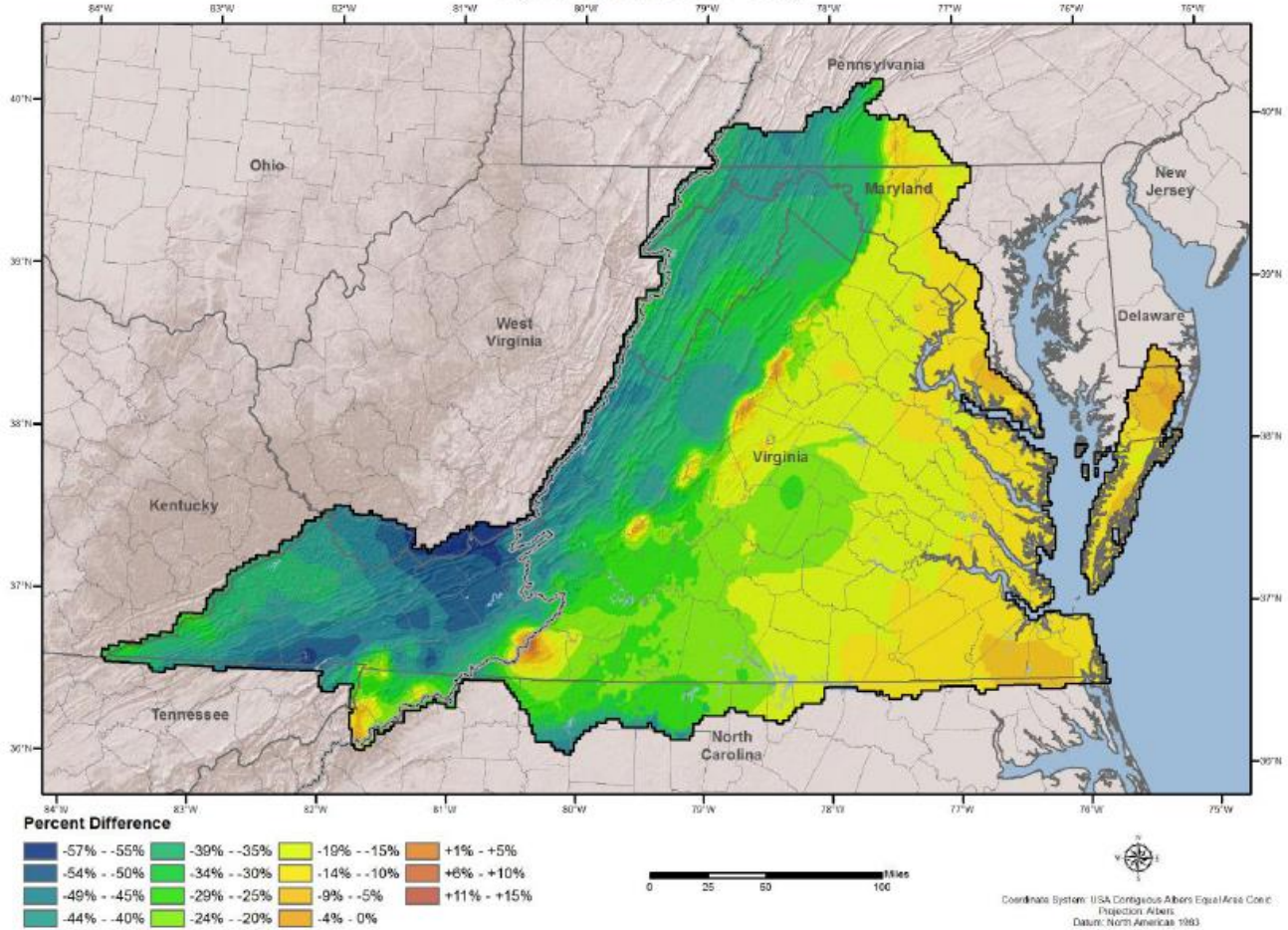


Figure 43: Percent difference of HMR 51 values compared to largest PMP values from all three storm types; 24-hour 10 square miles. Note that the scale in the legend is specific to the image. Taken from AWA (2015), their Figure 10.12.

Having conducted the rainfall analysis for each of the three 2016 events, we can use HMR51 and the Virginia DCR study to estimate how each event compares to PMP as shown in Table 13. Without having performed a comprehensive rainfall depth-area analysis, we use the 10 mi² PMP estimate to the gage-level analysis that was conducted in the current study (10 mi² is the smallest spatial area for which PMP is estimated in HMR51). For Hurricane Matthew, however, there is reasonable confidence (see 40 dBZ coverage area [orange bars] in Figure 40) that areas covering 200 mi² received over 12 inches of rainfall. Therefore, we also present an estimate for the 200 mi² area for Matthew. For the 10 mi² area, fractional PMP ranges from 0.21 for the July 31 event to 0.36 for Matthew. However, for the 200 mi² area, Matthew had a fractional PMP of 0.50, which is higher than many design standards for small- to mid-sized water control

structures (e.g. FEMA, 2016). Thus, this analysis confirms that of the three events, Matthew was the most severe in terms of heavy rainfall production.

Table 13: Fractional PMP estimates for each of the three events considered in this study.

Event	Max Rainfall		Fractional PMP	
	Duration	Amount	10 mi ²	200 mi ²
July 31, 2016	<6 hour	6.19 inches	0.21	---
Tropical Storm Julia	24 hour	10.20 inches	0.26	---
Hurricane Matthew	12 hour	12.47 inches	0.36	0.50

Hyetograph Deliverables

Five Microsoft Excel-compatible, comma-separated value format files have been provided showing 6-minute normalized rainfall accumulation fraction (column “norm_sum”), incremental rainfall amounts (column “amount”) and accumulated rainfall amounts (column “accum”) for two “Check Storms” based on Tropical Storm Julia (High, Low) and three “Check Storms” based on Hurricane Matthew (High, Mid, Low).

CHAPTER 4: REVIEW OF RAINFALL DESIGN GUIDANCE

Introduction

Despite a growing amount of evidence, both historically observed and future climate projections, that shows increases in heavy rainfall occurrence, implementing this data into design rainfall remains a challenge. The principle obstacles include (1) uncertainty regarding whether historical statistically “significant” trends, if detected, will continue, and (2) significant spread in GCM projections. Integrating improved statistical methods involving the latest climate change guidance to 1) quantify uncertainty and 2) improve development of procedures for design rainfall used in hydraulic engineering applications is an active area of research at the national and local level. Fundamental to the design of effective and resilient stormwater infrastructure is the need to quantify the type, frequency, and magnitude of precipitation events likely to impact the area.

The vocabulary and metrics used to measure precipitation by the climate science community (e.g. heavy or very heavy rainfall) is different from that used by engineers (e.g. 6-Hour or 24-Hour duration). The need to equate these differing metrics for purposes related to water resources engineering applications is addressed in the Federal Highway Administration (FHWA) Hydraulic Engineering Circular #17 (HEC-17):

“Groisman et al. (2005) equate very heavy precipitation to a return period of approximately one daily event in 3 to 5 years for annual maximum daily precipitation. Hence, the frequency and intensity of precipitation emphasized in much of the climate literature is at the lower end (smaller magnitude, more frequent) of the range of events typically used by the engineering community... precipitation rates typically associated with significant flooding are approximately 3 in/h, 5-16 in/day, and 17 to 20 inches in three days (Perry et al. 2000).”

In order for the practicing engineer to incorporate climate model projections in their analyses, a clearly defined methodology for translating interpreted results from GCM’s into actionable mechanisms for use in design rainfall is required. Another challenge is that design values for water resources applications are determined by peak rainfall totals. However, it is well known that GCM output underestimates local-level rainfall. This requires the downscaling of the raw data to a “point” (i.e. gauge) level, using a combination of dynamical and statistical based methods, as was performed using the Norfolk gauge in Chapter 2.

In this memo, federal and state guidance on resilient design standards are summarized. In addition, a summary of interviews conducted with practitioners about their experience with

updating rainfall design guidance is presented. Finally, in the conclusion section of this report, a recommendation is put forth regarding how to deal with potential changes in heavy rainfall frequency and intensity.

Federal Guidance

Federal agencies are assessing the impact of climate change in their areas of jurisdiction. The U.S. Army Corps of Engineers (USACE), Environmental Protection Agency (EPA), Federal Emergency Management Agency, and the USGS are developing methodologies to integrate the Intergovernmental Panel on Climate Change's (IPCC) 5th Assessment Report (AR5) climate projections. Of particular interest are projections of precipitation and temperature and their impact on the design parameters used to manage flood control and other water resources projects under their authority. Similar efforts are being undertaken by the National Weather Service (NWS) to evaluate non-stationary in observed rainfall data. For example, as part of the latest rainfall guidance NOAA Atlas 14, trends in heavy rainfall were analyzed regionally. Although regional-scale trends were not conclusive enough to warrant a full non-stationarity analysis in the actual guidance, local-scale changes, such as those in southeast Virginia, were more notable.

The USACE has summarized its guidance to incorporate climate impacts into inland hydrological analysis in the Engineering Construction Bulletin 2016-25. This bulletin recommends a qualitative analysis to determine observed changes in climate as well as potential future trends projected by the climate models. (See also Public Tools Developed by USACE for Climate-Impacted Hydrology¹)

The EPA has published a Storm Water Management Model Climate Adjustment Tool (SWMM-CAT), a software utility that allows the user to compute location based adjustment factors to be applied for 24-hour design storm; these adjustment factors are derived based on CMIP3 climate data projections statistically downscaled to a roughly 12 km (7 mi) horizontal resolution. To obtain the future design rainfall, the adjustment factors are intended to be applied on national standards for design rainfalls. In 2016, EPA published a web-based application, Climate Resilience Evaluation and Awareness Tool (CREAT), as an information

¹ USACE's climate projections use statistically downscaled Coupled Model Inter-Comparison Project Phase 5 (CMIP5) climate data projections published through a collaborative effort that also includes the USBR, USGS, Lawrence Livermore National Laboratory, and other partners. The tools are a means of detecting a climate trend; guidance on attribution of the trend to climate change and how to incorporate the detected change into hydrologic analysis is not available.

tool to assist drinking water, wastewater, stormwater utility owners and operators to understand and address climate change risks. For projected climate conditions, CREAT uses CMIP5 projections for RCP 8.5. Total storm precipitations for future periods is one of the parameters estimated by CREAT for the purpose of estimating future threats to the water industries. Although the EPA's methods are certainly a step closer to real rainfall compared to raw GCM data, each product still lacks the resolution to inform local-level analysis as is required for informing design. Recall that this was addressed in Chapter 2 by using the Norfolk Airport rain gauge as a method of bias correcting downscaled model data to design-scale resolution.

In order to estimate the changes in the 1% chance floodplains, the Federal Emergency Management Agency (FEMA) has developed climate regression equations within Hydrologic Unit Code -2 (HUC-2) regions as the geographic unit. The United States and its unincorporated territories are covered by 21 HUC-2 watersheds with drainage areas ranging from 3,515 to 615,000 square miles. Generalized Least Square multiple linear regression analysis was used to develop climate regression equations that relate 1%-annual chance and 10%-annual chance peak discharges at stream gage stations to the watershed characteristics and extreme climate indices of the contributing watershed. A total of 7,306 stream gages with 20 or more years of annual peak flow record were selected for this study from the 9,322 stream gages included in the USGS Geospatial Attributes of Gages for Evaluating Stream Flow (GAGES II) database. The regression-based methodology was extended to incorporate a climate change component based on IPCC CMIP5 projections. However, this approach is more geared towards informing future conditions in ungauged locations. Due to a significant amount of scatter around the regression equation approach, its direct application for a well gauged location like the Virginia Beach area is likely limited.

HEC-17 attempts to fill in the need to evaluate the potential changes in the frequency and severity of storms and floods on bridge and design practices for federal highways. Current guidance recommends the use of NOAA Atlas 14 for design precipitation, however methodologies to evaluate the stationarity or non-stationarity are recommended if a trend is detected at a given location:

“Planners and designers assessing the historical record for precipitation trends should be careful to define the season, magnitude, duration, and frequency of the precipitation statistic of interest to understand the risks to plans and projects revealed by the historic data. As discussed, less extreme precipitation data may exhibit trends, but may not result in changes in the types of floods of interest to engineers...Because of

the statistical nature of the analyses supporting Atlas 14, confidence limits for the precipitation estimates are available.”

HEC-17 goes on to provide the following guidelines:

“The objective is to estimate the projected change in the T-year 24-hour precipitation value as an indicator of the potential for climate change (climate non-stationarity) to affect the estimated design discharge based on historical data...Regardless of whether the design team is using rainfall/runoff or statistical models for the hydrologic analysis, this indicator is useful for evaluating the potential for changes in flood flows resulting from projected changes in climate for the T-year event.”

...FHWA recommends the use of multiple climate models. At a minimum, the design team should develop a climate change indicator for RCP 6.0 and FHWA recommends investigation of other emissions scenarios when possible as summarized in Section 7.3.

The development of this indicator begins by acquiring the downscaled daily precipitation data from the DCHP website, or equivalent database. The design team should download all years of available data (1950 through 2099) so that if there are changes in the periods of interest, all available data are present.

Once the daily data are downloaded, the indicator is developed by processing the data according to the following steps. If more than one emission scenario is examined, these steps are repeated for each scenario:

- 1. Average the observed daily precipitation data across all cells,*
- 2. Determine the maximum annual value for each year,*
- 3. Select the baseline and future periods,*
- 4. Compute the baseline and future T-year 24-hour precipitation for each model,*
- 5. Estimate the projected T-year 24-hour precipitation for each model,*
- 6. Compute the mean for the projected T-year 24-hour precipitation, and*
- 7. Evaluate the need for additional analysis.”*

The HEC-17 guidance, noted above, is very similar to the analysis conducted as part of Chapter 2. Although their recommendation was to use the RCP6.0 scenario, we believe this to be somewhat arbitrary and likely based on the assumption that most users may only consider one scenario. In fact, the consideration of RCP4.5 and two different sets of simulations of RCP8.5 provides a reasonably encompassing view of projections.

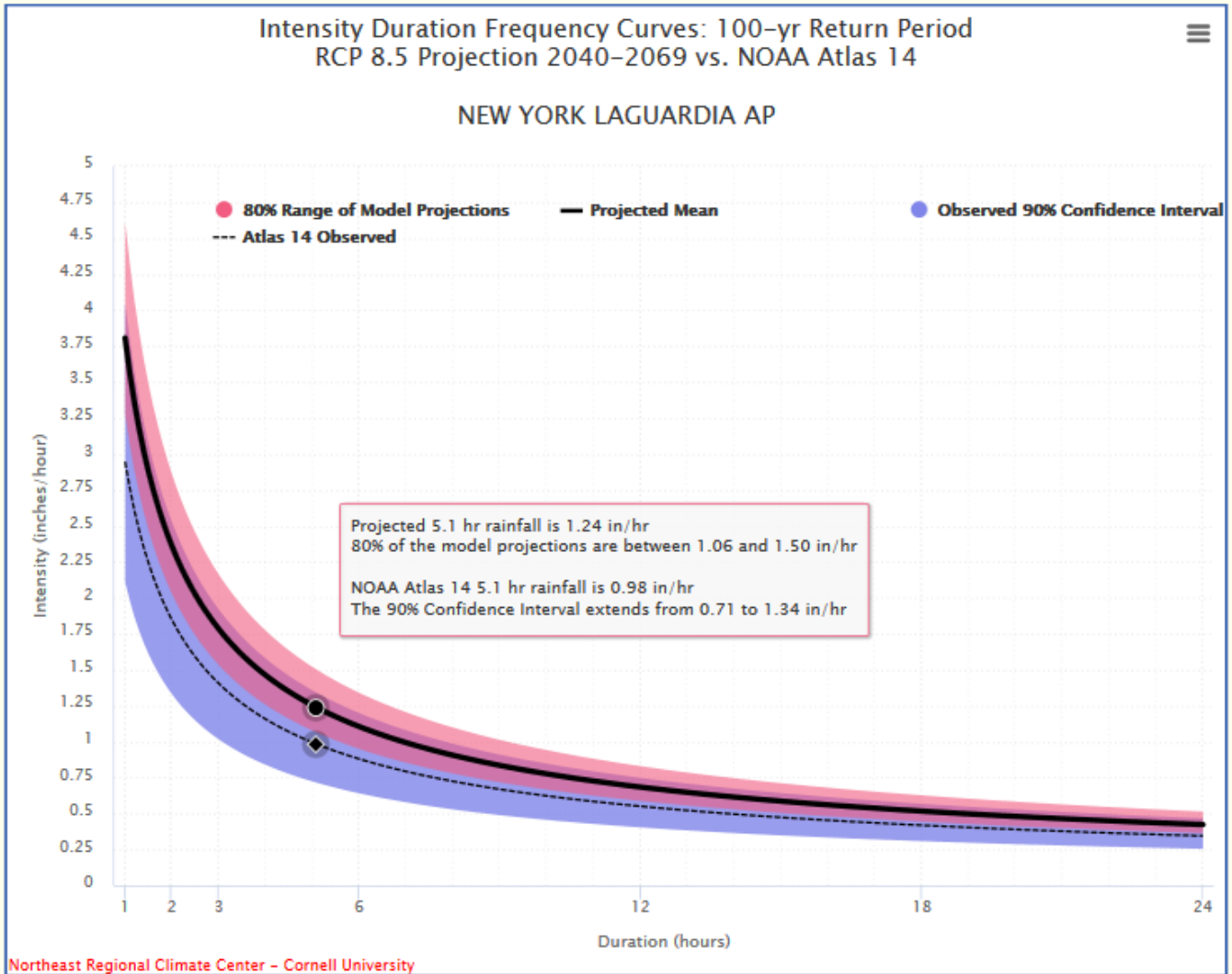
State Guidance

The State of New York has funded studies to use downscaled climate model projections to evaluate future temperatures, annual rainfalls, the possibility of droughts, etc. Principal among the NY studies is the Intensity Duration Frequency Curves for New York State: Future Projections for a Changing Climate, published by the Northeast Regional Climate Center (NRCC) of the Cornell University for New York. Projections of 24-hour rainfall for a location within the area of interest were estimated over a range of frequencies for the years 2045 (mid-term) and 2075 (long-term) and the RCP4.5 and RCP8.5 scenarios, compared to the current growth curve. An example of the web-based tool's output for the New York City area is shown in Figure 44. The analysis in Chapter 2 has many similarities to NRCC's study including similar downscaling method (though note that the NRCC study used several different downscaling approaches), the selection of the two emission scenarios and creation of uncertainty bounds.

In a separate study, the New York Department of Transportation in cooperation with the New York State U.S. Geological Survey used CMIP5 projections to produce potential future flow scenarios. These future projections for frequency discharges are offered through a web-based application titled 'Application of Flood Regressions and Climate Change Scenarios' (see report for details). This application computes peak discharges for 1.25-, 1.5-, 2-, 5-, 10-, 25-, 50-, 100-, and 500-year frequency events for three time periods, 2025-2049; 2050-2074; and 2075-2099. RCP 4.5 and 8.5 simulations of five of the CMIP5 models that best reproduced the past precipitation were used in the future peak flow estimation.

Interviews

Although the official guidance documents and methods described above are addressing the design rainfall issue, it is not clear to what extent the findings and relevant recommendations are being implemented at the local level. Phone interviews were conducted with engineers from Maryland, New York and Colorado (See Appendix E). Unfortunately, the take-away message is that all four agencies were using either the latest NOAA Atlas 14 guidance, or even the older Atlas 2 guidance. Engineers in Maryland and Virginia responded very similarly, stating that standard guidance was used, and no effort to augment current practice was being considered. Mr. Stewart from Denver's Urban Drainage and Flood Control District did state that the agency considered local rainfall trends, but found none. In turn, this reduced the interest in considering future projections, though he stated uncertainty regarding insufficient model resolution to simulate the region's heavy rainfall events was also a complication preventing the consideration of projections.



Duration (hrs)	Projected 2040-2069 Intensity Ensemble Member			Observed NOAA Atlas 14 Intensity with Confidence Interval (CI) Bounds		
	10 th	Mean	90 th	Low CI	Mean	High CI
1	3.27	3.81	4.61	2.11	2.95	4.04
2	2.03	2.36	2.86	1.33	1.85	2.53
3	1.53	1.78	2.16	1.02	1.40	1.92
6	0.95	1.11	1.34	0.64	0.88	1.20
12	0.59	0.68	0.83	0.40	0.55	0.75
18	0.44	0.52	0.63	0.31	0.42	0.57
24	0.36	0.42	0.51	0.26	0.35	0.47

Figure 44: Snapshot from the Northeast Regional Climate Center’s web-based tool showing changes in the IDF for the New York City area.

CONCLUSIONS

A comprehensive analysis of historical and future projections of heavy rainfall, as well as a comprehensive evaluation of three heavy rainfall events responsible for flooding in the City of Virginia Beach during 2016 has been conducted. The salient findings are discussed below.

Historical Analysis

- A meteorological analysis of VB's heavy rainfall climatology revealed many more Tropical-related events as well as Bullseye, worst-case scenario-type hits over the past 15-20 years; this could be driving part of the recent increases in heavy rainfall occurrence and intensity even though it is difficult to attribute such forcing to climate change.
- Gage-level analysis revealed a significant increase of 2.0 inches per century in the magnitude of Annual Maximum Series of 24-hour rainfall at the Norfolk Airport long-record gage; similar increases were noted when assessing the Peaks-Over-Threshold using a 24-hour threshold value of 1.25 inches.
- Extension of the Norfolk Airport gage using the nearby Diamond Springs gage showed lower increases than the Norfolk Airport gage alone, suggesting that heavy rainfall frequency and intensity increases have been especially large in the past 2-3 decades; this suggests climate change could be a driver of at least part of the signal, given that the last 30 years of data have been increasingly affected by a warming atmosphere (see Appendix A).
- A local-level analysis revealed a marked increase in 24-hour Annual Maximum Series intensity in a 60-mile radius around VB. A major part of this signal was from more available rain gages, or "gage inflation", which contributed to a better spatial sampling of heavy rainfall events. The local-level analysis also showed that design rainfall at a point-location such as the Norfolk airport gage may be starkly lower than a neighborhood-type approach. The latter can be impactful for flooding, since flooding is driven by rainfall volume and not point-rainfall.
- A regional-level analysis across the mid-Atlantic and Northeast states revealed widespread and significant increases in the AMS (*intensity*) and Peaks Over Threshold (*frequency*) across many gages. The results were statistically significant, and are thus unlikely to have occurred by chance. The regional-level trends provide more evidence for a climate change-related signal since many more storms are being considered than in the gage-level and local-level analyses.

Future Projections

- Two analysis were prepared: first, using high resolution (11 km) models that used the RCP8.5 scenario, and second, using medium resolution (44 km) models that used both the RCP4.5 and RCP8.5 scenario.
- Bias-corrected future projections of daily rainfall using multiple Regional Climate Models were able to reproduce the heavy rainfall statistics at the Norfolk Airport gage and thus were suitable for preparing gage-level projections.
- High resolution RCP8.5 projections of Peaks-Over-Threshold using the two-year and five-year events showed strong increases in heavy rainfall occurrence. For the two-year event, the historical rate of 4.6 events per decade was projected to increase to 8.8 in 2045 and 9.0 in 2075. For the five-year event, the historical rate of 1.6 events per decade was projected to increase to 4.3 in 2045 and 4.7 in 2075.
- For both high resolution and medium resolution RCP8.5 simulations, projected increases in the Precipitation-Frequency curve were shown for nearly all return periods in 2045 and for all return periods in 2075. The range of projected increases by 2045 was 17-24% (aside from 8% decrease in the one-year event), with statistical significance for events of ten-year intensity or less. The range of projected increases by 2075 was 21-41%, with statistical significance for events of 20-year intensity or less.
- For the medium resolution RCP4.5 simulations, projected changes included an up to 20% increase in the 1- and 2-year event, but little to no change for less frequent events.
- A non-linearity in the response of heavy precipitation to climate change is noted, with much stronger sensitivity in the RCP8.5 scenario.

It is recommended that differences in the model bias (Figure 16 and 23) be investigated further. For example, it would be useful to investigate the fidelity with which models reproduce the different AMS-producing processes identified in Table 1. This will also help explain the differing sensitivity of the projections to model resolution (e.g. Table 7).

Check Storm Analysis

Findings for each examined event in terms of 1) observed rainfall as compared the areas precipitation-frequency curves, 2) comparison to the NOAA Type C design storm, and 3) comparison to the region's PMP estimates are summarized below.

July 31, 2016

- Up to 6.66 inches over a two-hour period and 7.19 inches over a three hour period, translating to a 1 in 500 to 1000-year event for both durations.
- Highest totals were in the northern parts of the city, with substantially less rainfall further south.
- At the six-hour duration, this event translates to a fractional PMP of 0.21.

September 19 – September 22, 2016 (Tropical Storm Julia)

- Exceptionally long duration event with heavy precipitation observed for a 72-hour period.
- Shorter-term rainfall amounts were not particularly noteworthy; for example, the maximum six hour rainfall was 4.82 inches, which translates to a 1 in 25- to 50-year event.
- At the 24-hour duration, two of 28 gages used the analysis exceeded the 1 in 100-year rainfall amount (9.41 inches). Most of the other gages recorded 24 hour amounts that corresponded to the 1 in 10- to 25-year recurrence interval.
- Due to the long duration, none of the individual gage hyetographs resembled the design storm.
- At the 24 duration, the maximum observed rainfall corresponded to a fractional PMP of 0.26.

October 8 – October 9, 2016 (Hurricane Matthew)

- The most severe of the three events, when considering duration and intensity collectively.
- In contrast to Julia, produced one, sustained 12-15 hour period of very heavy rainfall across the entire region.
- For durations shorter than three hours, rainfall was in the 1 in 2 year to 1 in 10 year range.
- For all durations longer than three hours, rainfall exceeded 1 in 100-year amounts. At the 12 hour duration, multiple gages observed rainfall exceeding 12 inches, which corresponds to a 1 in 500- to 1000-year event.
- None of the gage hyetograph distributions resembled the design storm, mainly because the event never had a peak in rainfall intensity. Instead, continuous rain rates were observed over an 8-10 hour period during the event's peak intensity.

At the 12 hour duration, the maximum observed rainfall corresponded to a fractional PMP of 0.36 for a 10 mi² area, and a fractional PMP of 0.50 for a 200 mi² area.

Rainfall Design Guidance

Having conducted national-, state- and local-level analysis of heavy rainfall trends and projections, our experience is that several factors must be analyzed to establish the necessity of updating guidance.

1. Consistency between historical observations and historical model simulations.

All IPCC simulations are initialized in 1950 or earlier for a good reason: it is essential that models can accurately capture any already documented heavy rainfall trends. Indeed, this is the case across most of the eastern United States, where both long-term rain gauge data and GCMs have shown increases in heavy rainfall occurrence and

intensity. A lack of such agreement instantly increases the skepticism with which to view future projections. Although a model's inability to reproduce past climate does not necessarily imply it will be wrong in the future, it does warrant an extra amount of investigation that is unlikely to be funded by a local agency.

2. Limited uncertainty bounds in future projections.

Although uncertainty in temperature projections are relatively low, even at a local-level, the same is not always true for precipitation. If the uncertainty in future precipitation is so large that it completely overwhelms the historical uncertainty range, there is little motivation for more detailed investigation. We have seen this first hand when assessing the USACE's Climate Hydrology Assessment Tool. At this point, the issue goes back to the academic community with the aim of reducing the uncertainty range through more realistic modeling.

From the findings in Chapter 1 and Chapter 2, it is clear that both factors above are met in the Virginia Beach area. Analysis of historical observations shows a robust, statistically significant increase in heavy rainfall not only in the immediate area but also in the region. Meanwhile, future projections using the RCP4.5 and RCP8.5 scenarios both show increases in heavy rainfall. The observations made in this document on heavy precipitations trends justify consideration of increased design rainfall intensities. Key results to consider include:

- Historically, precipitation Annual Maximum Series have trended upward between 3-7% per decade. Using an average of 5% would suggest a 20% increase given a 40-year time horizon.
- Future projections support increases of 5% for the intermediate scenario to 24-27% in the high scenario by 2060. A blend of the two to account for uncertainty in the actual outcome warrants a 15-16% increase.
- Current Atlas 14 guidance for the 10 year rainfall event may be 7-10% below the actual localized value based on analysis of two long-record rain gages in the area. If such is the case, then even using the intermediate RCP4.5 projections of 5% would already warrant a 12-15% increase in the Precipitation Frequency curve.

Based on the above, we recommend a 20% increase in rainfall intensity above current standards. Table 14 summarizes the recommended changes, compared to the current NOAA Atlas 14 that is used by the City.

Table 14: Recommended Precipitation-Frequency curve values at key return periods, based on a 20% increase of NOAA Atlas 14.

Return Period	Historical Value (Atlas 14)	Recommended New Value	Increase
years	inches	inches	%
1	3.00	3.60	20
2	3.65	4.38	20
10	5.64	6.77	20
25	6.99	8.39	20
50	8.26	9.91	20
100	9.45	11.34	20

REFERENCES

Applied Weather Associates, 2015: Probable Maximum Precipitation Study for Virginia. Prepared for the Virginia Department of Conservation and Recreation (DCR). Accessed from the [Virginia DCR website](#) on February 25, 2017.

Bonnin, G., and co-authors, 2006: NOAA Atlas 14 Volume 8, Version 3, Precipitation-Frequency Atlas of the United States. NOAA, National Weather Service, Silver Spring, MD.

Bonnin et al, 2011, Trends in Rainfall Exceedances in the Observed Record in Selected Areas of the United States, Journal of the American Water Resources Association http://amazon.nws.noaa.gov/articles/HRL_Pubs_PDF_May12_2009/Geoff_Bonnin/10.1111_j.1752-1688.2011.00603.x.pdf

Burns et al., 2015. Downscaled Projections of Extreme Rainfall in New York State, Northeast Regional Climate Center, Cornell University, Ithaca, NY <https://pubs.usgs.gov/of/2015/1235/ofr20151235.pdf>

Castellano et al, 2015. Climate Resilience Evaluation and Awareness Tool, Version 3.0 Methodology Guide http://ny-idf-projections.nrcc.cornell.edu/idf_tech_document.pdf

Castro, C. L., H. I. Chang, L. O. Mearns, and M. S. Bukovsky, 2015: Trend of climate extremes in North America: A comparison between dynamically downscaled CMIP3 and CMIP5 simulations. In *American Geophysical Union Fall Meeting Abstracts*.

Cubasch, U., D. Wuebbles, D. Chen, M.C. Facchini, D. Frame, N. Mahowald, and J.-G. Winther, 2013: Introduction. In: *Climate Change 2013: The Physical Science Basis. Contribution of Working Group I to the Fifth Assessment Report of the Intergovernmental Panel on Climate Change* [Stocker, T.F., D. Qin, G.-K. Plattner, M. Tignor, S.K. Allen, J. Boschung, A. Nauels, Y. Xia, V. Bex and P.M. Midgley (eds.)]. Cambridge University Press, Cambridge, United Kingdom and New York, NY, USA.

EPA, 2016. Climate Resilience Evaluation and Awareness Tool, Version 3.0 Methodology Guide.

Executive Order 11988, Floodplain Management, 1977, 42 CFR 26951, 3CFR 1977.

FEMA, 2016. Federal Flood Risk Management Standard (FFRMS)
https://www.fema.gov/media-library-data/1422649643416-0ff9e51d11442790ab18bae8dc5df4b/Federal_Flood_Risk_Management_Standard.pdf

Federal Emergency Management Association (FEMA), 2016. *South Carolina Dam Failure Assessment and Advisement, DR-SC-4241*. Accessible from:
<https://www.hSDL.org/?view&did=800246>.

Federal Highway Administration, HEC 17, Highways in the River Environment - Floodplains, Extreme Events, Risk, and Resilience, 2nd Edition, 2016, FHWA-HIF-16-018
<https://www.fhwa.dot.gov/engineering/hydraulics/pubs/hifi16018.pdf>

Groisman et al, 2005. Trends in Intense Precipitation in the Climate Record. *Journal of Climate* 18:1326-1350.

Hanson, L. S., and R. Vogel, 2008: The probability distribution of daily rainfall in the United States. In *World Environmental and Water Resources Congress 2008: Ahupua'A*, pp. 1-10.

Hayhoe, K. A., 2010: A standardized framework for evaluating the skill of regional downscaling techniques. Doctoral dissertation, University of Illinois at Urbana-Champaign.

Kam, J., and Co-authors. (2016) Multimodel Assessment of Anthropogenic Influence on Record Global and Regional Warmth During 2015 [in “Explaining Extremes of 2015 from a Climate Perspective”]. *Bulletin of the American Meteorological Society*, 97 (12), S4 –S8, doi:10.1175/BAMS-D-16-0149.

Liguori, S. and Rico-Ramirez, M.-A., 2014: A review of current approaches to radar based quantitative precipitation forecasts, *International Journal of River Basin Management*, 12:4, 391-402, DOI:10.1080/15715124.2013.848872

Melillo, J. M., T. Richmond, and G. W. Yohe (eds.), 2014: *Climate Change Impacts in the United States: The Third National Climate Assessment*. U.S. Global Change Research Program.

Menne, M. J., et al., 2012: An overview of the global historical climatology network-daily database. *Journal of Atmospheric and Oceanic Technology*, 29, 897-910.

Merkel, W.H. and co-authors, 2015: Design Rainfall Distributions Based on NOAA Atlas 14 Rainfall Depths and Durations. Accessed from the [NRCS website](#) on March 15, 2017.

Merkel, W.H. and co-authors, 2011: Rainfall Distributions for Ohio Valley and Neighboring States based on NOAA Atlas 14 Data. Accessed from the [NRCS website](#) on March 20, 2017.

NOAA, Current. Precipitation Frequency Data Server <http://hdsc.nws.noaa.gov/hdsc/pfds/>

NOAA, 2006-2016. Precipitation Frequency Atlas of the United States, NOAA Atlas 14, Volumes 1 through 10 <http://www.nws.noaa.gov/oh/hdsc/currentpf.htm>

NRCS, 2015. National Engineering Handbook, Chapter 4: Storm Rainfall Depth and Distribution, September 2015 Draft
https://www.wcc.nrcs.usda.gov/ftpref/wntsc/H&H/NEHhydrology/ch4_Sept2015draft.pdf

Perry, C.A., B.N. Aldridge, and H.C. Ross, 2000. Summary of Significant Floods in the United States, Puerto Rico, and the Virgin Islands, 1970-89. U.S. Geological Survey Water-Supply Paper 2502, Reston, VA.

Prein, A. F. et al., 2017: The future intensification of hourly precipitation extremes. *Nature Climate Change*, **7**, 48-52.

Schreiner, L.C., and J.T. Riedel, 1978: Probable Maximum Precipitation Estimates, United States East of the 105th Meridian. Hydrometeorological Report No. 51, U.S. Department of Commerce, Silver Spring, MD, 242 pp.

Thiemeßl, M.J., Gobiet, A. and A. Leuprecht, 2011: Empirical-statistical downscaling and error correction of daily precipitation from regional climate models. *International Journal of Climatology*, **31**, 1530-1544.

USACE, 2016, Guidance for Incorporating Climate Change Impacts to Inland Hydrology in Civil Works studies, Designs, and Projects, Engineering Construction Bulletin 2016-25 http://www.iwr.usace.army.mil/Portals/70/docs/frmp/eo11988/ECB_2016_25.pdf

USACE, 2017. US Army Corps of Engineers Nonstationarity Detection Tool User Guide http://corpsmapu.usace.army.mil/rccinfo/nsd/docs/Nonstationarity_Detection_Tool_User_Guide.pdf

United State Department of Agriculture – Soil Conservation Service, 1973: A Method for Estimating Volume and Rate of Runoff in Small Watersheds. *Technical Paper 149*. USDA-SCS, Washington, DC, USA.

APPENDIX A: Historical Climate Modeling

A substantial amount of evidence (e.g. Cubasch et al. 2013) exists showing that climate change has already begun to affect the distributions of atmospheric variables. Figure A-1 shows the simulation of global temperature from a complementary set of Global Climate Model experiments with (red line) and without (blue line) anthropogenic emissions of greenhouse gases (see Kam et al. 2016). Note the simulations with anthropogenic emissions are in excellent agreement with historically observed temperature (black line). The modeling suggests that, at least for temperature, the separation point after which the anthropogenic-forced climate differs from its natural state occurred in the late 1970s. This provides a complication for the stationarity analysis herein, since choosing stations (even those with long records) that have limited observations after the 1970s will be less affected by climate change than those with a more recent record. To address this issue, we removed stations that did not have a qualifying record after 2007, providing about 30 years of “climate-change affected” data.

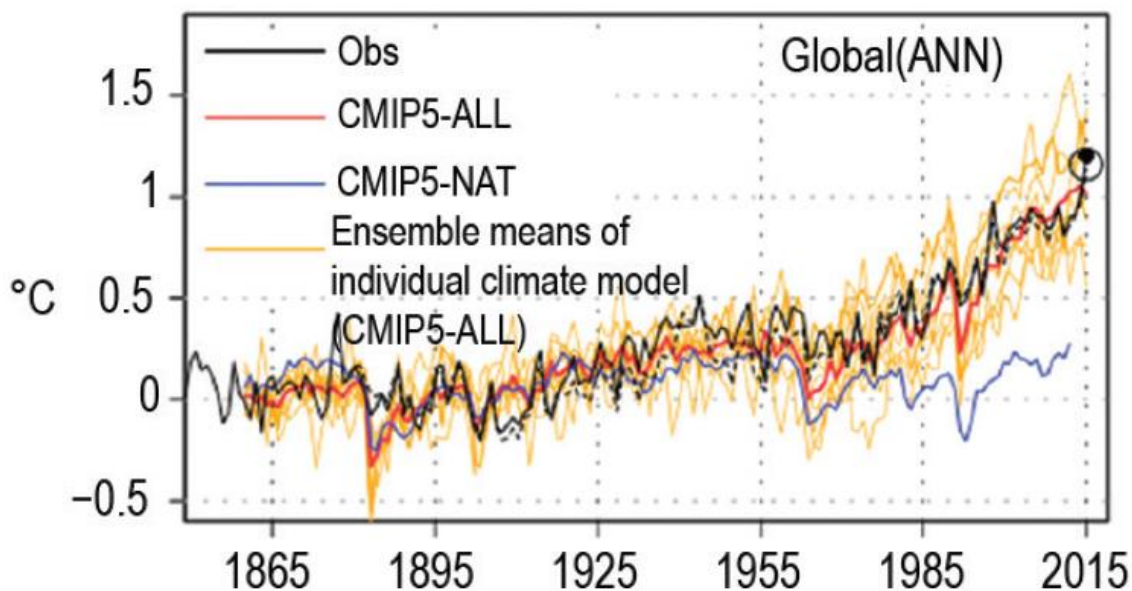


Figure A-1: Annual global mean surface temperature anomalies (°C). Red (CMIP5-ALL) and blue (CMIP5-NAT) curves indicate ensemble mean simulated anomalies through 2015 and 2012, respectively, with each available model weighted equally; orange curves indicate individual CMIP5-ALL ensemble members. Black curves indicate observed estimates from HadCRUT4v4 (solid) and NOAA NCEI (dotted). All time series are adjusted to have zero mean over the period 1881–19. [Reproduced from Kam et al. 2016; their Figure 2.1(e)].

APPENDIX B: NOAA Atlas 14 Point Rainfall for Virginia Beach



NOAA Atlas 14, Volume 2, Version 3
 Location name: Virginia Beach, Virginia, USA*
 Latitude: 36.7692°, Longitude: -76.047°
 Elevation: 6.32 ft**
 * source: ESRI Maps
 ** source: USGS



POINT PRECIPITATION FREQUENCY ESTIMATES

G.M. Bonnin, D. Martin, B. Lin, T. Parzybok, M.Yekta, and D. Riley

NOAA, National Weather Service, Silver Spring, Maryland

[PF_tabular](#) | [PF_graphical](#) | [Maps_&_aerials](#)

PF tabular

PDS-based point precipitation frequency estimates with 90% confidence intervals (in inches) ¹										
Duration	Average recurrence interval (years)									
	1	2	5	10	25	50	100	200	500	1000
5-min	0.415 (0.378-0.458)	0.481 (0.436-0.533)	0.534 (0.484-0.592)	0.623 (0.561-0.690)	0.701 (0.629-0.774)	0.777 (0.696-0.859)	0.842 (0.751-0.931)	0.905 (0.803-1.00)	0.977 (0.860-1.08)	1.05 (0.920-1.17)
10-min	0.663 (0.603-0.731)	0.769 (0.697-0.853)	0.855 (0.775-0.947)	0.996 (0.897-1.10)	1.12 (1.00-1.23)	1.24 (1.11-1.37)	1.34 (1.19-1.48)	1.44 (1.27-1.59)	1.55 (1.36-1.71)	1.66 (1.45-1.84)
15-min	0.829 (0.754-0.914)	0.967 (0.876-1.07)	1.08 (0.980-1.20)	1.26 (1.14-1.40)	1.42 (1.27-1.56)	1.57 (1.40-1.73)	1.69 (1.51-1.87)	1.81 (1.61-2.00)	1.95 (1.71-2.15)	2.08 (1.82-2.31)
30-min	1.14 (1.03-1.25)	1.34 (1.21-1.48)	1.54 (1.39-1.70)	1.83 (1.65-2.02)	2.10 (1.88-2.32)	2.36 (2.11-2.61)	2.59 (2.31-2.86)	2.82 (2.50-3.12)	3.10 (2.72-3.43)	3.37 (2.94-3.74)
60-min	1.42 (1.29-1.56)	1.68 (1.52-1.86)	1.97 (1.79-2.18)	2.38 (2.14-2.63)	2.79 (2.51-3.08)	3.20 (2.86-3.54)	3.57 (3.18-3.95)	3.95 (3.51-4.37)	4.44 (3.91-4.92)	4.93 (4.30-5.46)
2-hr	1.68 (1.53-1.86)	2.00 (1.80-2.22)	2.39 (2.15-2.65)	2.93 (2.63-3.24)	3.50 (3.13-3.87)	4.08 (3.63-4.51)	4.63 (4.10-5.11)	5.21 (4.59-5.76)	5.97 (5.20-6.60)	6.72 (5.82-7.44)
3-hr	1.82 (1.64-2.03)	2.15 (1.93-2.41)	2.58 (2.32-2.88)	3.18 (2.85-3.55)	3.84 (3.42-4.28)	4.53 (4.00-5.03)	5.19 (4.56-5.75)	5.90 (5.15-6.54)	6.84 (5.91-7.58)	7.81 (6.68-8.66)
6-hr	2.21 (1.99-2.48)	2.62 (2.35-2.95)	3.14 (2.81-3.53)	3.88 (3.45-4.35)	4.71 (4.17-5.26)	5.57 (4.90-6.21)	6.41 (5.60-7.14)	7.33 (6.35-8.15)	8.56 (7.34-9.52)	9.85 (8.33-10.9)
12-hr	2.63 (2.35-2.96)	3.10 (2.76-3.51)	3.73 (3.32-4.21)	4.63 (4.10-5.22)	5.66 (4.98-6.37)	6.76 (5.90-7.58)	7.84 (6.78-8.78)	9.04 (7.74-10.1)	10.7 (9.02-12.0)	12.4 (10.3-13.9)
24-hr	3.01 (2.76-3.30)	3.66 (3.36-4.02)	4.72 (4.33-5.20)	5.63 (5.14-6.18)	6.98 (6.32-7.63)	8.13 (7.32-8.90)	9.41 (8.39-10.3)	10.8 (9.55-11.8)	12.9 (11.2-14.2)	14.7 (12.6-16.2)
2-day	3.48 (3.19-3.83)	4.21 (3.86-4.64)	5.42 (4.96-5.96)	6.45 (5.89-7.09)	8.01 (7.24-8.78)	9.36 (8.40-10.2)	10.9 (9.65-11.9)	12.5 (11.0-13.7)	15.1 (13.0-16.6)	17.3 (14.6-19.1)

APPENDIX C: Hurricane Matthew

Snapshot of Hurricane Matthew's position, via the National Weather Service's watches/warnings from the National Hurricane Center's Advisory issued on Sunday, October 9, 2016 at 5AM. This represents approximately the time of peak winds in the Virginia Beach region. This image was prepared using HURREVAC software (v.1.5.3).

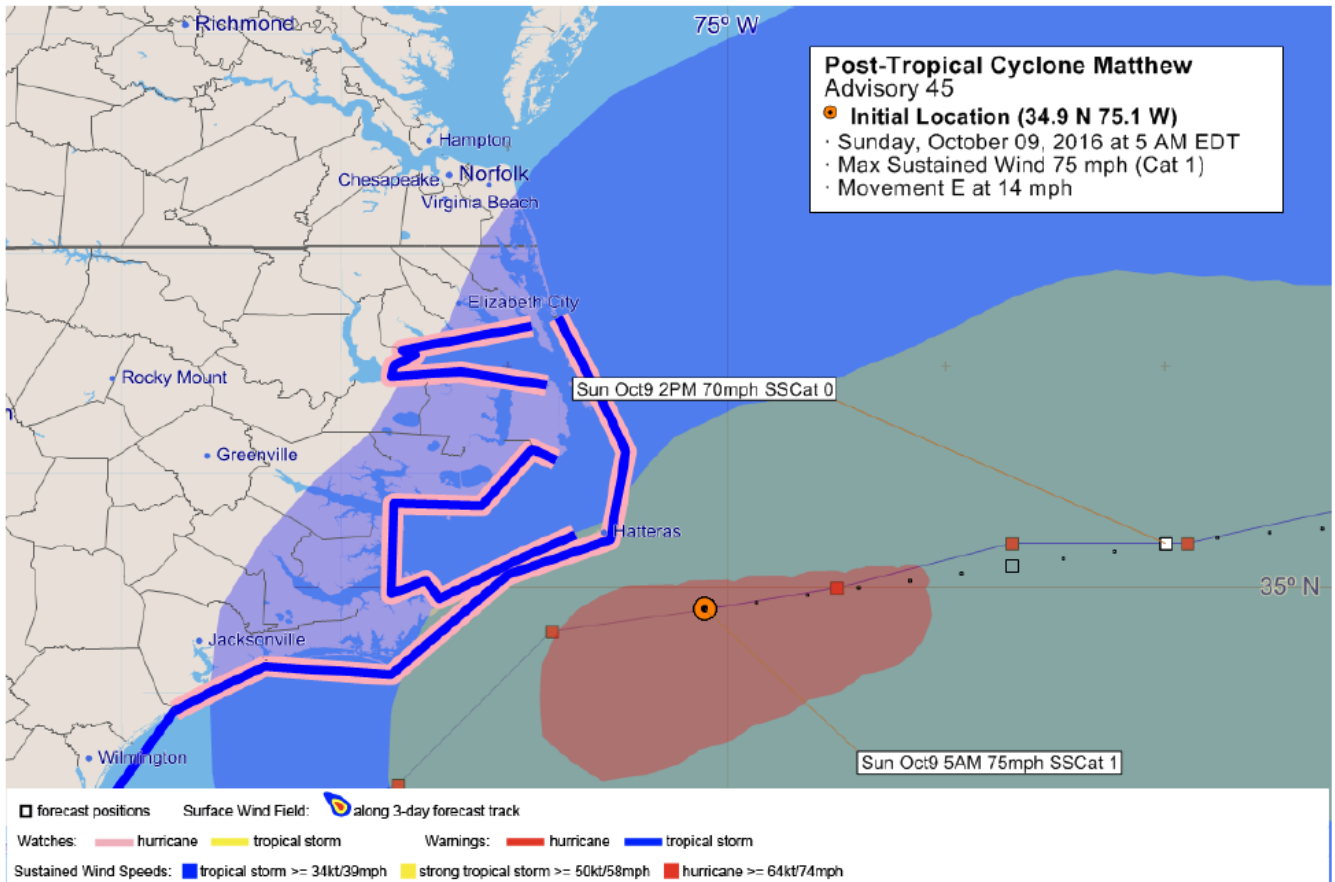
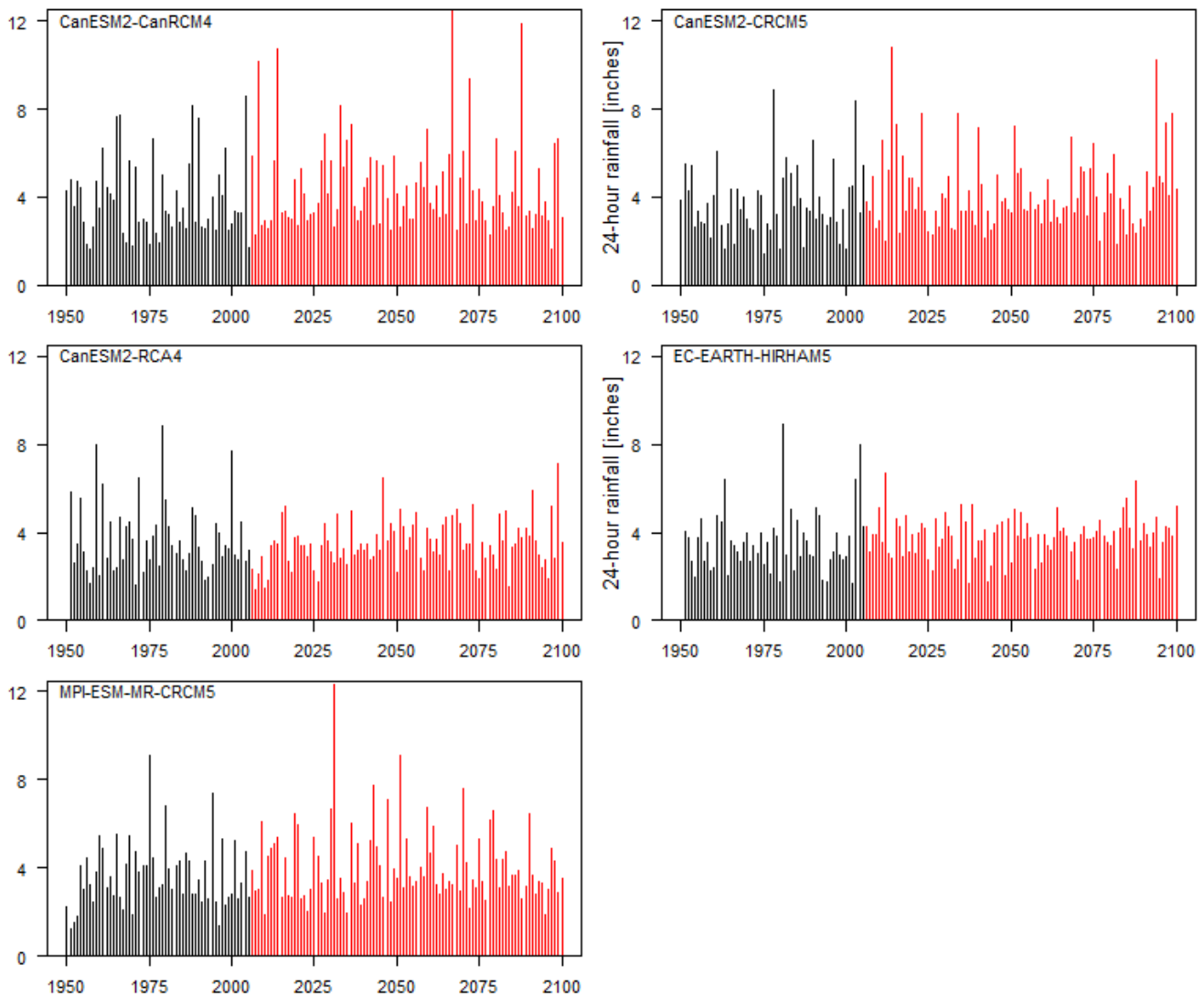


Figure A-2: Approximate time of wind speeds during Hurricane Matthew in Virginia Beach.

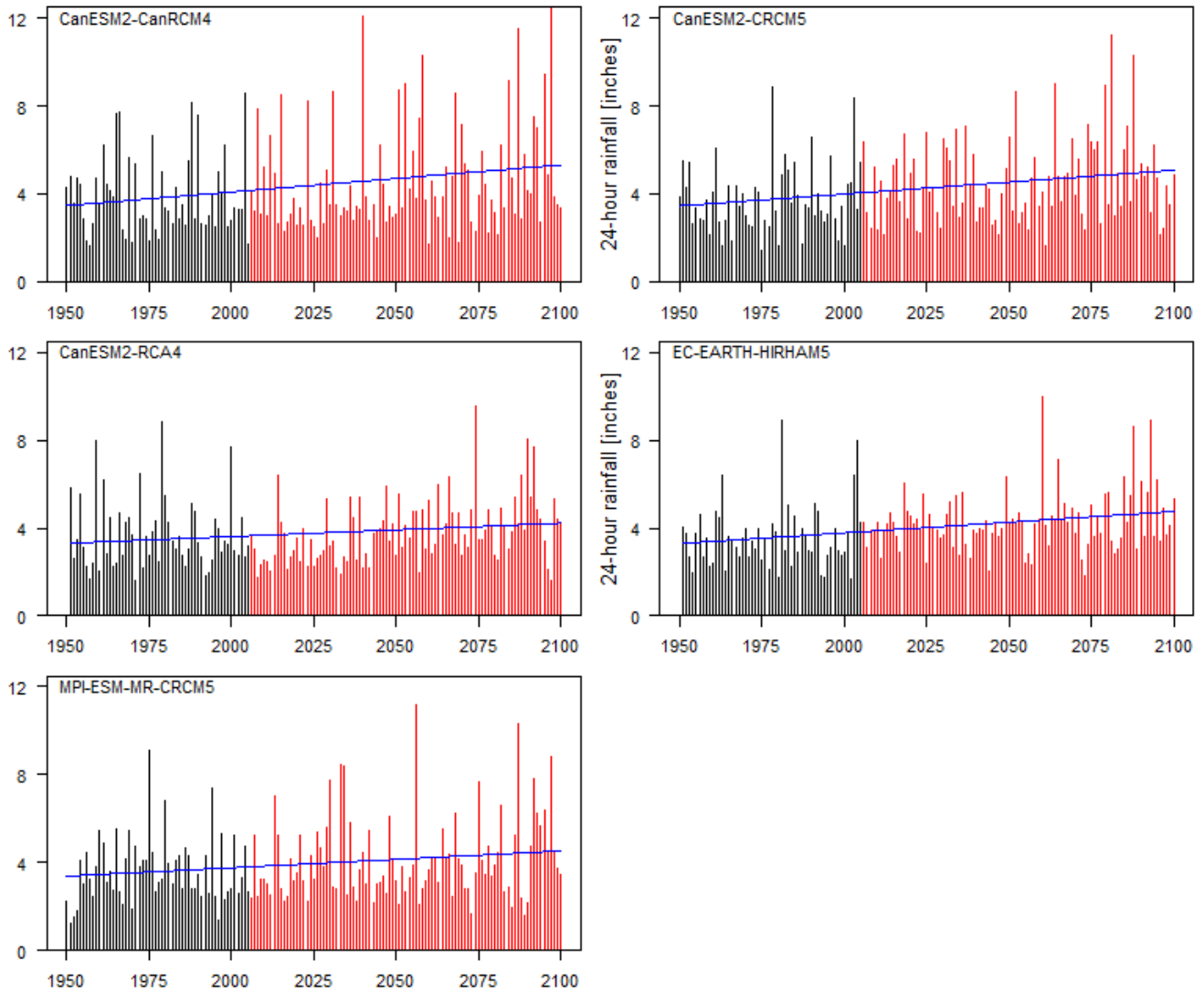
APPENDIX D: PROJECTED ANNUAL MAXIMUM SERIES

Shown below are bias-corrected Annual Maximum Series (AMS) of 24-hour rainfall for each model, grouped by the emission scenario and model resolution. A trend line (blue) is shown if the trend in AMS over the entire simulation (1950-2100) is non-zero with at least 90% confidence. A lack of a trend line implies no significant trend.

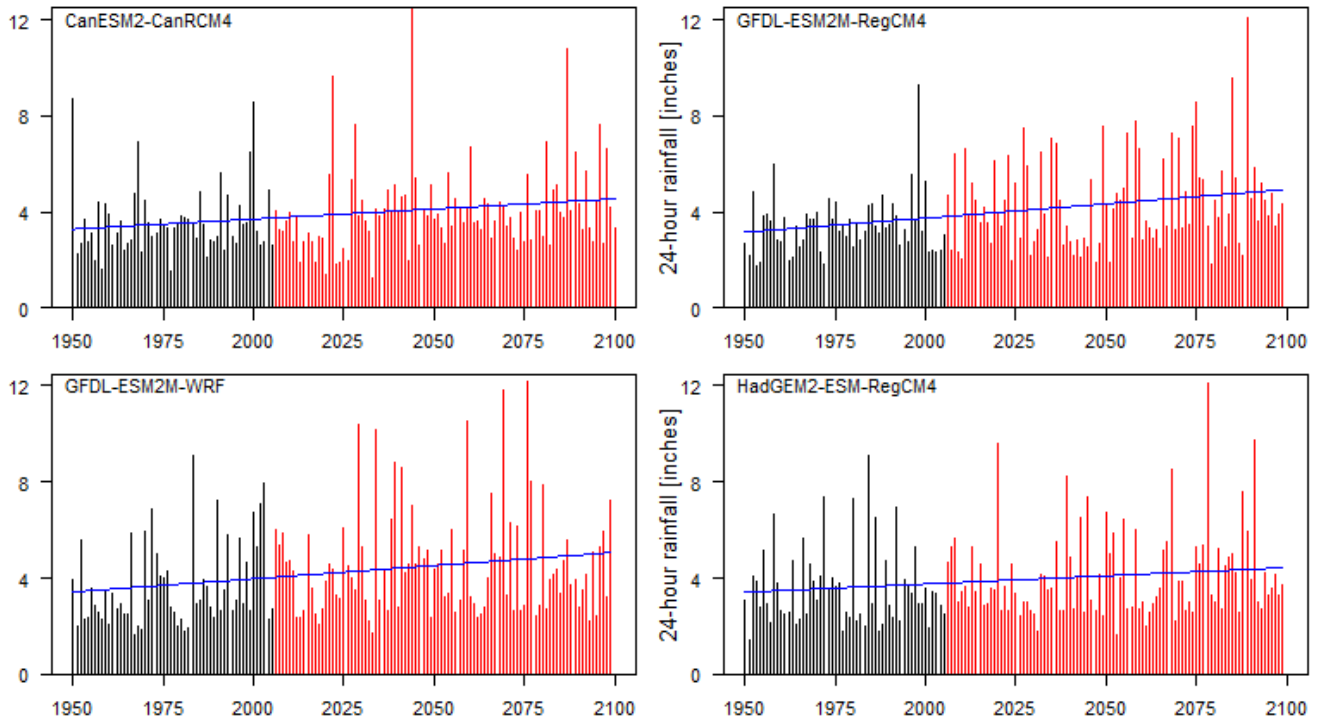
RCP4.5, 44-km resolution



RCP8.5, 44-km resolution



RCP8.5, 11-km resolution



APPENDIX E: INTERVIEW SUMMARY

Table A-1 provides a summary of the responses we obtained from four practicing engineers across the United States, regarding their views and experiences on resilient design rainfall practices. Each interviewee was asked the following three questions:

1. Many long-term historical precipitation gages, for example see Figure A-3, have shown increases in heavy, very heavy and extreme precipitation. This is especially true in the central and eastern United States. Has your organization considered trend analyses on local rain gage data to inform decision making for updating design guidance? If so, what was learned and how were the results implemented, if at all? If not, do you foresee such an analysis in the short term (next year)? Medium term (next 5 years)? Long term (10+ years)?

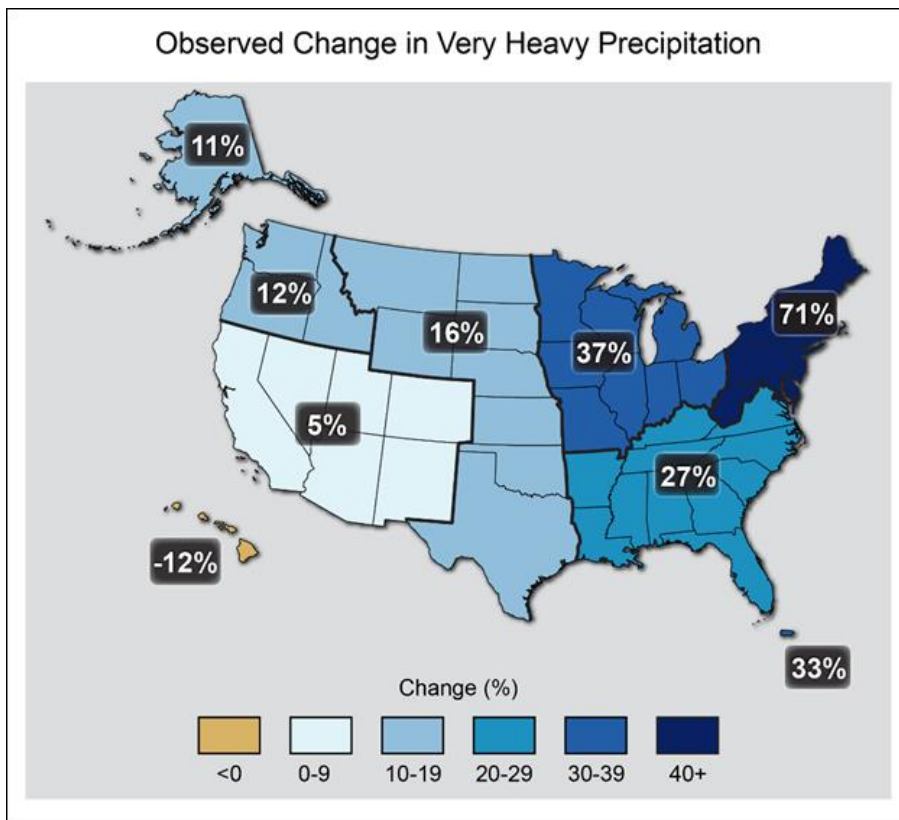


Figure A-3: Observed change in heavy precipitation events (i.e. downpours, the heaviest 1% of annual rainfall events). Source is 2014 National Climate Assessment, <http://nca2014.globalchange.gov/report/our-changing-climate/heavy-downpours-increasing>.

2. The latest climate modeling experiments project robust increases in heavy precipitation for many areas within the United States, see Figure A-4. For example, maximum 24-hour

rainfall is expected to increase by 20% or more, while heavy hourly rainfall could increase by more than 30%. Has your organization considered incorporating climate projections of future rainfall in decision making and/or design standards (see Figure A-4 for an example of such as analysis)? If so, what was learned and how were results implemented? If not, can you provide a reason why this is not being considered (e.g. science is uncertain, there is already slack in design standards to absorb these chances, etc.)?

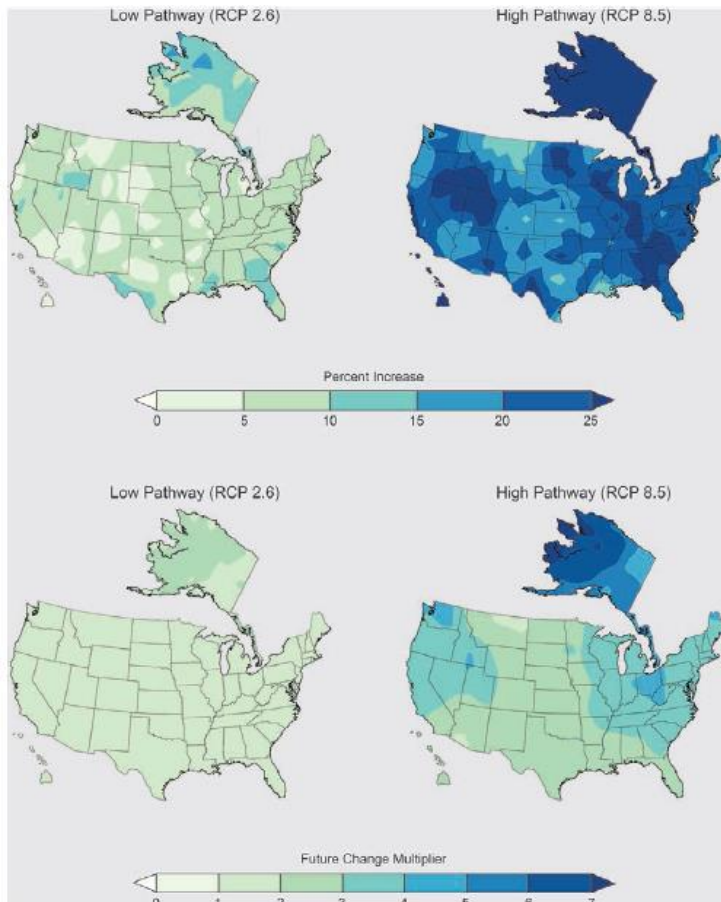


Figure A-4: (top) Projected change (%) in the 20-yr return value of annual maximum daily precipitation at the end of this century (2081–2100) relative to the recent past (1986–2005) for the lower (left) RCP2.6 and higher (right) RCP8.5 scenarios. (bottom) The relative rate at which the 1986–2005 20-yr return value of annual maximum daily precipitation is projected to occur during 2081–2100. A value of two would mean that such an extreme event happens twice as often. Referenced from Wuebbles et al. (2014).

3. Assuming that extensive evidence did exist in both points (1) and (2), which would carry more weight in influencing design standards

Table A-1: Responses from four practicing engineers regarding their experience with updating design rainfall.

Contact Name	Organization	Question 1	Question 2	Question 3	Notes
Kevin Stewart, Manager of Flood Warning Services	Urban Drainage & Flood Control District (Denver, CO)	The extent to which UDFCD looked into this was to compare the rainfall frequency curves of the latest Atlas 14 data with its predecessor Atlas 2. Atlas 2 has guided design in Denver area since its release in 1973. Atlas 14 found either similar or lower rainfall frequencies compared to Atlas 2. However, UDFCD chose to stick with Atlas 2 because they thought it well captured the regions climate, along with a slight buffer. They have no plans of investigating historical rainfall trends given the lower Atlas 14 findings. They authored a position paper on why they stayed with Atlas 2. See notes for link.	Not aware of any significant upward projections for the CO region. Also, concerned about inadequate resolution of climate models.	No opinion.	Link to position paper: http://udfcd.org/wp-content/uploads/uploads/resources/position%20papers/UDFCD_Position_on_the_2013_NOAA_Precipitation-Frequency_Atlas.pdf
Darold Burdich	Fairfax County DEP, Stormwater	Not sure, but does not think so. Stated that Consultants do this work, using whatever is the accepted criteria.	N/A	N/A	N/A
Karl Berger	Metropolitan Council of Governments	Standard guidance is in use, will email county engineers (MD, DC & NOVA) to get more info.	Have discussed this, but not involved in design.	N/A	N/A
Matthew Waters	Annapolis Public Works	NOAA Atlas 14 and guidance in the MD Drainage manual are applied.	No consideration has been made for deviating from current guidance.	No opinion.	N/A

